January 2019

3d Scanning And The Impact Of The Digital Thread On Manufacturing And Re-Manufacturing Applications

Mojahed Alkhateeb
Wayne State University, mmalkhateeb@kau.edu.sa

3D SCANNING AND THE IMPACT OF THE DIGITAL THREAD ON MANUFACTURING AND RE-MANUFACTURING APPLICATIONS

by

MOJAHED MOHAMMAD F. ALKHATEEB

DISSERTATION

Submitted to the Graduate School

of Wayne State University,

Detroit, Michigan

in partial fulfillment of the requirements

for the degree of

DOCTOR OF PHILOSOPHY

2019

MAJOR: INDUSTRIAL ENGINEERING

Approved By:

_____

Advisor Date

_____

_____

_____

DEDICATION

To my parents and wonderful family

ACKNOWLEDGEMENTS

First, I would like to thank Dr. Jeremy Rickli for his guidance, ideas and support and also for allowing me to take the lead in the MaRSLab and work as a graduate research assistant. I value his guidance, as well as his efficiency and responsiveness in reviewing my work. I would also like to thank Dr. Ana Djurich for allowing me to use the robot in her lab to conduct the experiments and being there when needed. I would also like to extend my thanks and appreciations to Dr. Qingyu Yang and Dr. Evrim Dalkiran, who have served as my dissertation committee members, for their valuable comments and constructive suggestions on this work. The MaRSLab Lab has been like my home since I started my Ph.D. journey. I would also like to thank King Abdulaziz University and the Government of Saudi Arabia for providing the financial support throughout my study.

I would like to convey my appreciation to my friends Dr. Mahmoud Alzahrani for his support in programming the point cloud comparison tool, Dr. Mohammad Mkaouer for his support in programming and encouragement throughout my Ph.D. journey, and my colleague Shengyu Liu for her help with conduction the CT scanning experiment, and Nicholas Christoforou for his help with the analysis of the smoothing factors. I must also express my sincere thanks to Ms. Sara Tipton for proofreading and editing my research.

My journey in pursuit of this research program would not have been possible without the sacrifice and constant prayers from my family especially my parents, Eng. Mohammad Alkhateeb and Dr. Omaima Abulfaraj, my wife, Amenah Baroum, and our wonderful daughter, Maha, who did not complain too much when I picked her up late from school. They are the driving force in my life and career, and without them, the journey would have been less meaningful.

I pray to Allah, whom I owe the knowledge, strength and determination to complete this research, to bless us all.

TABLE OF CONTENTS

LIST OF FIGURES

LIST OF TABLES

CHAPTER 1: INTRODUCTION

1.1 BACKGROUND AND MOTIVATION

Traditional inspection methods in manufacturing required technical individuals that use a variety of gauges and tools. These techniques require time which is not consistent because performance involves human interaction. The issue is because of the variations involved, there is no standard due to the nature of human error and variation. With the increasing demand for quality and speed in manufacturing, the importance of automation in the processes, and the use of machinery to conduct inspection, attracted developers to provide automated solutions. Automation of inspection techniques has improved both the accuracy and the speed of inspection processes. Developers have invented devices that measure the coordinates of the part being inspected automatically by using a device called Coordinate Measurement Machines (CMM). CMMs inspect the part by using a touch probe that contacts the surface of the part and makes multiple contacts with the part being inspected to collect points on the surface. These points are then fed to a computer device and compared with the original value to decide if the measured part within the tolerance is specified. The technology is very precise and accurate. However, the process is slow in acquiring the dimensional information, as is it required to make a movement and contact the part each time a point is collected [10]. Contacting the part in order to collect data points is not efficient for collecting a large number of points and would require a long time in the manufacturing facility. Non-contact inspection methods, such as laser line scanners, can obtain a large number of data points in a short period of time [11] in comparison with the contact type of inspection [1]. However, in many non-contact inspection methods, human involvement is required, which is a time-consuming technique that is run on a trial and error basis in manual inspection [12]. In order to avoid human involvement in inspection and make the process more time efficient and error free, it is important to facilitate the use of automated planning for inspection in laser scanning [13]. 3D scanning technology can be automated to generate plans for inspections for consistent and repetitive measurement. These consistent plans are dependent on the

dimensional information of the specific part that is being inspected and are tailored to the specific features on the surface. In order to generate the best automated plan for the 3D scanner to follow, the relationship between point cloud quality and scan parameters must be defined. With the advances in CAD/CAM and machining technologies manufacturers are able to make complex, compound curved parts, but parts need to be inspected. Traditional methods may not capture all the data needed, especially if the parts have compound curves, surfaces with multiple features, and other organic shapes. 3D scanners are the perfect tool to use in order to inspect these organic shaped surfaces and ergonomically designed parts [14]. In addition, traditional inspection of free-form surfaces requires highly skilled technical individuals, which takes a long time. 3D scanners have made it possible to accurately and quickly measure free-form surfaces due to their ability to measure a fine detailed surface quickly and cover the surface faster than the CMMs while not having a visibility problem [1]. When automating a 3D scanner, depending on the size and the type of the scanner, the scanner is either mounted to a robotic arm and the part is on a turntable [15, 16, 17, 10] or mounted on a robotic arm; the part is fixed, and the the scanner moves around the part [18, 19], or it can be in place at the end probe in CMM [20]. In all cases the scanner is programmed to make a movement over the part to scan it; these movements are based on the location of the part being inspected in the robot/CMM workspace. When using the scanner mounted to a robotic arm, the data gathered from the scanner are then stored in the scanner workspace. In this dissertation, it will be referred to as the C-track workspace. The relationship between the workspaces are not known, so there is a need for it to be derived in order to reference a point on the surface of a part to be revisited. In this thesis I divided the work into four tasks the that will be divided into four chapters. The first task is to connect the workspaces together and find the relationship between the robot workspace and the scanner workspace. The second task is to conduct experiments with systematically varied parameters to study the effect on the scan quality caused by the view angle of the scanner to the test object being inspected, the stand-off distance between the scanner and the test

object, and the speed of the movement of the reboot arm, as well as the resolution setting selected on the scanner. The third task is to study the effect of the changes in the point cloud or the digital representation of the object for the remanufacturing applications, this will be following all the steps in the remanufacturing facility starting from the inspection and digitization phase all the way to the remanufacturing phase that is material deposition. The fourth task is to use machine learning to optimize the parameters of the scanning technology in order to get the best scanning outcomes and study the accuracy of the model.

1.1.1 Contact and Non-Contact Inspection

Contact measurement methods acquire surface geometric information using tactile sensors such as gauges and probes that physically touch the part being inspected such as CMMs. (Figure 1.1.a). On the other hand, non-contact measurement methods acquire surface geometric information by using some sensing devices such as laser/optical scanners, X-rays, or CT-scanners [1].

In contact inspecting methods there are several factors that do not need to be taken into consideration, since it would not affect the process of measurement dimensional information of the inspected surface. These include view angle, standoff distance, and speed. Speed is not critical for individual point measurement because CMM speed does not affect the ability to capture a point as long as the probe is making contact with the surface. The contact inspection methods, such as CMM, is accurate although it does not allow for the collection of many data points as quickly as a non-contact inspection method (Figure 1.1b). Optical CMMs are one of the technologies that are not as clear in terms of contact or non-contact; non-contact optical CMMs systems have an optical eye to measure the dimensions of the object. However, they have some mechanical constraints as the part has to fit in the area designated for use. The main difference between Optical CMMs and a 3D scanners is the ability of the 3D scanner to collect more data points and scan larger objects. Portable optical CMMs come with a scanner and a portable probe that contacts the part while scanning. Although it has a probe, it is considered contactless as it moves freely around the surface

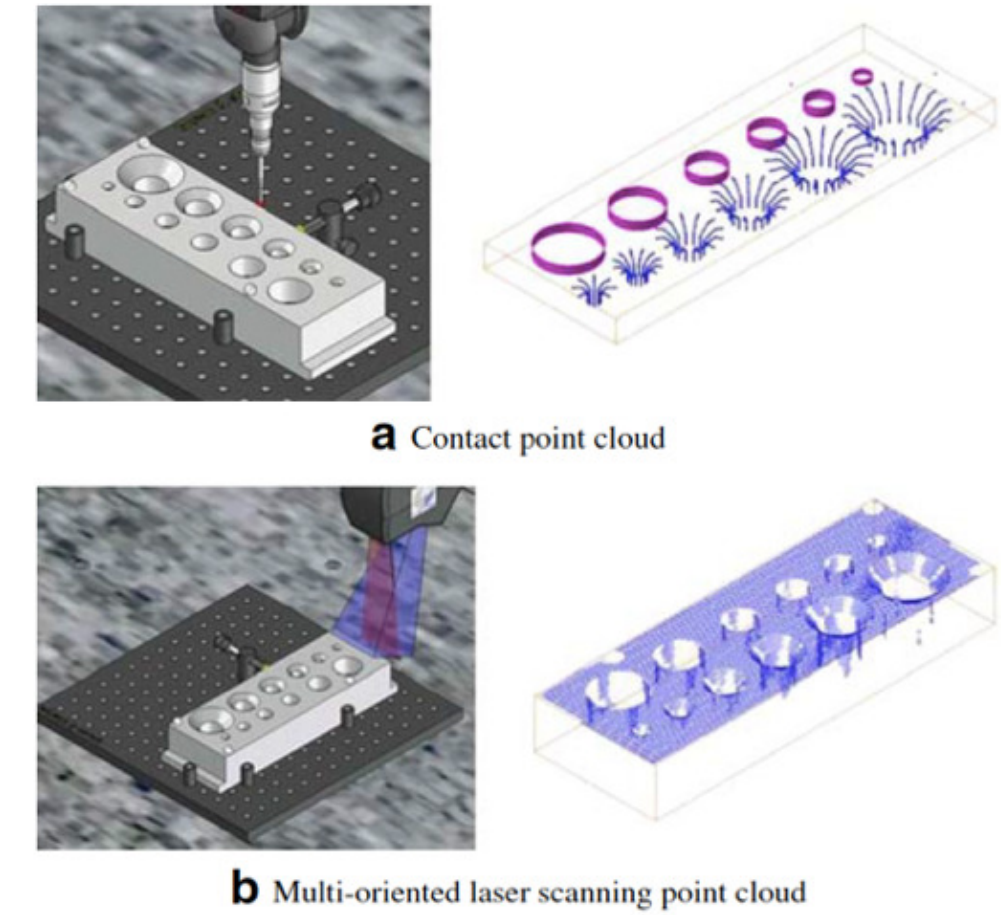

Figure 1.1: Point cloud artifacts C(a,b) collected by CMM and laser scanner [1]

and only collects points based on its location on the part and on what angle it is. It provides the ability to measure large objects by freely walking around them and has no mechanical constraints. CT-scanners on the other hand provide a solution to inspect the geometry of the part along with the internal structure and the condition of the part by projecting x-ray signals in different frequencies and provide a visual representation of the part.

1.1.2 3D Scanning Technologies That Are Being Used for Various Application

Commercial laser scanners can be attached to a robot or coordinate measuring machines (CMMs) for dimensional inspection, reverse engineering [21, 22], and re-manufacturing [23]. Compared to a contact method, such as CMM using a touch-trigger probe, laser scan-

ners have the advantage due to their ability to gather many points in a short time with high speed, high resolution, and without contact sensing [24]. This advantage has also attracted non-manufacturing fields due to the technology's ability to do touchless scanning. 3D scanning has been used in many applications, some related to civil engineering and surveying, and others related to medical applications and historical preservation of heritage [24]. This includes historians who capture dimensional data about sculptures to digitally record and preserve historical artifacts [25]. Physicians use laser scanners as a surface measuring tool for clinical assessment of patients [26]. Depending on the intended use of a 3D scanner, there are multiple scanners to select from. No one single scanner can fulfill all the required needs of different applications. It depends on the size of the object being scanned and the scanner's features. Scanners can be categorized into two types: ranging scanners and triangulation scanners. Ranging scanners scan buildings and large objects with lower precision compared to triangulation scanners. These scanners are fixed in one place and a laser beam is projected from the scanner to scan up to 360 degrees around the scanner; these scanners are not ideal to scan objects as they only scan one side that is visible on the object. Scanners are not the same in their abilities and features. Some are small and easy to transport and have the ability to run on a battery, while others are bulky and hard to move. Other features are related to the ability of the scanner such as resolution, speed, field of view, and range limits. Scanners are also not the same in their ability to scan when there is interfering radiation [27]. This research will be working with a triangulation scanner. Which has the ability to scan medium to large objects such as a car hood or a door, and it also provides the ability to be moved around the object to cover the surface from all angles.

1.1.3 Challenges in 3D laser line Scanning in Manufacturing

Although laser scanners can obtain a large number of data points in a short period of time as shown in Figure 1.2, there are challenges that hinder their use as an inspection tool in manufacturing applications, due to some trial and error and the iteration it is taken by the workers in taking the measurements.

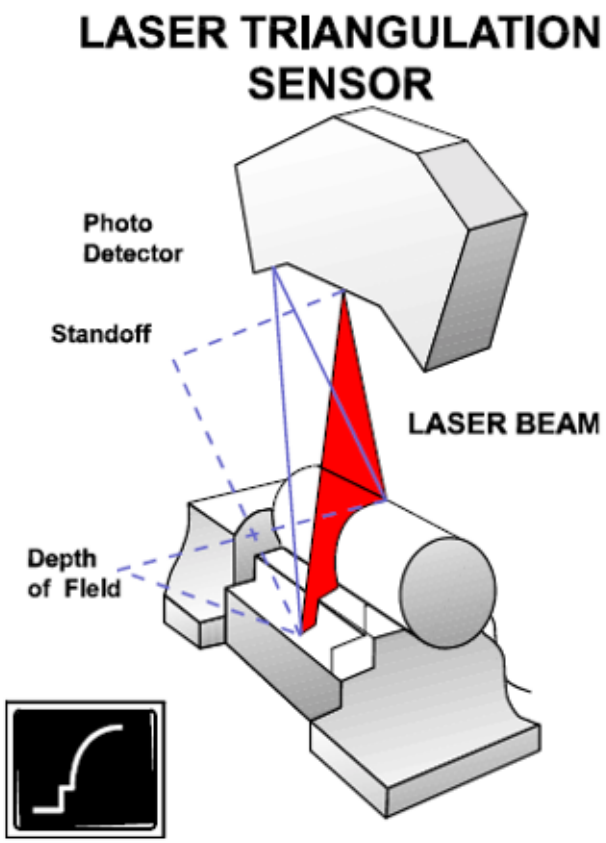

Figure 1.2: Impression of a side of the object in one instance

There is a need for development of automated laser scanning system models that avoid the trial and error caused by manual scanning [12]. Since there is a lack of knowledge on the effect of the different parameters the scan quality, the outcomes of automating the process will not be a clear and accurate point cloud that can be used in the manufacturing industry as a tool for inspection. When scanning manually, it is difficult to keep track of all the details about the standoff distance, and the view angle due to fatigue that occur while holding the scanner and inability to manually control it. Automating the process will make it possible to scan a specific part while keeping track of scanning parameters such as view angle and standoff distance by integrating it into the scan trajectory. This will result in consistently getting a complete point cloud that represents the surface each time.

1.1.4 Motivation and Significance

There has been little research focused on the effect of scan quality by the integration of the 3D scanner with a robotic arm and testing the system as a whole in an effort to automate the system. Understanding the effect of integrating these components together is important in designing an optimized trajectory path in the future. Analysis predicts that there will be a compound annual growth rate of 13.81 % annually in the market of 3D Scanning over the period of 2013-2018. ("Global 3D Scanning Market 2014-2018"). This research is motivated by the importance of a defect detection method which can be used in today's fast paced manufacturing facility. There is a continued demand for better quality in manufacturing. Manufacturers are concerned about utilization by having a flexible line manufacturing facility that is able to handle multiple products with minimum modification to the line itself [28]. Having flexible technology that can be used with different setups is a key component in a flexible manufacturing facilities. 3D scanning can be used in flexible manufacturing facilities as an inspection tool for defects due to its ability to scan a variety of products with little modification [14]. However, the current manual approach, although it is lean and flexible, needs to be automated, as that would reduce the inspection time approximately 30% [29] and generate more consistent scan data. This can be solved by generating a scan path trajectory based on each part using a vision system that identifies the part on the production line and activates the specified scan trajectory for the part being inspected. National Institute of Standards and Technology (NIST) is initiating a project to demonstrate how a standardized 3D model of a product can integrate and streamline production from the initial design through the final inspection in a continuous, coherent data-driven process. This tightly integrated, seamless string of activities is what manufacturers call a "digital thread" [30]. Products and Manufacturing Information (PMI), proposed by NIST, will include non-geometric attributes in a 3D CAD model that will be important for manufacturing product components and assemblies [31]. The automated laser line scanning system will help in increasing the information content by adding the original manufactured

dimensional information to the digital thread, and making the scanned data more effective. The availability of PMI will make it possible to reverse engineer a product and use the scanning technology to collect geometric information. The collected scanned dimensional information along with the PMI information can be used in remanufacturing applications and inspecting the part to be remanufactured. This can also be used to sort the quality of the parts received at the remanufacturing facility for quick decisions about accepting or rejecting the part based on the feasibility of the part received. Despite the continued improvement in accuracy, there is still a problem, as most of the current scanning techniques and procedures cause very bad scanning artifacts, such as noise, outliers, missing areas, and incomplete geometry [5]. Researchers have been addressing this with two strategies. The first strategy is by point cloud processing to remove errors [5]. The second strategy is point cloud path planning to minimize the amount of work in point cloud processing. Within the second strategy there are researchers that are looking at the noise caused from the part being inspected and the effect of the surface finish [32]. Others are looking at the problem from the parameters on the scanning procedure [18, 6]. Understanding the effect of different parameters on the quality of the scan is important as it can lead to better scan quality and reduce the noise and inconsistency in the data; it also reduces the effort of cleaning the dataset after scanning. Extensive cleaning can eliminate points that are important in identifying the defect and make the technology not applicable for use as an inspection tool. Having better scanning quality by using the right parameters will reduce the processing time that will also save inspection time. It will also improve the quality of the generated trajectory as it is generated based upon the best parameters in accordance to the curvature of the part being scanned. Experiments in this study are expected to explain the effect of the parameters on the scan quality that is required to benchmark future scan path planning methods. In order to automate the technology and take it from its manual current state, there is a need to investigate scanning techniques and define it based on the best outcomes unlike its current trial and error technique. Manual scanning often results in numerous bad

scanning artifacts and can require scanning the same part multiple times to capture what was missed. This is a time consuming process that has to be avoided in automatic inspection. This cannot be achieved unless the parameters are defined and taken into consideration in the scan planning process. It is important for any exploration and understanding of the problem to understand the effect of the parameter in order to suggest an improvement or to optimize the process [32]. Parameters effect on the scan quality are still not well addressed in the literature along with the limitations of the 3D scanning technology.

1.1.5 Research Problems

Current point cloud measurement procedures are time consuming and do not produce good scan quality. Because current scan procedures are based on manual trial and error, they produce scans that cannot be used as a basis for inspection due to variability in the procedure and noise in the scans that produce many artifacts and outliers. There is a need to develop an automated laser scanning system to avoid these variations and have a consistent data capable for identifying defects. In this research, I am investigating the cause of having an artifacts in the point cloud data and studying its causes. In order to do so many components need to be added to reach to the results. First, by learning how to program the robot using a Teach Pendant, and became familiar with the process of scanning using the 3D scanner. Also becoming familiar with the field and gather the necessary knowledge. The parameters that were considered in designing the path were the standoff distance and the view angle. The change in these parameters effects the distance between the two neighboring paths. The lower the standoff distance, the smaller is the width of the laser beam. Also, when the view angle is smaller and the scanner is perpendicular, the smaller the laser beam is. Due to the complexity of the scanned object in the initial experiments, ideal point cloud were not achieved. It wasn't clear what the factors that impacted the scan quality were. Therefore, I concluded that there is a need to study scan parameters in order to know the factors that affect the scan quality that prevent having noise, outliers, holes, and low sampling density of point clouds. This also showed that in order to get the right parameters there is a need

to select a test object that does not contribute to the noise in the scan and we can easily distinguish the effect of the parameters by using a designed test bed. For doing so a test bed that allow to hold some parameters constant while changing others to understand the effect of individual parameter was designed. The selection of the test bed is very important in characterizing the impact. Failure to design and select the right test bed will result in a misleading information about the impact of the parameter on the scanning quality. However, although in the optimal parameters were selected in the performed scan we found out the resulting point cloud wasn't clean as well and there are many noise, and outliers. This prevent the use of the point cloud as gathered for digital additive remanufactuing and lead us to the second phase of exploring the different phases that the point cloud go through in the remanufactuing process that adds up to the total error. Finally, the need for optimizing the parameter is important to get the optimal point cloud; therefore it is important to use some optimization and machine learning tools to predict the right parameters. A study was made to study the accuracy of the prediction tool in finding the right parameters based on the results of an experiment made on CT-scanner; doing so will generate the knowledge needed to automate the system. These activities led to a greater understanding on how to design a trajectory and scan a part in the most optimized and efficient way. The robot that was used is FANUC S-430 IW, and the scanner is Creaform MetraSCAN-R. This contribution is significant because it is expected to automate the use of laser line scanners and make it more consistent, reliable, and efficient as a quality monitoring tool for condition assessment in the manufacturing and remanufacturing inspection operation. Thus, it eliminated variation caused by manual scans.

1.1.6 Research Challenges

Currently there are two workspaces: the robot workspace and the C-track workspace. The robot workspace is used to move the robot and record the location of the end effector while moving. The C-track workspace is the dimensional information of the scanned object. Deshmukh et al. [33] created a model that made it possible to determine the position and

orientation of a robot arm, laser scanner, laser beam, and component with respect to the robot workspace. The points that are collected are stored in the VX element on a different workspace; one of the challenges is finding the transformation matrix that connects the C-track workspace to the robot workspaces. Understanding this relationship and the effect of moving the C-track is important as it will affect the way the experiment is conducted. The relationship is also important in identifying points to scan in the inspection process and knowing what point the scanner is pointing at on the C-track while moving in the robot workspace. After finding the relation and its effect, the experiment was made to validate the model. Deshmukh et al. [33] worked on a model that integrates three components in the automated laser line scanner as this is necessary to know in automating the system; the three components are the robot, the laser scanner and the component surface. They created the fundamental kinematic models required for advanced automated scan path planning and generated the forward and inverse kinematics models. The model created was the first used for this application and had some assumptions in the modeling of the kinematics equations. This made it challenging to use the model as the results of using it are not known. One of the challenges is how to define point cloud quality.There are four parameters that define the quality of point cloud that were introduced by [34, 35]: density, completeness, noise, and accuracy. Boehler et al. [32] measured the quality by the deviation of a single point from the object's surface. However, the deviation of a single point is not the right approach to use as there are variations that prevent us from getting the exact point each time a scanning is performed, as mentioned by the same researcher due to some variability in the rate the scanner capture and the moving speed. In this research, I defined the quality as the density, completeness, and noise of the gathered point cloud. Since selecting the right test object affects the ability of the scanner to scan and produce a quality point cloud, part of it is the lack of knowledge on the effect of the different parameters on the scan quality, and this makes it challenging to select the right test object for the experiment. Not finding the right test object will result in misleading information that will prevent us from knowing the effect

of the parameters.

1.1.7 Research Objectives

The research objectives are understanding the effect of: view angle, standoff distance, scanning speed, and resolution setting on the scan quality by conducting a point cloud measurement experiments with systematically varied scan parameters. This experiment will help defining the effect of different parameters on the scan quality. Previous researches did not address the effect of speed, view angle, standoff distance, and resolution and the interaction between them in the scan quality; these are important in designing the automated system. Understanding the effect of the parameter will be a foundation for designing the automated scan system that will help achieve a faster inspection time that suite the industry. This research is expected to model the location of a point on the surface in an attempt to predict the measured point cloud, to model of relationship between the C-track workspace and the robot workspace, to characterize the impact of point cloud measurement parameters on the scan quality, and to verify the points prediction by feeding the location of the point to be collected by the scanner. By accomplishing all three objectives linking the robot and the scanner workspaces, predicting the location of the laser beam on the point being scanned, designing the experiment with a systematically varied scan parameters, understanding the error contribution factors from all the activities in the remanufactuing application, and the possibility to optimize and predict the parameters of the scanner to achieved the best results will addresses the research gaps in 3D scanning as an inspection tool and study the effect of the scanning parameters on the scan quality. These steps will make it possible to have an automated system capable of having a consistence scans that can be used as basis for inspection for many applications.

1.2 LITERATURE REVIEW

This review covers the relevant literature in the area of the research in ten different sections: free-form surface inspection methods; computer aided inspection planning; point cloud quality for contact and non-contact inspection; 3D scanning applications; strategies

for improving the point cloud; point cloud analysis; factors that affect scanning quality in other research papers; robot kinematics; 3D scanning parameters; and manufacturing digital thread and the point cloud smoothing.

1.2.1 Free-form Surfaces Inspection Methods

Advances in CAD/CAM have given manufacturers the ability to make complex and curved surfaces. With the demand for ergonomically designed parts that have multiple features and other organic shapes, traditional inspection methods may not be the right tool to use. The reason is that the surface being created from curves does not have a specific feature or shape. 3D laser line scanners are ideal for inspecting a free-form surface [14]. Free-form surfaces exist in many forms and fields around us from manufacturing and designing of molds and dyes and to the first clay models of products such as a car body. All CAD software has the ability to draw a free-form surface; this is important because it gives the ability to generate dimensional information and compares it with the inspection data. With the ability to make and machine a free-form surface, the demand for inspection arises. Inspection techniques for free-form surfaces are not as mature as they are related to products with regular features, like plane or cube. Future research on free-form surface inspection is predicted to focus on the development of techniques that give better accuracy and efficiency and reduce cost [13].

1.2.2 Computer Aided Inspection Planning

Past Technology

Research prior to 1995 showed the focus was on two and a half dimensional features, and the goal of the system for Computer Aided Inspection (CAIP) was tolerance-driven or geometry-based system driven [36]. The tolerance-driven CAIP system focuses on features that have specific tolerance requirements. ElMaraghy et al. [37] developed one of the earliest CAIP systems. The system depends on a knowledge-based approach in generating inspection tasks. The system was developed using purpose logic programming language and uses a feature oriented approach in modeling inspection. In designing the system, they considered the characteristics of the CMMs, the geometry of the object being inspected and the function

of the object in designing the system. Most of the research at that time focused on developing conceptual level CAIP systems for CMMs. These systems require inspection operator input for feeding the system the important inspection features to look for or tolerances that need to be checked. Geometry-based CAIP system focuses on planning how to obtain a complete geometric description of an object using the inspection data. Inspection of part surfaces is made automatically using a tactile sensor. The tactile sensor collects points on the part surface; then the measured data are aligned with the CAD design data model, and the error is calculated [38]. The system usually ignores tolerance information and focus is on the matching geometry between the designed shape and the inspected object. Geometry-based CAIP systems are not as widely used as tolerance-driven CAIP systems. Furthermore, geometry-based CAIP systems tend to acquire more data points and thus require more time; this caused the technology to become un-popular and made the industry search for an alternative [36]. The alternative way had to be more efficient to gather a large number of points in a short period of time such as 3D laser line scanners if they can be efficiently implemented [36].

Recent Technology

In the past 20 years, researchers have started to look for computer-aided inspection planning system with one or more modules. These include inspection feature selecting and sequencing, measuring/sampling point's selection and optimization, collision-free path planning and generation, and inspection execution [36]. On-Machine Inspection (OMI) has been widely preferred to directly inspecting in manufacturing and quality control. This feature is vital for an automated production system that identifies the error earlier in the machine and saves time for. OMI processes integrate design, machining, and inspection aspects of manufacturing and allow the product to be inspected and accepted on the machine while being made [36]. Inspection-related information, such as dimensions, tolerances and geometric items, are becoming available for use and can be retrieved from Standard for the Exchange of Product (STEP) model data and used in creating inspection process plans [36]. The technology used in this research is stand-alone and not installed on-machine; this will allow

the technology to be used to inspect a variety of products. Non-contact devices, such as 3D optical scanners, are gradually maturing for use in inspection. This kind of research has caused non-CMM measurement methods to become a major research trend [6]. Automated planning for free-form surface inspection for CMM and laser-scanning is becoming important as it reduces human involvement in order to make the process more time efficient and error free [13].

Inspection Methods Limitations

Laser line scanners can be used as a substitute for tactile probes for CMMs. The difference is that it is not touching the surface, but only the laser line is projected on the surface; it also has the ability to collect a larger number of data points compared to tactile CMMs, and has the ability to measure larger objects than CMMs. There are many types of CMMs, some with mechanical, optical, laser, or white light, and they are all used for inspection. Although both types are used as inspection tools and to generate dimensional information, procedures for evaluation differ between the CMM and laser line scanner. Therefore, error specifications with the scanners are difficult because there are many factors that influence scan quality such as surface quality, surface orientation, and scan depth. Nevertheless, there are benefits for using each type of inspection methods. Inspection methods can be contact and non-contact or a combination of both [13]. Contact sensors require touching the surface of the object in order to register the coordinates of the point. It has to take the measurements multiple times in different locations to have a data cloud of points that gives a dimensional representation. As mentioned previously, the CMM is an example. Li and Gu [13] mentioned that the visibility problem for a scanning system is similar to the accessibility problem for CMM; they both require planning and optimizing of the scan path. When using the CAD model, the important point to be inspected is generated based on the optimized path. Non-contact measurement systems are systems that gather points on the surface of the part by directing pulses of light and calculating the time it takes the pulse to return back to the sensor. These 3D scanners are categorized in terms of use and accuracy into two categories: Ranging/Terrestrial scanners and Triangulation/Shape scanners [27]. 3D scanners are used

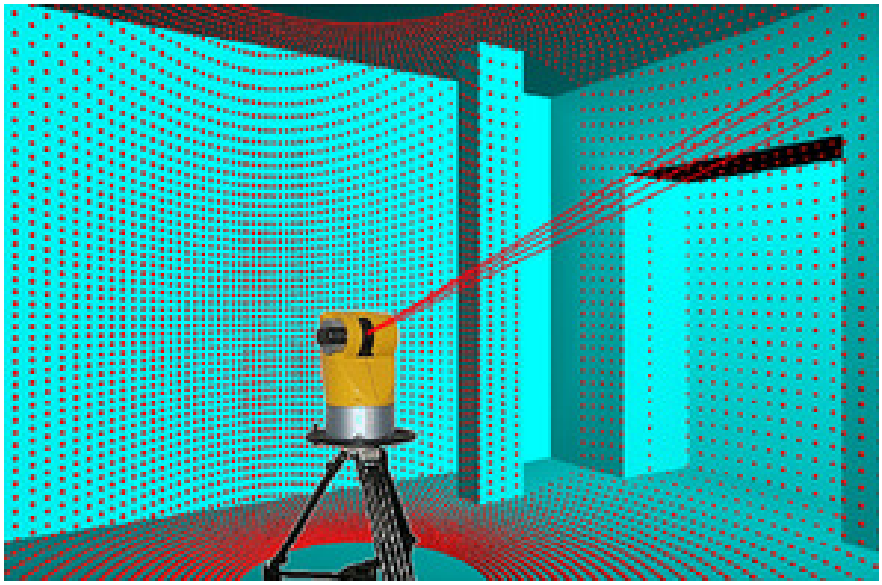

Figure 1.3: Bulk/Terrestrial scanners [2]

for Modeling From Reality (MFR) as you are gathering dimensional coordinates from an existing product or a clay model. Li and Gu [13] suggested that many non-contact inspections, human involvement is still required, which is a time-consuming technique. It is expected to enhance the accuracy of a non-contact measure approach by using higher accuracy sensors and optimizing the measurement parameter. 3D laser line scanners are important in quality control as they have the ability to scan from 50-100 times faster than CMMs [13]. There are two types of laser scanners; the first is ranging scanners - Bulk/Terrestrial scanners. This type of scanner is used for scanning large objects with low procession. It is used in many fields ranging from surveying in architecture, engineering, and construction (AEC) to preservation of cultural heritage [39, 40, 25]. Terrestrial scanners work by placing the scanner at the distance recommended by the manufacturer from the surface it is intended to scan. Pulses are released, and their time traveled to the object and back to the scanner is measured; the distances are calculated based on the time of travel, and a data point is recorded see Figure 1.3 [27].

Due to their being no uniform method for measuring the accuracy of terrestrial laser scanners and testing facilities until recently. The analysis works through different face poses

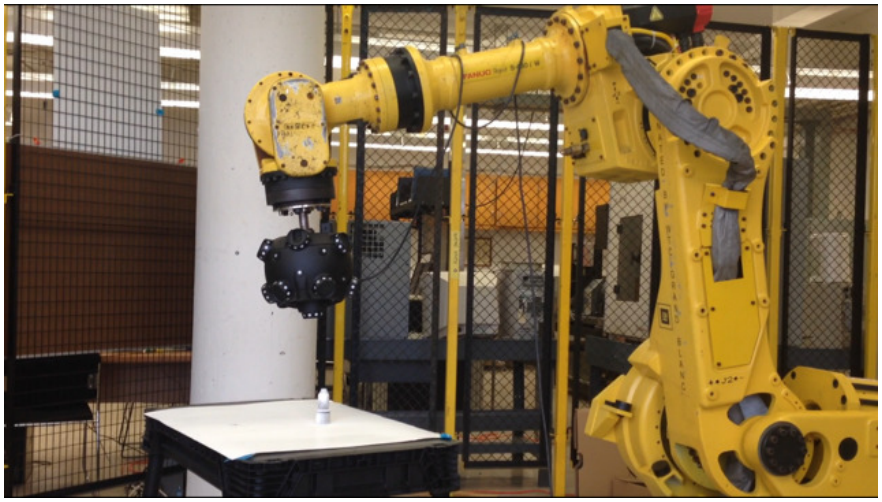

Figure 1.4: Triangulation scanners or shape scanners attached to a robot

using different scanners, compares the different scans together, and then ranks them by the accuracy and repeatability of the scanner [41]. In addition, the results and the technology are not the same as with dimensional laser scanners as terrestrial scanners have measurements errors of magnitude greater than shape scanners. Furthermore, manuals and pamphlets about product specifications should not be trusted; care given to the scanner and the the setup and calibration of single setup varies between one product to another and one scan to another [32]. The second type is triangulation scanners, such as shape scanners. This type of scanner is used for scanning with high precision. Unlike the first scanner, this scanner moves along the object it is going to scan, and a laser beam is projected on the surface of the part being inspected. A camera predicts the distance from the lens to the surface based on the shape of the laser beam, see Figure 1.4. This kind of scanner comes in single camera solution - double camera solution [27]

Unfortunately, there haven't been many complete studies on the triangulation scanner as there have been for ranging scanners. There have been multiple studies on small aspects in the scanning process. such as digitizing errors [4]; cleaning point cloud [5], effect of standoff distance and view angle [4, 6]; and generating a path [10]. However, there has not been a complete study of all the necessary parameters to be considered to have an accurate consistent point cloud and make the system able to be automated while mounted to a robot.

1.2.3 Point Cloud Quality for Contact and Non-Contact Inspection

The advantage of using a 3D scanner over a touch trigger probe is the ability to measure contactless and capture a large number of points in a short period of time. Touch trigger probes capture one data point per touch. In order for a touch trigger probe to capture the same number of data points that a 3D scanner collects it would take a long time and thus makes the technology infeasible. On the other hand, the disadvantage of laser line scanning at the moment is its limited accuracy and the strong influence of the surface quality on the accuracy. As it is difficult to inspect shiny surfaces such as machine steel and aluminum using a 3D laser line scanner [4]. Laser line scanners are less accurate than conventional touch-trigger probes like CMMs. While there are standardized procedures to evaluate the accuracy of touch-probe sensors, these are not appropriate for use with 3D scanners because error specification 3D scanners are difficult due to influencing factors such as surface quality, surface orientation, and scan depth that are not relevant in CMMs [6]. There is a need for standardized procedures to evaluate 3D scanner accuracy due to uncertainties in the 3D scanning such as surface quality, surface orientation and scan depth [6]. While it is known that the best view angle for scanning is when the scanner is normal to the surface, this is not always possible due to visibility problems [1]. The visibility problem for scanning systems is similar to the accessibility problem for CMMs [13].

1.2.4 3D Scanning Applications

There is a global demand for a freeform and ergonomic product that comes in complex shapes, but they are hard to design and require a long time to do so. Manufacturers are using reverse engineering techniques in product design to save time and shorten time for development by scanning existing shapes and modifying them [42]. They are also being used for remanufacturing purposes in which commercial laser scanners have been mounted on robots or CMMs and used for reverse engineering and re-manufacturing applications [4, 43, 44, 12]. It also has been used to reproduce existing components [23]. Manufacturers

have also been using 3D scanners to design molds for use by scanning the clay model of their first product, collecting the dimensional information and feeding it to CAD software in the design process. In this work the applications will use the technology as an inspection tool to gather the dimensional information for manufacturing and remanufacturing facility by collecting all the necessary points from the surface.

1.2.5 Strategies for Improving Point Cloud

There are two strategies for improving point cloud. Researchers have been addressing this in two ways. The first strategy is by working on the gathered point cloud and processing it to remove errors. The second strategy is by working on the scan parameters, and investigating the different parameters in an effort to understand their effects on the quality of the point cloud.

Point Cloud Processing

Cleaning of the point cloud is a necessity at this time. When manually scanning sometimes points are collected by mistake. These points can be the fixture of the part, a hand movement in the background, or a loose wire. Point cloud processing works after the point cloud is gathered to identify these outliers based on predefined boundaries and to clean the data. Researchers have been working on point cloud processing for many reasons.

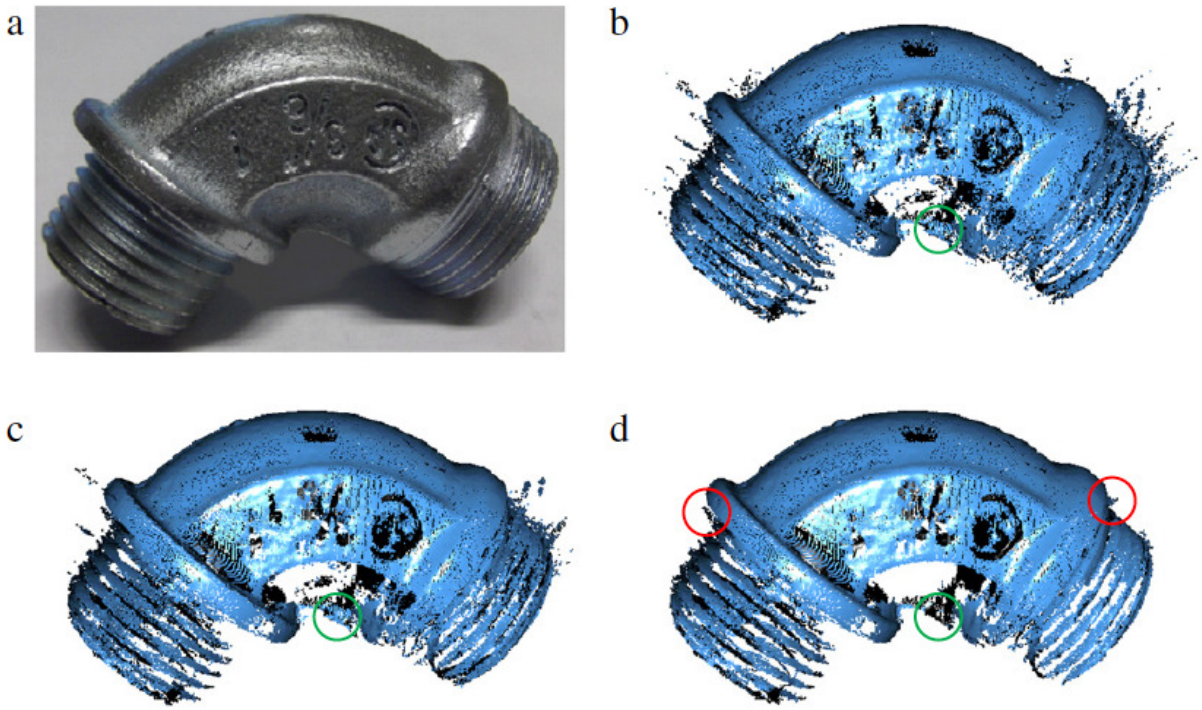

Figure 1.5: (a) picture of the part; (b) raw data collected by the scanner; (c) combined three method used in the literature; (d) the proposed method [3]

Wang and Feng [3] suggested that the collected point cloud is usually full of measurement outliers. They classified the outliers as sparse outliers, or isolated or non-isolated outlier clusters. They worked on developing a tool that works on all kinds of outliers. They suggested that the non-isolated outlier clusters are the most challenging to detect and current clustering methods will mix the non-isolated cluster with surface points, which will cause a noise in the gathered point cloud. They studied all the existing tools such as plane fitting criterion, miniball criterion, and nearest-neighbor reciprocity criterion [5], and they developed a tool that works on the data gathered by using the majority voting principle to make an improvement to the current outlier detection techniques see Figure 1.5. They suggested that the outliers are known to be associated with the scan path and it is possible to identify the outliers with redundant scans by changing the scan path.

Parameter Investigation

This strategy includes both parameter investigations that are related to the setup of the scan such as the view angel, standoff distance, as well as point cloud path planning.

Some researchers have studied the effect of in-plane and out-of-plane angles that have an important effect on the measured standard deviations because the measurement noise is mainly concentrated in the depth direction of the scanner. They have found that proper orientation while scanning can reduce outlier extensity and that outliers are dependent on the orientation of the scanner [6, 20].

Lee and Park (2000) [10] made an effort to automate the scanning process first by generating a path that considers all the accessible directions while considering the constraint in laser scanning operations. They made sure to fulfill the view angle, depth of view, in relation to the part, avoiding collision with the probe as well. They then calculated the number of scans and the most desired direction for each scan and generated the scan path that gives the least scan time. They suggested that the algorithm they used will enable automatic inspection by building a consistent and efficient scan plan. However, they concluded that the accuracy and efficiency of algorithms need to be further improved. Furthermore, the algorithm they used didn't take into consideration the shape of the part and didn't maintain the curvature of the part and distance while scanning.

Feng et al. [4] studied the effect of standoff distance and view angle on scan quality. In the experiment they mounted a commercial laser line scanner to a CMM robot. The experimental results showed that the random errors of the scan data are close to the nominal values provided by the manufacturers. Moreover, they found that there is a relationship between scan depth (standoff distance) and the projected angle (view angle) see Figure 1.6 [4]. However, they did not study the effect of speed on the scan quality, but this is an important factor to consider for the use of the technology as an inspection tool.

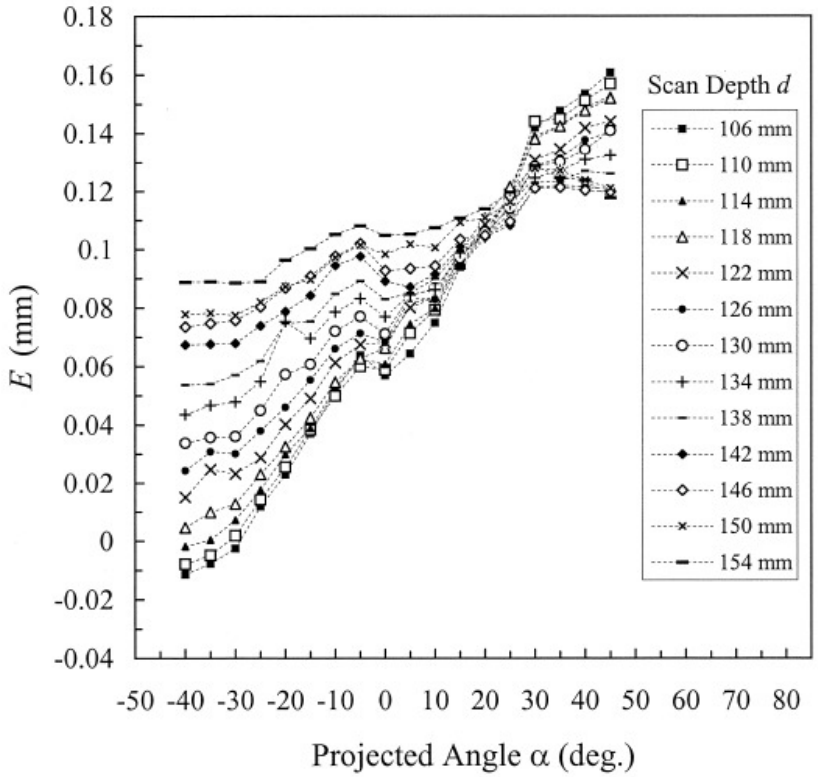

Figure 1.6: The systematic error of the scanned data in relation to the view angle and standoff distance [4].

Researchers have studied the digitizing errors of 3D laser scanners, and have suggested that the measurement is affected by object geometry and its position in the work window[4] . Other researchers have investigated the influence of surface reflectance, wetness, and color selection on the measurement of the terrestrial laser scanners and found that there is an effect from surface wetness, color selection, and material scanned on the quality of the point cloud measured, which has an effect on scan quality [45]. The accuracy information provided for the laser scanner by the manufacturers is generated for a controlled environment and thus cannot be generalized for the manufacturing environment [18]. Thus, there is a need to investigate the accuracy and test the equipment to generate general knowledge on the best use for the technology in order to mount it to a robot and automate it.

Although different parameters have been investigated in the literature by many researchers, there has not been a complete study on all the necessary parameters to be consid-

ered as in the automated scanning system. The resolution setting and the speed of moving the robotic arm are very important factors in automating the inspection process. If the speed of the robot is causing noise to the gathered data cloud, understanding the speed and the resolution effects are very important. Not knowing the effects of all the parameters will make optimizing the measurement and achieving the best path plan impossible.

1.2.6 Point Cloud Analysis

Most 3D scanning technology is improving steadily. However, most available scanning techniques still produce artifacts, such as noise, holes, outliers, or ghost geometry see Figure 1.7. Post processing is important for creating 3D model. The point cloud gathered from the available scanning techniques showed a demand for a scan cleaning tool to work on the acquired data points in order to create a digital 3D surface data. Weyrich et al. [5] developed tools that work directly on the acquired point cloud to clean and improve it. They also suggested that post processing of point cloud should be performed before surface reconstruction could be made (they called their tool a point cloud cleaning toolbox). The post processing of a 3D scan repair in point cloud is done by erasing irrelevant points, removing outliers, Smoothing MLS, and doing point relaxation, MLS spray scanning, and automatic hole fitting. It is challenging to scan a part and compare it to a point cloud as shown in [32]. Points collected with a contact system were faster and easier to deal with in processing due to the homogeneity of the points collected and the amount of points [1].

There are two methods of alignment between design and measurement data. The first is automatic, where best fit and features are based on the alignment of the object. The second is semi-automatic, where users need to do an initial alignment by manually arranging the design model and closely measuring the data. Then, the system will do the remainder of the registration operation. There are multiple commercial packages used for inspection and comparison of contact and noncontact measurement. Most can handle free form surfaces; however, user interference is often required. These packages have the function of inspection and comparison. Some of the popular brand names for packages used for inspection are:

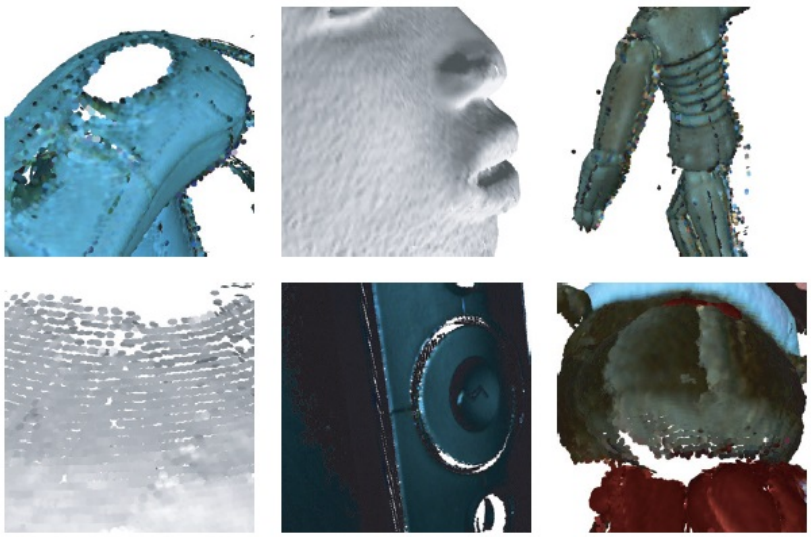

Figure 1.7: Scanning errors "Typical artifacts of raw scanner data. Top Row: Holes due to sensor restrictions, noise, outliers. Bottom Row: Low sampling density due to gracing sensor views, low sampling density at delicate surface details, and holes due to critical reflectance properties." [5]

Polyworks, Rapid form, Geometric, Imageware, Metrics, and Spatial Analyzer [13].

1.2.7 Factors That Affect Scanning Quality in Previous Studies

The literature has covered factors that affect scan quality. Some are related to a free form surface while others are irrelevant to the technology used in this study. The best orientation is when the laser beam is normal to the surface. However, despite the effect of the change in the angle, this is not always possible as there will be some accessibility problem that will prevent achieving a normal angle [1]. Boehler et al. [32] investigated the accuracy of different terrestrial 3D scanners by having different test targets and comparing the quality of the measurement obtained. They studied plane surfaces with different reflectivity at different ranges and noise caused by the range or range effect on scan quality. The parameters they looked at were angular accuracy (view angle effect), range accuracy (standoff distance), resolution, edge effect, surface reflectivity (lighting), and environmental conditions (temperature). They designed their experiment by selecting a box and a sphere. The box studied the range accuracy, resolution, and surface reflectivity. The sphere to study

the angular accuracy since the way the scanner works is by changing the lens angle and the mirror in a fixed increment and collect points; when the angle increment is large, fewer details and resolution will represent the sphere. The experiment was done in a controlled temperature room at about 20 degrees C. However, the technology they used is different from the one used in this study as the application it is used for since in this technology the scanner is fixed. However, the similarity will be in the surface reflectivity, and the speed of movement if it is faster than the scanner capturing capabilities. Martins et al. [46] worked on a model to prove the effectiveness of automated laser line scanners and their ability to substitute manual scanning. They concluded that the technology can be used. However, it requires optimizing the number of viewpoints and the path to be taken in order to get more reduction in scanning costs and improve the performance of the system [46]. Manorathna et al. [18] showed that the angle of steepness affects the number of points collected, and thus the angle hinders the scanner ability to collect data points. In the experiment they compared the number of ideal laser lines that can capture around 1280 laser points when normal to the surface versus when it is on an angle. Li and Gu [13] suggested that the accuracy of the non-contact measurement approach is expected to be enhanced by optimizing the measurement parameters. Optimizing the measurement parameters comes after knowing the relationship that the parameters have on the scan quality. Without knowing this, it is difficult to get meaningful information. This led me to the importance of studying scanning parameters in order to know the relationship and define it. With all the development in the accuracy of these instruments, the most available scanning techniques cause severe scanning artifacts such as noise and errors in the scans that are not present in the actual model [5]. Thus, there is a need to study 3D shape scanner techniques. In recent years, some researchers have proposed to developing automated planning for visual or laser inspections [13]. However, in order to successfully develop automated planning for visual or laser inspections that does not produce artifacts or missing points and holes, there is a need to understand what causes the artifacts or outliers to avoid them. By experimentally testing the scan parameter and

its effect on the scan quality, a better automated system can be developed. There is a need for standardized procedures to evaluate 3D scanners accuracy due to uncertainties in the 3D scanning such as surface quality, surface orientation and scan depth [6]. In order to achieve a standardized procedure, there is a need to accomplish four tasks that will make it possible. First is linking the workspace of the robot to the scanner workspace. This will let me know the location of the robot on the surface of the part being inspected and will collect the right point cloud. The second task is designing an experiment with a systematically varied scan parameters to study the effect of the parameters on the quality of collecting point clouds. Third, is studying the effect of the parameters and the post procession application on the point cloud in the remanufacturing digital thread. Finally, is by studying the alternative for quality perdition by selecting the right parameters for the CT-Scanning application, which can be generalize for other scanning technology. In the experiment I studied factors that hindered me from getting a consistent and efficient scan plan to be able to get quality scans with the least amount of noise and outliers in the scan and the least amount of post processing effort to make a decision about the condition of the part. Thus, the interactions between the different scan parameters are important, and from the literature done, there has not been one complete study that provides the necessary knowledge to generate a scan path. Moreover, past studies do not provide quantitative details that can be used as constraints for future scan trajectory, but they were based on the best results for an individual setup. Because speed is an important factor in the manufacturing environment, Li and Gu, [13] suggested that the increasing of speed and using of higher accuracy sensors and optimizing measurement parameters to use the technology for inspection purposes should be fully explored, in the experiment I am going to test the effect of standoff distance, view angle, speed, and resolution and their effects on scan quality. While the investigation of the accuracy of different kinds of surveying scanners has been done, there is still need for results that can be generalized to be used as input for the industry for inspection purposes in order to get the best point cloud quality that is consistent and clear.

1.2.8 Robot Kinematics

Commercial laser line scanners can be attached to a robot or coordinate measuring machines (CMMs) for dimensional inspection, reverse engineering [21, 22], and remanufacturing [23]. Laser line scanners have an advantage due to their ability to gather many points in a short time with high speed, and high resolution, and without contact sensing [24]. This advantage has also attracted non-manufacturing fields due to its ability to scan without contact. 3D scanners are designed for different applications. There are scanners that are small and easy to transport and have the ability to run on a battery while others are bulky and hard to move. Other features are related to the ability of the scanner such as resolution, speed, field of view, and range limits. Also, scanners are not the same in their ability to scan when there is interfering radiation [27]. The Creaform MetraScan-R scanner is one that was be used for the work. It is a triangulation scanner that can scan medium to large objects such as a car hood or a door, and it provides the ability to move around the object covering the surface from all angles. Although laser line scanners can obtain many data points in a short period, there are challenges that hinder its use as an inspection tool in manufacturing applications. Currently the process is labor intensive. There is a need for development of automated laser line scanning system models to avoid the trial and error caused by manual scanning [12]. Since there is a lack of knowledge on the effect of the different parameters on scan quality, the outcomes of automating the process are not perfectly predictable. When scanning manually, it is difficult to keep track of all the details about the standoff distance and the view angle due to fatigue that occurs while holding the scanner and the inability to manually control it. Automating the process will make it possible to scan a specific part while keeping track of scanning parameters such as view angle and standoff distance by integrating it into the scan trajectory. This will result in consistently getting a complete point cloud that represents the surface each time. Martins et al. [46] worked on a model to prove the effectiveness of automated laser line scanners and its ability to substitute manual scanning. They concluded that the technology can be used. However, it requires

optimizing the number of viewpoints and the scan path trajectory in order to get more reduction in scanning costs and improve the performance of the system [46]. Previous research has developed algorithms that determine robot poses in relation to component surface [47], and the relationship between a six degree of freedom robot and laser line scanner with and without an external tracking device [17, 48, 49]. The length of the laser beam is considered as the stand-off distance between the component surface and the scanner; it is assumed to be constant [12] and in our experiment was set at 300 mm. Larsson and Kjellander [19] created an automated system with a turntable that captures the component surfaces automatically in the form of point cloud datasets by having a preprogrammed path with pre-determined scan parameters.

There have been few efforts focused on the points collected on the surface of an object in addition to the position and orientation of the robot end effector [33]. Deshmukh et al. [33] linked the automated laser line scanning system with the component surface and established the forward and inverse kinematic models that are required for advanced automated scan path planning. What is missing is the relationship between the component surface and the data gathered from the C-track and the relationship of the C-track to the data gathered.

The location of an external tracker such as the C-Track is a less explored area that is important to fully discover and understand in order to create a trajectory that fully covers the points in the inspection process and create a trajectory that saves time while fulfilling the purpose. Thus, knowing the kinematic relationship between the robot workspace and the location of the laser beam and the relationship between the robot workspace and the C-track workspace is important.

In our system the scanner collects data points by moving the robot from one location to another. The location of the scanner is registered by the C-Track in the data collection process. Knowing the kinematics of the robot and the location of the laser beam is important as it will link the two workspaces, the C-track and the robot.

1.2.9 3D scanning parameters

Previous studies have focused on some parameters that affect the cleanliness of the collected point cloud from the noise. Based on the nature of these parameters, we can divide them into two general categories: hard parameters and soft parameters. Hard parameters, such as view angle, standoff distance, and speed, would require a physical change while soft parameters, such as lighting, color, and resolution, require changes in the parameters that have no movement or angle or distance or speed change from the object being scanned. In this research, the main focus will be on hard parameters and only one soft parameter will be addressed, resolution.

Hard parameters have been the focus of several studies. Gistel et al. [6] along with Wang et al. [20] and Gerbino et al. [50] studied the influence of changing the view angle on the laser scanner 3D point cloud quality. Based on their observations, using different view angles resulted in different standard deviation of the collected points and, as a result, different scanning qualities [6, 20, 50]. In addition, Wang et al. [20] found that using an appropriate view angle can particularly reduce the outlier's intensity and improve the scanning quality [20].

Based on the findings of Martinez et al. [1], the best orientation is when the laser beam is normal to the surface. However, despite the effect of the change in the angle, this is not always possible as there will be some accessibility problems that will prevent having a normal angle. This was confirmed by a similar study done by Manorathna et al. [18]. They compared the number of points captured by the scanner when it is normal to the surface versus when it is on an angle. Based on their findings, best results are achieved when the laser beam is normal to the surface. Both Feng et al. [4] and Van et al. [6] studied the effect of the view angle in conjunction with the standoff distance on the quality of the collected point cloud. They did several experiments with different standoff distances and view angles as can be seen in Figure 1.8, and based on the results, both parameters had a significant effect on the scanning quality.

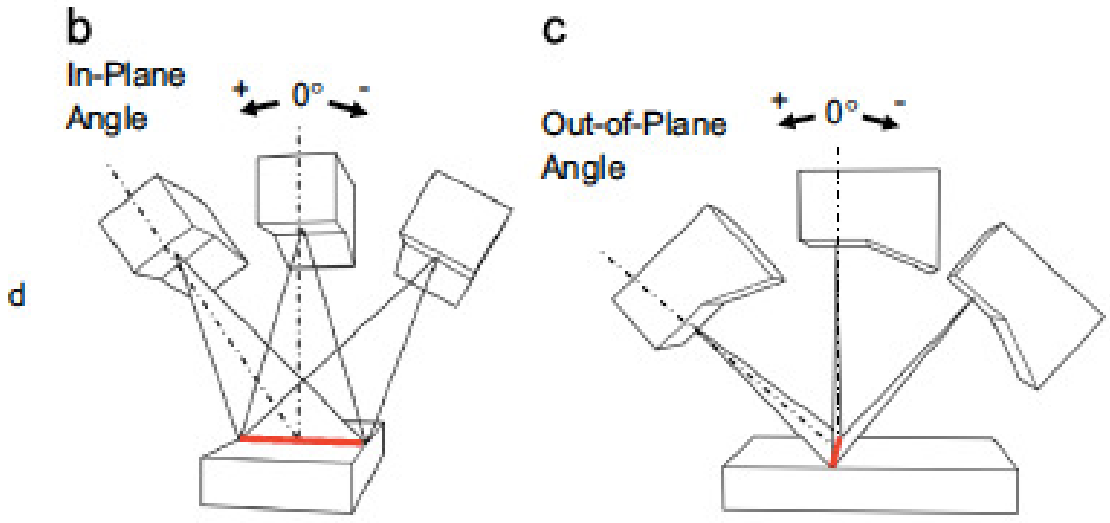

Figure 1.8: In plane and out of plane view angle [6].

On the other hand, some researchers have focused on the soft parameters. Blanco et al. [51] showed that different light sources have different impacts on the quality of a digitized surface [51]. This is particularly important when scanning a reflective surface such as machined aluminum. Rico et al. [52] studied another soft parameter named surface roughness. They introduced a measure called flatness value which is an index for the surface roughness. Their findings showed that using different flatness values results in changing the scanning quality [52].

Other researchers have investigated the effect of a combination of hard and soft parameters on the scanning quality. Vukavsinovic et al. [53] studied the influence of the view angle, distance, object color, and scanning resolution on the scanning quality. They suggested a set of guidelines to be followed in order to achieve a better point cloud quality. Based on these guidelines, it is important to maintain a uniform color and the right thickness on the whole surface when coating. In addition, the object being scanned should be as close as possible to the measuring sensor. Finally, the trajectory should follow the object geometry and maintain the same stand off distance to the object being scanned in order to reduce the noise generated. Bohler et al. [32] investigated the accuracy of different terrestrial

3D scanners by having different test targets and comparing the quality of the measurement obtained [32]. They studied plane surfaces with different reflectivities at different ranges and the noise caused by the range or range effect on the scanning quality. They examined several parameters including angular accuracy (view angle effect), range accuracy (standoff distance), resolution, edge effect, surface reflectivity (lighting), and environmental conditions (temperature). They designed their experiment by selecting a box and a sphere. The box was used to study the range accuracy, resolution, and surface reflectivity.

Moreover, some studies have focused on the general aspect of the feasibility of using 3D laser scanners as inspection tools and their efficiency. Martins et al. [46] worked on a model to prove the effectiveness of automated laser line scanners and their ability to substitute manual scanning. Based on their conclusion, this technology is applicable. However, it requires optimizing the number of viewpoints and paths to be taken in order to get more reduction in scanning costs and improve the performance of the system [46]. Li et al. (2004) suggested that the accuracy of the non-contact measurement approach is expected to be enhanced by optimizing the measurement parameters. Optimizing the measurement parameters requires knowing their effects on the scanning quality [13]. Without knowing these effects, it is difficult to obtain meaningful information. With all the development in the accuracy of the instruments, most available scanning techniques cause severe noise and errors in the scans that are not present in the actual model [5]. Although previous studies have investigated the effect of several parameters on the scanning quality as indicated in Table 1.1 at the end of the Introduction chapter on page 50, they did not cover two particularly important parameters, the scanning speed and resolution [53]. These two parameters should be further investigated before using the 3D scanning technology as an efficient inspection tool in the industry.

1.2.10 Manufacturing Digital Thread And Point Cloud Smoothing

Additive manufacturing is flexible with workpiece geometry and can be used when many other manufacturing methods cannot be implemented [60]. It has been shown that material deposition along with the complimentary operations can satisfactorily provide the

flexibility and agility needed to remanufacture high value EoL cores to original equipment manufacturer specifications [61, 62, 63, 64, 65, 66]. However, there are challenges preventing the technology from being the mainstream, such as production rate and cost of production [64]. This is because the deposition rate is slow, so making a single part requires hours or days depending on the size of the object. Thus, remanufacturing using additive manufacturing should be optimized to remanufacture a product that has higher imbedded energy as the time spent in longer than when using traditional manufacturing methods. Rickli et. al [9] made some progress towards describing the framework for salvaging failed builds and remanufacturing via additive manufacturing; however, significant theoretical and practical challenges still exist. In order to proceed with additive remanufacturing processes, digital translation of the physical shape needs to be captured [63]. This allows the realization of the defect and generates the appropriate corrective additive manufacturing procedure. While laser line scanners have been used more often for inspection and reverse engineering in industry [66], it is also being used for remanufacturing purposes where commercial scanners are mounted on a robot or CMM and used for reverse engineering and remanufacturing applications [4]. Because speed is an important factor in the manufacturing environment, Li et al [13] suggested the increment of speed, sensor accuracy, and measurement parameter optimization should be fully explored for technology implementation and to understand the effect that the speed has on the quality of the collected point cloud. Digital translation of a part is captured by a point cloud output from 3D scanning the surface of the object. The points are collected in Cartesian coordinate form and then converted to a mesh format. However, raw data from optical devices such as 3D laser scanner contain noise. Studying the effect of this noise and how it propagates within additive remanufacturing is essential to compensate for the error in meshing and slicing operations. Moreover, this will only reduce the errors to a certain extent and will give a better point cloud that have fewer errors. Smoothing a point cloud can be done by taking the original point cloud and applying the nearest neighbor algorithm to correct the noise in the gathered point cloud, though other

smoothing algorithms do exist. Rosli et. al [67] created a model that could adapt the density of the model based on bootstrap error estimation to avoid over smoothing using Bilateral Filtering. However, point cloud smoothing can eliminate some important features from the point cloud such as sharp edges. This is a common limitation for the point smoothing because it is based on averaging of neighboring points. With the additive remanufacturing model presented in this paper, it is essential that smoothing preserve the features of an end-of-use part that require reprocessing. Bi and Wang [68] summarize a general point cloud processing procedure that features six key steps. First, the point cloud must be filtered of noise and unwanted surfaces. Next, the point cloud is registered with a model to locate similar and dissimilar dimensions. Third, surfaces not fully captured by the scanner and/or lost in the noise filtering are reconstructed. Fourth, the point cloud is smoothed. Fifth, a feature detection algorithm is used to compare the scanned point cloud with model. Last, a data comparison tool is used to compare the model with the gathered data. While Bi and Wang [68] provide a useful strategy to process point clouds, variation still exists in each of their six steps, depending on the application. For example, Piya et al [69] demonstrate how their prominent cross-section (PCS) method serves to repair damaged turbine blades. The PCS method is an adjusted point cloud processing approach that groups the final four steps of Bi and Wang's [68] workflow into one algorithm. Although Piya et al [69] show a successfully rebuilt turbine blade, their method is limited to 2.5-D geometries. As mentioned in the introduction, multiple researchers have developed smoothing strategies that attempt to retain model integrity [70, 71]. Their strategies are tested on damage-free models; however, applications with damaged models could contribute to determining the effects smoothing has on the damaged regions. Brown et al. [60] investigated the nonsystematic translation errors on the digital design and their root causes on the steps of additive manufacturing by proposing feedback loops to ensure digital design integrity starting from tessellation all the way to toolpath generation. Brown et al. [60] focused on CAD to mesh in the additive manufacturing sequence. This literature is relevant as it focuses on the digital design integrity

for additive manufacturing, and since the technology that is used in this remanufacturing work are additive manufacturing the paper offers an additional aspect that is important regarding digital design data integrity. This paper attempts to propose a model for the effect of the point cloud data of each of the five steps in the remanufacturing process. These steps include scanning, smoothing, meshing, slicing, and material deposition. This paper covers the changes in the point cloud collected by the 3D scanner from the collection phase to the material deposition phase. As a result, it is critical to investigate the scanning process for the collection of the point cloud and the smoothing of the point cloud up until a satisfactory point cloud is achieved. The generated point cloud then can be used to proceed with the following steps in the remanufacturing activity while ensuring that the errors generated in these steps are determined to compensate for it in the following steps to achieve the desired results.

1.3 APPROACH

There are multiple tasks that were addressed to answer the proposed research question. This first task is linking the C-track workspace to the robot workspace and defining the relationship between the two workspaces as this is important to plan for the trajectory of the scanner and the point cloud reconstruction. The second task is to know the effect of the different scanning parameters on the overall point cloud quality. Knowing this will make it possible for future optimization of the parameters to be selected right in order to decrees the noise in the point cloud made by the process of the scanning as it was shown in the literature and the primary experiment it is very important to select the right parameter to eliminate or reduce the noise in the point cloud. In this task, experiments were conducted with systematical varied scan parameters. These parameters will be the view angle, standoff distance, speed, and resolution. The goal of the research is to establish the knowledge of the impact of measurement parameters on the scan comparing to the CAD model of the test object being scanned. This will lead to a good understanding of scan parameter effects on quality and inspection method performance that will allow for an automated inspection

system capable of capturing consistent, accurate, and clean point clouds. The third task was to study the effect the point cloud on the remanufacturing digital thread. The parameters of the 3D scanner can only be improved to a certain extent. The noises on the point cloud can be generated due to many factor other than the parameters. Therefore, in order to use the point collected form the 3D scanner for remanufacturing application. There is a need to clean the point cloud. This task follow the point cloud life cycle for the remanufacturing application and address all the processes that effect the point cloud such as the smoothing and cleaning the point cloud, meshing, slicing, and the actual material deposition and determine the sources of error and the extent of error from each step. The fourth task is to study the applicability of the implementation of predictive model to optimize the parameters of a CT-Scanner. As the parameter of the scanner need to be optimized in order to select the right parameters to select and get the best scan quality. For this task experiments were made with five parameters that are the voltage of the x-ray source, the current or the x-ray source, the filterer installed on the x-ray source, and the integration time of the CT-Scanner. The results were analyzed and the predictive model were found to be applicable.

1.3.1 Linkage of C-Track in the Kinematic Model

Automated Laser Line Scanning (ALLS) is used for inspection by collecting the point cloud of the surface and storing it to a computer. The elements of an ALLS system are a laser line scanner attached to a six degree of freedom FANUC S-430 IW robot and a computer to collect the point cloud and make the comparison [33]. Creaform MetraScan-R system contains a laser projector, lens, and image sensor. The reflection of the laser light on the measured surface passes through the lens and is recorded via the image sensor. It forms a triangle between the scanner and the object and the camera, see Figure 1.9, (i.e. triangulation). The (x,y,z) of a point on a measured surface is determined from the coordinate system of the laser projector, the coordinate system of the lens, and the coordinate system of the image sensor.

The link between the robot workspace and the C-track workspace is not known. The

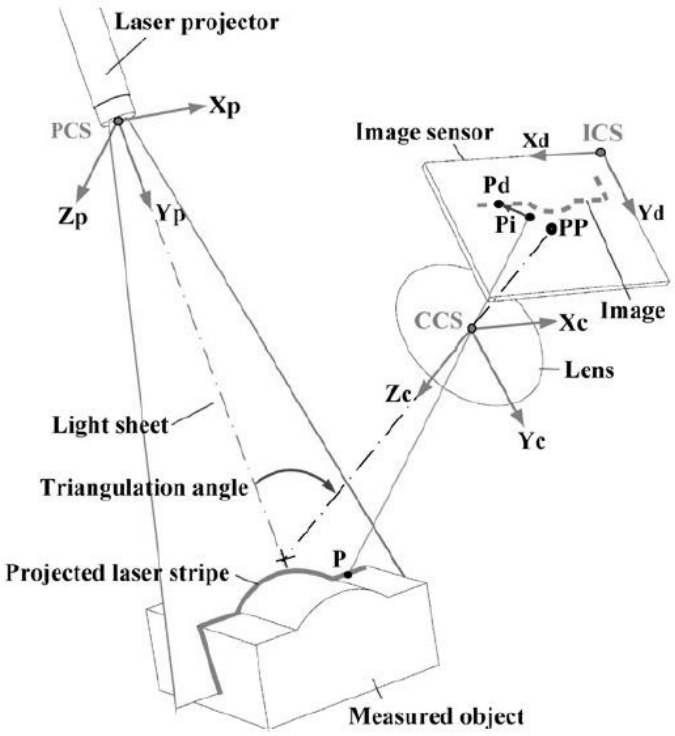

Figure 1.9: Point collection of general laser line scanners to be used as end effectors model [7]

scanner is running in the C-track workspace. The robot is running in the robot workspace. The relationship between the two workspaces must be known in order to design a trajectory that takes into consideration the dimensional information of the test object being inspected. In the model made by Deshmukh et al. [33] all the equations were defined in relation to the robot workspace including the component surface. However, the point on the surface and acquired point cloud collected by the 3D scanner cannot be compared because the relationship between the C-track (scanner) workspace and the robot workspace was not found. In this task I will select a specific point to scan and gather the data from the scanner in the C-track workspace, measure the location of the point in the robot workspace, and derive the equation for the kinematic relationship between the two workspaces.

1.3.2 Prediction of the Location of the Laser Beam

Using equations by Deshmukh et al. [33], I validated the model by creating a test board that has four points that are pre-selected. The location of the four points within the

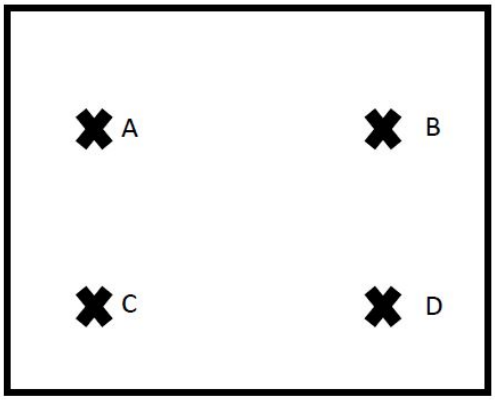

Figure 1.10: Point location validation board

robot workspace are known. Then, using the inverse kinematics equation provided from her model I derive the location of the robot end effector to have the laser beam exactly on the center of the points A, B, C, and D see Figure 1.10. After getting the laser beam on the point selected, the location of the point in the C-track workspace was be recorded for future reference to define the transformation matrix between the two workspaces.

1.3.3 Systematical Varied Scan Parameter Experiment

The objective of this task is to understand the impact of point cloud measurement parameters on scan quality. Collecting a large point cloud dataset with systematically varied scan parameters is important in understanding the impact of parameters. Automated point cloud measurement is critical to isolate all sources of variation that is caused by manual scanning. The approach that will be used to obtain a sufficient database is physical measurements using the automated point cloud measurement test bed in the engineering technology lab with varied scan parameters. In doing this experiment, six tasks are to be completed as the following sections listed below:

Understanding the Difference Between Vertical and Horizontal View Angles

Previous researchers have studied the view angle for scanners that have only one laser line [6]. In their test they studied the effect of vertical vs horizontal change in the view angle see Figure 1.11 and they found that there is an effect on the noise by changing the angle Figure 1.12.

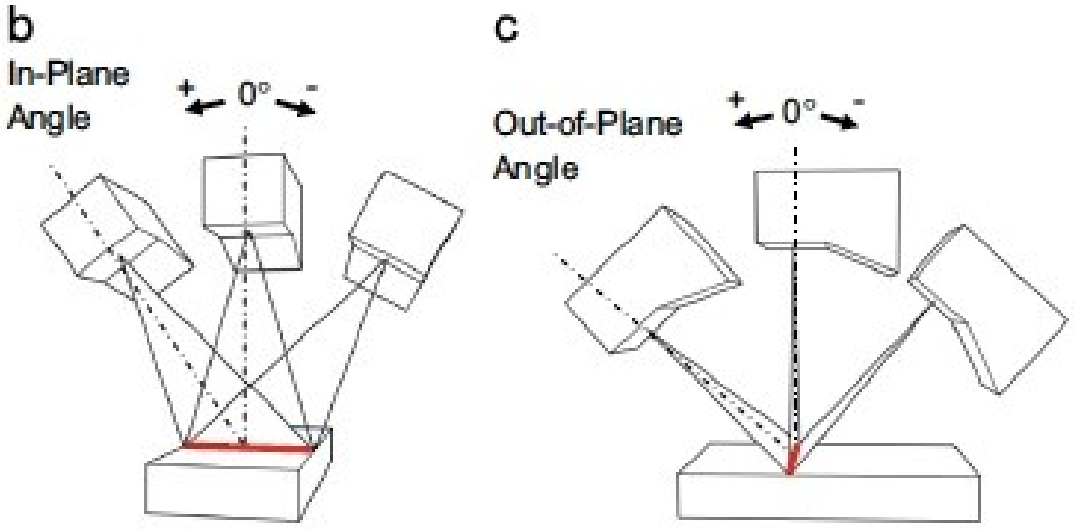

Figure 1.11: In-plane and out-of-plane view angle image [6].

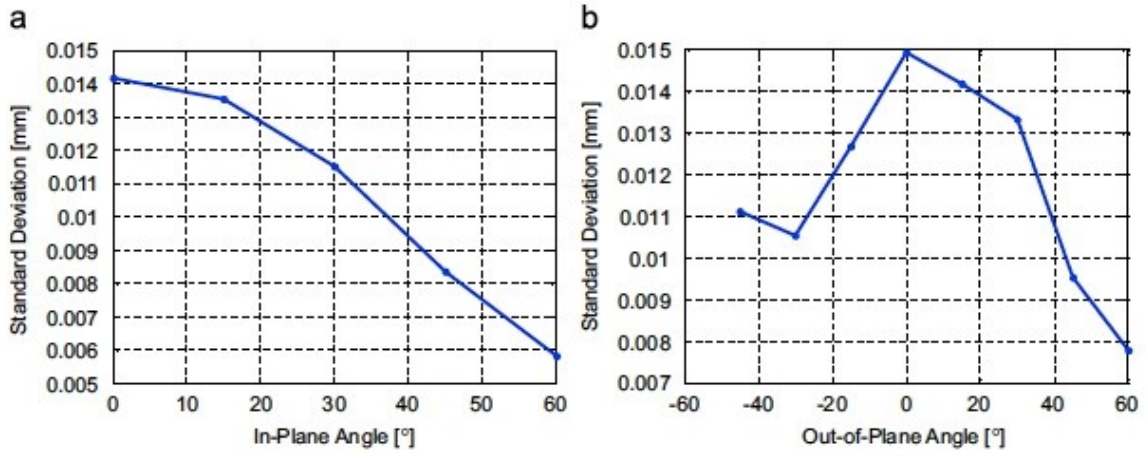

Figure 1.12: The effect of In-Plane vs Out-of-Plane angle image [6]

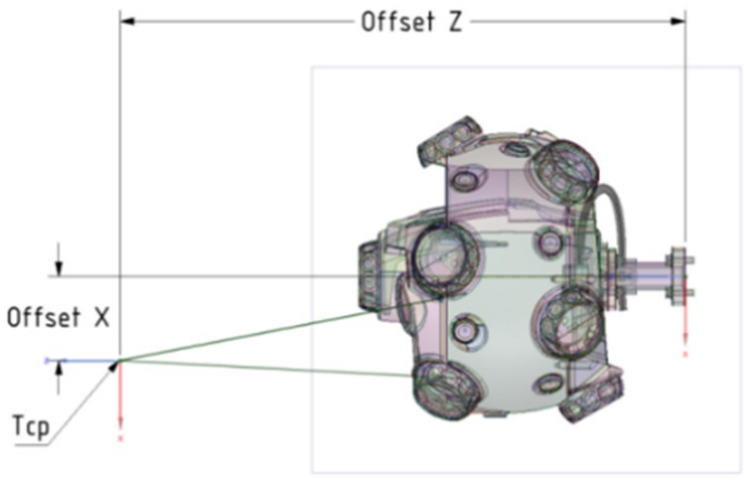

Figure 1.13: The used 3D scanner drawing from Creaform training materials

However, because there are two laser lines in the scanner used in my experiment, I would like to study if the results from the previous studies are relevant to this experiment, and thus whether the effect that the angle has on the scan quality for the vertical angle is different than the horizontal angle or if it is irrelevant in our type of scanner. In order to know if the results they received would be similar to what I would expect and to know the characteristics of the scanner, I repeated the experiments they performed exactly and compare the results for this reason and also to test the model used for comparing the point cloud in my experiment.

Since the shape of the scanner is not the same as the scanner they used, I will define the angle that is vertical from the scanner as the Out-of-Plane Angle. This angle is vertical to the two cameras on the scanner around the x-axis see Figure 1.12. The other angle is horizontal from the scanner as the In-Plane Angle around the y-axis. An experiment will be conducted, and three different view angles will be made to understand the effect between the vertical and horizontal angles. The three inputs parameters were 70 degree angle, 80 degree angle, and 90 degree angle. The previous study changed one factor at a time and compared the effect by the number of data points gathered using each view angle. However, I compared the results by running a simple one line trajectory to scan a flat surface. This is an important step as the outputs from this step will be given to the next experiment,

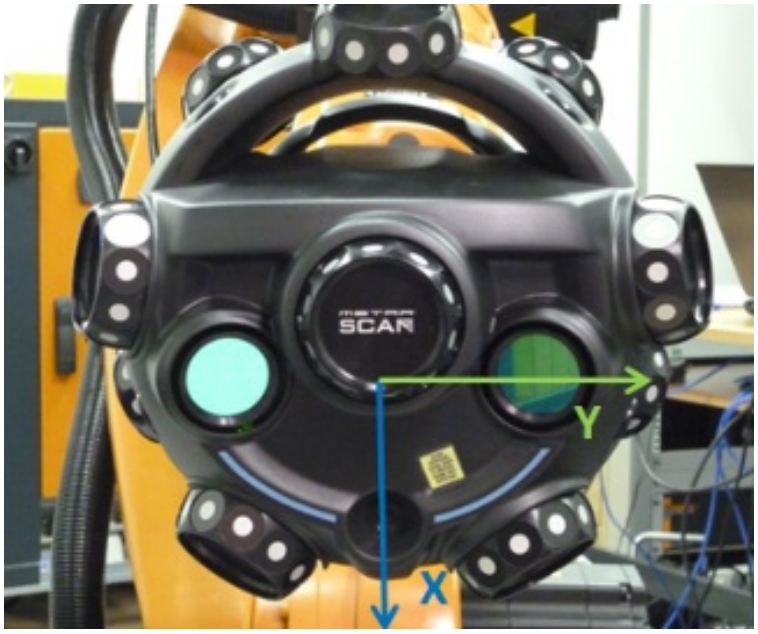

Figure 1.14: The actual used 3D scanner from Creaform training materials

which will involve multiple parameters with multiple levels. Knowing the importance of the orientation of the scanner is essential in order to generate the ideal trajectory to scan any part in the future. With hand held scanner, the two cameras are always on top, but when it is attached to the robot, the orientation is not being accounted for while moving. This test will define the importance of keeping track of the orientation of the scanner while scanning.

Designing the Trajectory for the Scan

In generating the trajectory, I used what ElMaraghy and Yang [29] did. Based on the CAD model of the test object selected, they decomposed the whole surface into different patches based on the view angle and standoff distance and generated a linear zigzag path to scan the patches. I created a tool with Matlab that generate the zigzag based on the dimension of the test object and the view angle and the standoff distance. The kinematic model will be added into consideration to know the location of the point that I am collecting, as it will contribute to the knowledge of standoff distance and view angle in designing the trajectory. The trajectory will then be programmed to the robot software which is ROBOGUIDE. The setting for the viewing and standoff distance will be added to the path in the program. Each setting will require a separate program to execute.

Setting Up and Designing the Point Cloud Measurement Test Bed

This test setup provided the required tools to investigate the effect of the view angle on the component surface, stand-off distance, and scan speed on scanning quality. Since Manorathna et al. [18] suggested that the accuracy of the information provided for the laser scanner by the manufacturers is generated for a controlled environment, it thus cannot be generalized for the manufacturing environment. The experiments were done in the manufacturing engineering laboratory with a setup similar to the manufacturing environment, and the robot used is similar to the robots used in industry to test the influence of certain factors. The robot that was used is 6-DOF Fanuc S430iw industrial robot Figure 1.15. The laser line scanner Creaform MetraSCAN-R is attached to the robot as the end effector and uses as external locating system separate from the robot location system to locate the laser line scanner and obtain the position in space of measured point (x,y,z) coordinates. In designing the test bed, I took into consideration the reachability of the component surface based on the limitation of the robot, especially the selected measurement parameters. This is critical as it insures elimination of user-induced system noise. The software that will be used for simulation is Fanuc ROBOGUIDE.

Figure 1.15: The robot attached to the laser scanner.

Designing a Component Surface Electronically and Material Selection

In designing the component surface, the first step is to design a similar surface electronically using CAD software. The CAD model will be then converted to triangles and points will be generated to represent the dimensional information of the part. In selecting the material to be used it is important to consider the surface finish of the test object. Specular, shiny, dark surfaces must be avoided because they generate spurious points that do not lie on the actual object surface [1]. Therefore, I used a white board with matte finish as the experimental components as recommended by Manorathna et al. [18] as it is the best surface to use in order to avoid noises in the measurement process. My goal in doing the experiment to test the parameters and surface reflectivity is not one of them. Thus, I should eliminate all factors that might affect surface reflectivity in order to minimize possible errors.

Designing An Experimental Component Surface And Fixture Design

It is crucial to design the experiment to reduce or eliminate the chance of having an un-controlled variation in point cloud measurement and inspection from unexpected source such as a complicated component surface geometry or surface reflectance. The goal of the

component(s) is to represent a benchmark surface able to characterize the effect of scanner view angle, stand-off distance, and scan speed on scanning quality. The selected component surface as mentioned will be simple, with three edges to test the effect of the characteristics. Once a scan path has been designed and generated for the experiment. It will remain the same and won't change for all the replication throughout the duration of the project to control the variation caused by the scan trajectory as much as possible since it is not under the scope of study. The experiment will determine the factors that affect the accuracy of the scan quality. This will also increase the quantifying effect of the parameter on the scan quality. The part selected is a flat work piece surfaces. This work-piece is a simple flat surface with no curvature or features to show the effect of changing the parameters.

Figure 1.16: Experimental Components Selected

Scanners run on a frequency in collecting data points, when scanning the same test object twice using the same path and parameter will not collect the exact same point twice but will collect points that represent the shape[32]. However, automation will reduce variation and improve consistency in the point cloud measurement. The first component, Figure 1.16, is a simple, flat surface with no curvature or features. The flat surface is selected for the experimental test object because it is trivial and does not contain any surface features also as recommended by Gestel et al. [6] artifact that are complex, which gives results that are difficult to analyze; also flat surfaces are easy and fast to scan and can easily represent the measurement task. Therefore, I used the flat surface for the experiment. A half-sphere won't allow me to study the effect of the factors one at a time since the sphere is curved; also, the scanner will be able to collect multiple points at multiple distances and view angles and won't show the effect as clear compared to the flat surface.

The Design of Point Cloud Measurement

Experiments performed with the automated point cloud measurement test bed will target four scanning parameters: (1) view angle of the laser line scanner to the component surface, (2) scanner stand-off distance, and (3) scan speed and (4) resolution. While there might be other parameters that are important that have an impact on point cloud quality, the focus will be on only the four mentioned parameters due to the expected improvements that these parameters will have on the point cloud quality by optimizing the parameters settings. The settings that were selected for each parameter tested are provide in Table 1.2. The values used are within the limits specified. The view angles values used for the scanner are within the limits specified, and the stand-off distance is within the minimum and maximum distance. The speed of movement was within the camera ability to capture. The resolution was within the camera's resolution ability. The experiment were conducted based on the plan provided in Table1.2.

Table 1.2: Parameters and parameter controls for the experiment

Parameter	Parameter Control	Number of inputs	Response
View Angle	Angle (di)	3	Quality (Q)
Stand-off	Distance (L-Pi)	3	
Scan Speed	mm/sec	3	
Resolution	mm	3	

In Table 1.2, the four parameters targeted in this research are controlled by four factors: the normality angle to the surface (di), stand-off distance (L-Pi), scan speed which is determined by the robot arm settings (mm/sec), and the selected scan resolution (mm). The study will investigate three normality inputs, three stand-off inputs, three scan speed inputs, and three resolution inputs. Normality input parameters will be the minimum angle, maximum angle, and normal to point surface. Stand-off distance inputs parameters will be the minimum distance, maximum distance, ideal distance. The scan speed input parameter will be high speed, ideal speed, and slow speed. The resolution parameter will be high resolution, ideal resolution, and low resolution based on the guidelines of the Creaform MetraSCAN-R

laser line scanner. The proposed multilevel factorial design for the experiment of the point cloud measurement experiments will yield eighty-one unique parameter combinations. The automated scan path for each of the proposed surfaces will be pre-programmed and will not be modified throughout the point cloud measurement experiments to reduce variation. However, there will be changes in the parameter being tested such as the laser line scanner normality, stand-off distance, scan speed, and the resolution parameters. All the parameters were be saved with the trajectory and loaded to the robot and ready for run prior to the experiment. In this experiment I had 81 runs. Each run took on average half an hour to conduct with a total running time for the experiments of 40 hours. Raw data were be collected along with the run order to look for variation or outliers if they exist in the process. The experiments took about two weeks once all the programming and setup were completed. Gestel et al. [6] mentioned that there are four parameters that define the quality of point cloud: noise, density, completeness, and accuracy. In their research they only studied noise and accuracy [6]. Lartigue et al. [35] suggested that noise is an indicator of data sampling errors and evaluated by the deviations between the points gathered and the surface model. The density is related to the point cloud density and the number of points collected that represent the part; the completeness is an indication or gaps in the point cloud; accuracy is an indication of measurement uncertainty [35] In my research I studied density, completeness, and noise. The data gathered from the test object were be compared to the data generated from the CAD model, the number of data points gathered does not affect the accuracy of the scan, but its coordinate will. I used the several measures including Mean Square Error (MSE) [32] . The mean-squared error (MSE) between two captured data c(x,y,z) and g(x,y,z) c is the data gathered from the CAD model and g is the data gathered from scanner. Boehler et al. [27] measured the quality by the deviation of a single point from the object's surface; in the process they noticed that while it is possible to record dimensional information of an object several times from different scanned points, it is impossible collect the exact same points in each time. Therefore, they collect the points then model it in a 3D shape, and

finally calculate the quality by the deviation of a single pint from each observation. Two strategies for scan path generation can be used. For the plane surface the global strategy was be used; it scans the test object all at once and maintains the same standoff distance above the artifact. However, this strategy might not fit right for other edged surface because there are multiple surfaces. The appropriate strategy to use is the multi oriented strategy where the artifact will be patched into small patches and scanned each patch individually on certain orientations, then travel to the other patch [1] .

1.3.4 Assumptions and Limitations

Limitations are the four mentioned parameters. In selecting the shape to scan and do the experiments on I selected the surface that is recommended in the literature that does not cause noise in the scanning process. different surfaces will not be taken into consideration. The same surface will be used in the two made models. I am not going to test different shapes other than the proposed shape as this shape test for what is need to know about the parameters. Moreover, this shape is supposed to study the parameters that I am testing and provide accurate results and thus the results might be generalized. While there is an effect on the surface reflectivity and the material used, I am not going to address this in the research, and it will not be within the scope of this work. In the literature it is recommended to stay away from using specular, shiny, dark surfaces because they cause noise in the gathered data [1]. It is recommended to use white and matte surfaces in designing the experimental components [18]. I followed these recommendations by MartÃŋnez and Manorathna [1, 18] in designing the test object. My assumption is that their recommendations will work with all 3D scanners, and by following their recommendations, I am reducing or eliminating the noise effect on the gathered data. There are factors that I am not going to investigate in the experiment, as these factors might add noise to the experiment such as signal radiation and the effect of sunlight in the experiment. All the experiment were made in the same setting in a similar time frame to reduce the variation that is caused by these factors. I also used one scanner calibration to reduce the effect of scanner calibration in the experiment. Results

were from the equipment tested and not general to all other devices and scanners.

1.4 CONTRIBUTIONS

There are four expected contributions that this work adds to the research knowledge and to the application field to achieve an automated inspection system. First is defining the relationship between the C-track workspace and the robot workspace this is necessary to know what is the point that is being collected on the surface and that it can be referenced in the robot workspace. The second contribution is on the role of the right parameter on the scan quality. The third is to show the error propagation in the point cloud for the remanufacturing process planning and how the digital thread is affected by the point cloud processing. The fourth is the use of the machine learning to optimize the scanning technology and predict the scan quality, the machine that was used in this work is CT-scanner.

1.4.1 C-track Transform and Model Validation

3D scanners digitally capture the shape of physical objects. Robots move the 3D scanner over the surface of on object to collect the point cloud of the surface, which are collected to form a digital representation of an object. In Deshmuk et al. [33] the component surface, robot, and scanner in three workspaces, but only the link that reflects the location of the component surface in the robot workspace was found. However, the point on the surface and acquired point cloud collected by the 3D scanner could not be compared because the relationship between the C-track (scanner) workspace and the robot workspace was not found. In this work, I derived the transformation for the robot space and C-track camera space to be able to know the location on the robot workspace that is derived by the 3D scanner. Knowing the relationship between all the workspaces is necessary for integrating the system and designing the Automated Laser Line Scanning systems (ALLS). Failure to connect the workspaces together will result in a disintegrated system. This will make me unable to use the gathered information about the component surface in designing a trajectory to scan a specific test object, or know the location of the test object in relation to the robot and the accurate location of the scanner. After linking the coordinate of the component

surface with the coordinates of the robot in the robot workspace, I will validate the model by comparing a single point on the surface with single point cloud point on the gathered scanned data. In this experiment I used a FANUC S430i robot, a Creaform MetraSCAN-R scanner, robot offline programming software such as Roboguide will be used to program the robot as well as the kinematic models that connect the component surface to the robot workspace [33] and a test object to validate the proposed link between the robot workspace and the component surface. Validating the model will provide the ground work to build upon for future applications with the ALLS, and this will make it possible to have an integrated system capable of knowing the points that should be visited in order to collect all the necessary points on the component surface. There are assumptions made in modeling the kinematics equations, one of which is that the laser beam is in the center of the scanner and at a specific distance from the robot end effector. However, in the actual scanner the laser beam is not located in the center of the scanner it is displaced from the center. This requires the model to be modified to fit the actual scanner. This is a necessary step to make as it will validate the model as well as it will like the C-track and robot workspaces. This work will be the basis for future applications with the 3D scanner. By knowing the relationship among all the workspaces, we will be able to design a system capable of identifying the location of the surface that was missing in the scan and to revisit it in the inspection process. It is essential to know where the defect is located exactly on the component to then easily revisit a specific area on the test object just by feeding the point to the robot.

1.4.2 The Role of the Right Parameter On the Scan Quality

The outcome of this research task is to find the effect of different parameters on scan quality. This is important as it works as the input for future optimization tasks and also for programming future scan paths [46, 72]. The long-term goal of the tasks is to develop an initial step towards 100% on line point cloud measurements in manufacturing systems. It will make the technology practical to advance the field and practice of manufacturing quality monitoring as it reduce the amount of noise and will increase accuracy and consistency in

the point cloud. It will also save time in the inspection process and make the technology appealing for the manufacturing industry.

1.4.3 Error Propagation in the Point Cloud for Remanufacturing Process Planning

In this research the sources of errors in the remanufacturing digital thread for additive manufacturing were studied, and the overall error was measured in different steps, starting from the scanning error after reducing the error by selecting the right parameters, to the error that is generated from smoothing and cleaning the point cloud, to the error generated from meshing the point cloud of the scan for measuring the amount of the defect to generate the correction plan for the material deposition, to the error of slicing in the plan for the movement of the material deposition, and finally to the error generated by the actual manufacturing and material deposition. The errors were calculated for the scanning phase, the smoothing phase and the mathematical models. Errors were found in the scanning, smoothing, meshing, and slicing.

1.4.4 Using a Predictive Model to Optimize the Parameters of a CT- scanner

The final goal of this research is to test the use of machine learning in predicting the scanner parameter. This research was conducted on a different type of scanner a CT scanner, which shows both the surface structure as well as the internal structure of the part. This can lead to a tool that can be integrated into a different scanner. In our case this can be integrated into the CT scanning software in which users would be prompted to input the approximate density and thickness of the item to be scanned. The tool would use our prediction models as a basis for simulating scan parameters and output a set of recommended parameters. The preliminary testing of the accuracy of the prediction shows that the model can be used as a prediction tool for the CT scanning application.

Table 1.1: Literature Review of Different Factors

Paper	View Angle	Stdff distance	Speed	Resolution	Color	Accuracy	Glossiness	Ambient light	Material	Geometry	Roughness	Laser intensity
Zaimovic et al. (2010)[54]	-	-	-	-	X	-	X	-	-	-	-	-
LemeÅą et al. (2009) [55]	-	-	-	-	-	-	-	X	-	-	-	-
Voisin et al. (2007) [56]	-	-	-	-	-	-	-	X	-	-	-	-
Voegtle et al. (2008) [57]	-	-	-	-	-	-	-	-	X	-	-	-
Lichti et al. (2002) [58]	-	-	-	-	-	-	X	-	X	-	-	-
Gerbino et al. (2016) [50]	X	-	-	-	-	X	-	X	-	-	-	-
Wang et al. (2016) [20]	X	-	-	-	-	-	-	-	-	-	-	-
Gestel et al. (2009) [6]	X	X	-	-	-	-	-	-	-	-	-	-
Feng et al. (2001) [4]	X	X	-	-	-	-	-	-	-	X	-	-
Blanco et al. (2009)[51]	-	-	-	-	-	-	-	X	-	-	-	-
Vukasinovic et al. (2010) [53]	X	X	-	-	X	-	-	-	-	-	-	-
Cuesta et al. (2009)[52]	-	-	-	-	-	-	-	-	-	-	X	-
Popov et al. (2010)[59]	-	X	-	-	-	X	-	-	-	-	-	X
MartÃŋnez et al. (2010) [1]	X	-	-	-	X	-	X	-	-	-	-	-
Martins et al. (2005) [46]	X	X	-	-	-	-	-	-	-	-	-	-
Li et al. (2004) [13]	-	-	-	-	-	-	-	-	-	-	-	-
Weyrich et al.(2004) [5]	-	-	-	-	-	-	-	-	-	-	-	-
Manorathna et al. (2014)[18]	X	X	-	-	-	-	X	-	-	-	X	-
Boehler et al. (2003) [32]	-	X	-	-	-	-	X	-	-	X	-	-
Alkhateeb et al. (2019)	X	X	X	X	-	-	-	-	-	-	-	-

CHAPTER 2: LINKAGE BETWEEN MEASURED AND COLLECTED POINTS WITHIN THE SCANNING PROCESS FOR THE INTEGRATED AUTOMATED LASER LINE SCANNING INSPECTION SYSTEM

2.1 Abstract

3D laser line scanning is a cutting-edge technology that digitally captures the shape of physical objects. 3D laser line scanner is skillfully designed and mounted onto the robot (FANUC S-430 iW) to automate the scan path and quality inspection processes. The robot's primary function is to transport the 3D laser line scanner above the surface of an object to collect point cloud datasets of the surface. Point clouds of the surface are collected and form a digital representation of an object. The kinematic relationship between the component surface of the part being scanned,the robot, and the scanner were previously derived. However, the location of the point on the physical surface and acquired point cloud collected by the 3D laser line scanner cannot be compared because a relationship between the robot and scanner workspaces was not found. In this work the transformation of the robot workspace and the scanner workspace was derived (C-track camera space) to be able to know the location of a point being collected on the robot workspace. Knowing the relationship between all the workspaces is necessary for integrating the system and designing an Automated Laser Line Scanning system (ALLS) with an external tracker. It will help in trajectory planning for the 3D scanner, which can lead to an autonomous system capable of automatically scanning and collecting points. Failure to connect the workspaces together will result in disintegrated systems, which would limit the ability to design a trajectory to scan a specific part, or know the location of the part in relation to the robot workspaces and laser line scanner.

2.2 Introduction

3D scanning is recognized as an advanced technology used for speed, accuracy, and coverage. With automated 3D technology, users can improve quality and compliance without

slowing down production. The processes used for 3D scanning make it faster to scan a part with complex dimensions while reducing time consuming orientation and alignment processes. As a result of remanufacturers encountering high uncertainties in component quality and factors related to sustainability, it is necessary to incorporate this advanced technology for the effectiveness and efficiency of quality inspection and condition assessment operations. By understanding the relationship of the missing links, which are the location of the C-track in the robot work cell and the point that is being collected, a trajectory can be created that takes into consideration points collected from one location to the next, which in turn allows users to make careful predictions. Within the automated system there are several components that contribute to the function of the automated scanning system. The components utilized consist of the robot, laser line scanner (Creaform MetraScan-R), and the C-track. The C-track has dual camera sensors fitted with high quality optics and lighting, enabling it to measure all reflectors in the parameters of the workspace. Besides the tracking capability of the whole systems reference model, the C-track ensures the exact localization of the laser line scanner (Metra Scan-R), in turn offering high end automated scanning solutions like scan trajectory optimization algorithms and optimized meshing output. There has been considerable research on automated scanning systems regarding path planning strategies [19]. However, there is no exact solution to explain the relationship between the robot and the C-track. Systems with encoders linking the robot arm and the scanner do not require this relationship. The relationship between the C-track and robot are required here because the C-track is external and independent of the robot. The relationship of the two is very important for this research because it will integrate the zero position of the C-track compared with both the end effector and the base frame of the robot. Knowing the location of the C-track is very important as when the area being scanned is in front of the C-track it can be reached by the robot. However, when the end effector is at this position it is causing an occlusion to the C-track. Thus, this area can't be scanned, so the locations shouldn't be considered while planning the trajectory, but another end effector view angle should be

considered. In this study, the link between the measured and collected points in the scanning process was investigated. To do this, the location of all the components in the workspace were taken into consideration. These components are the center of the robot, the kinematic model of the robot, the location of the end effector, the location of the end of the laser line scanner, the location of the laser beam in the space, and finally the location of the C-track in the work cell. These models establish an understanding of the relationship between scanning procedures and measured point cloud datasets and are the foundation for automated laser line scan monitoring and assessment. In the absence of these models, laser line scanning would continue to be a time and resource intensive monitoring and assessment strategy and have little relevance except in single workspace instances. The long-term goal that this research contributes to is to transform quality monitoring methods in new product manufacturing and condition assessment methods in remanufacturing operations. This can only become possible through laser line scan automation and scan trajectory optimization. However, efficient automation and scan trajectory optimization require a fundamental understanding of the kinematics of automated laser line scan systems (ALLS). After linking the coordinates of the component surface with the coordinates of the robot in the robot workspace, the model will be validated by comparing a single point on a surface with a single point. This experiment uses a FANUC S-430Iw robot, a MetraSCAN-R laser line scanner, robot offline programming software (Roboguide, Robcad, Workspace), and a test object to validate the proposed link between the robot workspace and the component surface. Validating the model will provide the foundation for future applications with the ALLS, and this will allow us to have an integrated system capable of knowing the points that should be visited in order to collect all the necessary points on the component surface. This work will be the base for future applications with scan path planning for 3D laser line scanning. In CMMs and other types of measuring systems there is a direct link between the internal moving system or the robot arm and the external scanner. In the scanning process the point cloud is encoded with the location of the point being collected. However, in the current system these two

components are not linked, which makes it challenging to predict the point to be collected by moving the robotic arm from one location to another without connecting the C-track and robot workspaces. The knowledge that will be gained from this work will make it possible to encode the point collected by the laser line scanner to the movement of the robot arm. The location of the reference frame of the C-track is also determined. In this experiment the zero frame of the robot and the C-track is measured while using all the tools needed to know its location precisely. All these steps and the outcomes of this work will improve trajectory planning for 3D laser line scanning.

2.3 The Current System

3D scanners have been mounted to robotic arms or other types of mechanical devices such as CMMS in an effort to automate the data acquisition process and inspect a part [21, 22]. This will substitute the old way of manual data acquisition which generates an inconsistent point cloud that cause noises and variability in inspection processes. Mounting the scanner to a robot with an external track results in two disintegrated workspaces The robot moves in the robot workspacem and the scanner moves in the workspace created by the C-track.

To my knowledge, this has not been studied before. It is important to find the relationship between the points that are being collected and the location of the scanner in the workspace because this will allow for the creation of a scan trajectory based on the feature of the part being inspected.

2.4 Elements of the Automated Laser Line Scanning System

The Automated Laser Line Scanning System (ALLS) studied here consists of a laser line scanner attached to a six degree of freedom FANUC S-430 IW robot as the tool frame, a robot controller, a program to move the robot, cables, a scanner controller, C-track, a power supply for the scanner, a computer, and software to collect and process the data points collected.

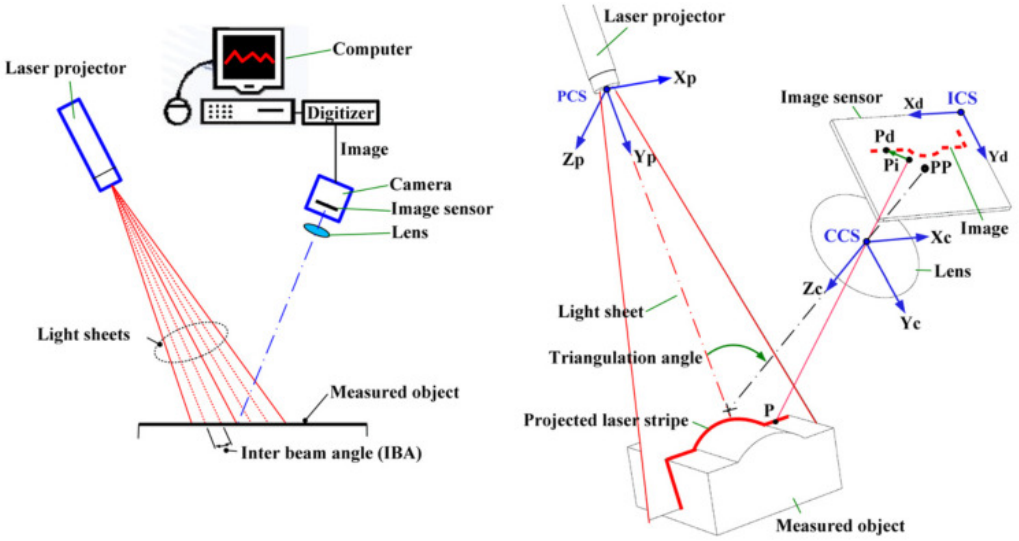

Figure 2.1: Point collection of general laser line scanners to be used as end effectors model (image from Bracun et al., 2006) [7]

2.4.1 Laser Line Scanner

As mentioned in Deshmukh et al. [33], the Creaform MetraSCAN-R scanner operates by the steering of laser beams, followed by a distance measurement at every pointing direction. A 3D laser scanner consists of a laser, a ranging unit, a control data unit, and a location tracker (C-track). The laser unit produces the laser beam that is needed for measurement. The ranging unit determines the distances and angles. When a laser stripe projects onto a surface of a component, the reflected beam is detected by cameras; this determines the distance based on the shape and speed of the reflection. The Creaform MetraScan-R system contains a laser projector, a lens, and an image sensor. The reflection of the laser light on the measured surface passes through the lens and is recorded via the image sensor. It forms a triangle between the scanner and the object and the camera (i.e. triangulation). The (X, Y, Z) of a point on the measured surface is determined from the coordinate system of the laser beam, see Figure 2.1. However, in our system the locations of the points are determined in relation to the location of the C-track.

The link between the robot workspace and the camera workspace (C-track) is not known. The scanner is running in the C-track workspace. The robot is running in the robot

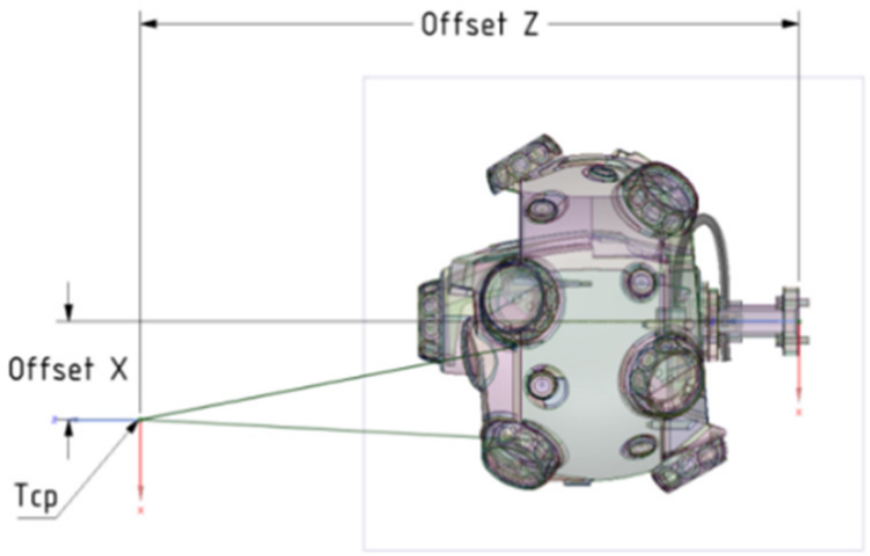

Figure 2.2: Offset of the Creaform MetraSCAN-R laser line scanner MetraSCAN training PPT)

workspace. The relationship between the two workspaces has to be known in order to design a trajectory that takes into consideration the dimensional information of the test object being inspected. In the model made by Deshmukh et al. [33] all the equations were defined in relation to the robot workspace including the component surface. However, the point on surface and acquired point cloud collected by the 3D scanner could not be compared because the relationship between the C-track (scanner) workspace and the robot workspace was not found.

2.4.2 FANUC S-430 IW Robot

The FANUC S-430 IW robot arm has six joints with six degree of freedom. The kinematics of each of the joint will be shown in the kinematic section (J1, J2, J3, J4, J5, and J6). The scanner is attached to the robot end effector J6 as a standoff distance. This distance is to account for the laser beam and the dimensions of the scanner. The tool center point of the laser scanner is defined in the tool frame to create a Z-offset that is the distance from the end of robot arm to the scanner end effector, see Figure 2.2.

2.5 Approach

In this experiment, tools such as a water level device, protractor, and laser pointer were used to measure and identify the angles and distance between the components in the work cell. First, the kinematics model for the FANUC S- 430 iW robot was validated by using the model suggested by Deshmukh et al. [33] as well as by adding the dimensions of the scanner and the laser beam along with the physical model. A simple program for the robot was created to locate a point on the work space. The scanner was left collecting points until enough data points were collected in the intersection between the two laser beams. In order to get accurate measurements and a collection of point cloud datasets that represent a specific point, the robot was in static mode and was not moving, which made it challenging to collect points. The point clouds collected were saved in a text file with three taped columns. To locate the reference frame for the C-track, another experiment was done, a manual scanning to determine of the actual axis (X, Y, and Z). The first step for the manual scanning was to scan the floor in the X-axis. Then a manual scanning for the Y-axis was done, followed by the Z-axis. After collecting the cloud measurement data, the data was plotted to determine the desired point for the actual study and further references. Moreover, the data gave a better reading for the axis of the research that was done earlier. The manual scanning showed the differences in X-axis, Y-axis and Z-axis, which made it clear that the reference frame for the C-track is between the two cameras in the C-track. Thus, the calculation for the location of the C-track used earlier will be the same in both cases, making it possible to predict the points to be collected by the scanner based on location of the C-track in a specific position with a specific orientation.

2.6 Methodology

The 3D scanner was attached to the end effector of Fanuc S- 430-iW and the C-track was placed on the negative Y-axis of the robot world frame Figure 2.3(a).

The distance between the robot and the C-track was measured using a measuring tape Figure 2.3. Also, the distance between the C-track and the Laser sensor that was attached

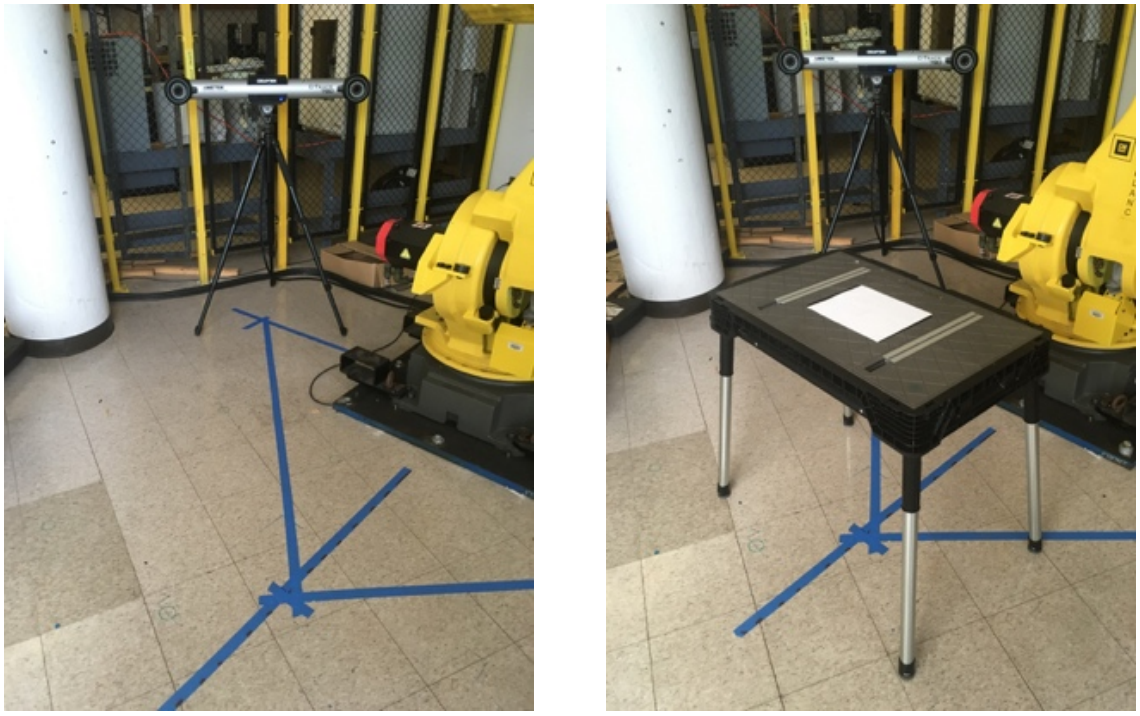

(a) (b)

Figure 2.3: The workspace of the robot (a): without the table (b): with the table.

to the robot's end effector was measured Figure 2.6. The robot was calibrated and set to the zero position for exact measurement Figure 2.4. Then, validation was performed on the robot to check the zero position using the kinematic model of the robot and compared with the actual data collected from the robot controller using the Teach Pendant see Figure 2.5.

The kinematics equation was implemented in Maple 17 to get the end effector position. After that, the MetraScan-R was attached to the end effector of the robot and the dimensions of the laser scanner were taken into account along with the standoff distance for the laser beam, the kinematic model that represents the actual setup was developed, Figure 2.5.

In Figure 2.4, A blank sheet of paper was placed on the test bed underneath the laser beams to test the trajectory, and the laser sensors were placed within range of the C-track in order to collect the point cloud datasets.

The distance between the laser sensor was then measured using a measure tape in order to validate the measurement in Maple 17 later on. Moreover, the workspace was measured and marked using tape for more accurate position repeatability of the process,

Figure 2.4: The robot calibrated and set up at zero position without the Scanner installed

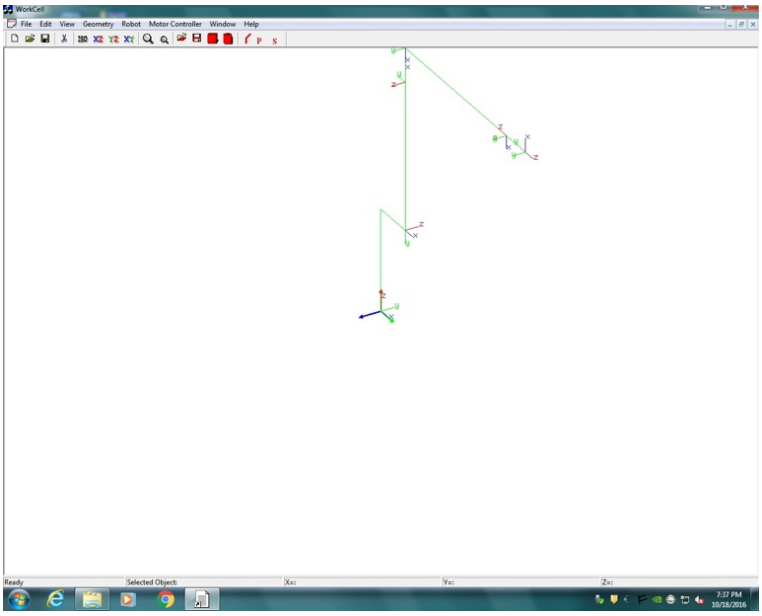

Figure 2.5: Drawing the representation of the robot kinematics Djuric, (2007) [8]

(a) (b)

Figure 2.6: The robot calibrated and set up at zero position with the scanner installed and the table placed with the laser beam in the zero position

Figure 2.6.

2.7 Kinematic Model and the Relationship between the C-track and the Robot Reference Frame

The relationship between the C-track and the robot reference frame was derived using forward kinematics and validated physically on the actual robot. To know the location of the robot end effector, the location of the laser beam on the workspace was noted along with the measurement of the 3D scanner, Figure 2.7. Using kinematic equations for six degree of freedom FANUC S430 IW, the robot end effectors was moved to a fixed point named the home position. The joint angles of the robot ($\theta 1 - \theta 6$) were determined while taking into consideration the limitation of the joints and validated with the actual robot based on research by [73, 74] while ensuring that the selected position for the home position was not in singularity[75]. The home position using the equations and the actual space of the robot in the work cell for FANUC S-430 IW robot with the model obtained by [74] was validated. Work by Deshmukh et al. [33] work was extended by incorporating the location of the C-track to the location of the point on the surface determined by the laser beam by using forward kinematic equations to obtain the validated position for the FANUC S-430 IW robot, laser scanner, and laser beam. The robot was calibrated and set to the zero position then joint 5 was moved -90 degrees to the ground see the robot D-H Parameters Table 2.3.

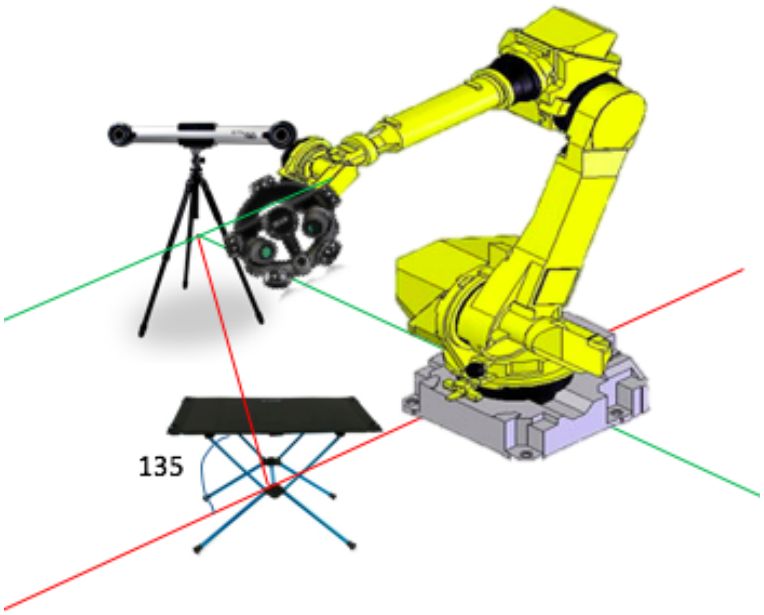

Figure 2.7: The robot work cell along with the calculation of the angles and the measurement of the workspace.

The equations for the forward kinematics are as follows: The general homogeneous transformation matrix for all the robot joints.

$$A = \begin{bmatrix} cos(\theta) & -cos(\alpha) * sin(\theta) & sin(\alpha) * cos(\theta) & a * cos(\theta) \\ sin(\theta) & cos(\alpha) * cos(\theta) & -sin(\alpha) * cos(\theta) & a * sin(\theta) \\ 0 & sin(\alpha) & cos(\alpha) & d \\ 0 & 0 & 0 & 1 \end{bmatrix} \tag{2.1}$$

Equation 2.1: The Homogenous Transformation Matrix A01 the relationship between reference frame and joint 1 in the robot.

Table 2.3: Robot D-H parameters

Th1: 0.00	D1: 740.0	A1: 305.0	Al1: -90.0
Th2: -90	D2: 0.00	A2: 925.0	Al2: 180.0
Th3: 180.0	D3: 0.00	A3: -250.0	Al3: 90.0
Th4: 0.00	D4: -1110	A4: 0.00	Al4: -90.0
Th5: -90.00	D5: 0.00	A5: 0.0	Al5: 90.0
Th6: 180.0	D6: -260.0+605	A6: 0.00	Al6: 180.0

$$A_{01} = \begin{bmatrix} cos(\theta_1) & -cos(\alpha_1) * sin(\theta_1) & sin(\alpha_1) * cos(\theta_1) & a_1 * cos(\theta_1) \\ sin(\theta_1) & cos(\alpha_1) * cos(\theta_1) & -sin(\alpha_1) * cos(\theta_1) & a_1 * sin(\theta_1) \\ 0 & sin(\alpha_1) & cos(\alpha_1) & d \\ 0 & 0 & 0 & 1 \end{bmatrix} \tag{2.2}$$

Equation 2.2: The Homogenous Transformation Matrix A12 the relationship between joint 1 and joint 2 in the robot.

$$A_{12} = \begin{bmatrix} cos(\theta_2) & -cos(\alpha_2) * sin(\theta_2) & sin(\alpha_2) * cos(\theta_2) & a_2 * cos(\theta_2) \\ sin(\theta_2) & cos(\alpha_2) * cos(\theta_2) & -sin(\alpha_2) * cos(\theta_2) & a_2 * sin(\theta_2) \\ 0 & sin(\alpha_2) & cos(\alpha_2) & d \\ 0 & 0 & 0 & 1 \end{bmatrix} \tag{2.3}$$

Equation 2.3: The Homogenous Transformation Matrix A23 the relationship between joint 2 and joint 3 in the robot

$$A_{23} = \begin{bmatrix} cos(\theta_3) & -cos(\alpha_3) * sin(\theta_3) & sin(\alpha_3) * cos(\theta_3) & a_3 * cos(\theta_3) \\ sin(\theta_3) & cos(\alpha_3) * cos(\theta_3) & -sin(\alpha_3) * cos(\theta_3) & a_3 * sin(\theta_3) \\ 0 & sin(\alpha_3) & cos(\alpha_3) & d \\ 0 & 0 & 0 & 1 \end{bmatrix} \tag{2.4}$$

Equation 2.4: The Homogenous Transformation Matrix A34 the relationship between joint 3 and joint 4 in the robot

$$A_{34} = \begin{bmatrix} cos(\theta_4) & -cos(\alpha_4) * sin(\theta_4) & sin(\alpha_4) * cos(\theta_4) & a_4 * cos(\theta_4) \\ sin(\theta_4) & cos(\alpha_4) * cos(\theta_4) & -sin(\alpha_4) * cos(\theta_4) & a_4 * sin(\theta_4) \\ 0 & sin(\alpha_4) & cos(\alpha_4) & d \\ 0 & 0 & 0 & 1 \end{bmatrix} \tag{2.5}$$

Equation 2.5: The Homogenous Transformation Matrix A45 the relationship between joint 4 and joint 5 in the robot

$$A_{45} = \begin{bmatrix} cos(\theta_5) & -cos(\alpha_5) * sin(\theta_5) & sin(\alpha_5) * cos(\theta_5) & a_5 * cos(\theta_5) \\ sin(\theta_5) & cos(\alpha_5) * cos(\theta_5) & -sin(\alpha_5) * cos(\theta_5) & a_5 * sin(\theta_5) \\ 0 & sin(\alpha_5) & cos(\alpha_5) & d \\ 0 & 0 & 0 & 1 \end{bmatrix} \tag{2.6}$$

Equation 2.6: The Homogenous Transformation Matrix A56 the relationship between joint 5 joint 6 in the robot

$$A_{56} = \begin{bmatrix} cos(\theta_6) & -cos(\alpha_6) * sin(\theta_6) & sin(\alpha_6) * cos(\theta_6) & a_6 * cos(\theta_6) \\ sin(\theta_6) & cos(\alpha_6) * cos(\theta_6) & -sin(\alpha_6) * cos(\theta_6) & a_6 * sin(\theta_6) \\ 0 & sin(\alpha_6) & cos(\alpha_6) & d \\ 0 & 0 & 0 & 1 \end{bmatrix} \tag{2.7}$$

To get the location of the laser beam, all the joint homogeneous equations were multiplied as given in equation 2.7.

$$T_{06} = A_{01} * A_{12} * A_{23} * A_{34} * A_{45} * A_{56} \tag{2.8}$$

For the previous equations, a program was made in Matlab to give the location of the end

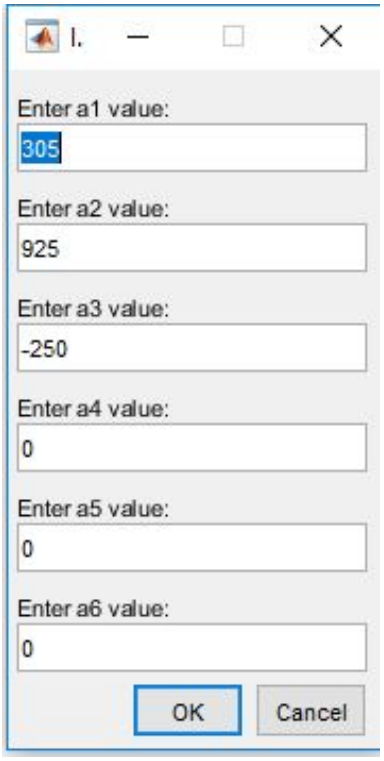

Figure 2.8: Matlab prompt to get forward kinematics by inserting D-H parameters and theta

effector using forward kinematics by taking the D-H parameters in an input dialogue length and angles of all joints of the robotic arm Figure 2.8. Defaults for the robot were inserted, and a theta value was given for a specific location

The location of the C-track in relation to the robot end effector is given by equation 2.9.

$$\vec{A} = \vec{B} + \vec{C} \tag{2.9}$$

The current location of the C-track is measured and given by the vector C-track and the location of the end-effector in the workcell space is given by T_{06}

$$C_{track} = \begin{bmatrix} 0 \\ -1330 \\ 1530 \end{bmatrix} \tag{2.10}$$

$$T_{06} = \begin{bmatrix} 1415 \\ 0 \\ 1050 \end{bmatrix} \tag{2.11}$$

The relationship between the location of the laser beam and the C_{track} is given by equation 2.12

$$X_{final} = C_{track} - T_{06} = \begin{bmatrix} -1415 \\ -1330 \\ 480 \end{bmatrix} \tag{2.12}$$

2.7.1 The Relationship between the C-track Reference Frame and the Robot Reference Frame

In this step the location of the origin of the C-track workspace was validated. The data collected by the scanning process was saved in (X, Y, Z) points. The points that were gathered did not consider the reference point as the center of the test object. The relationship between the point being collected and the shape of the part was not known. It was determined that the points gathered change every time the C-track is moved. However, this could not be linked to a specific reference, so three coordinates of three different points were collected. The coordinates of these points were gathered in relation to the camera workspace and the robot workspace. The relationship between the two workspaces were derived and programmed. The program takes the location of the C-track in relationship to the robot, and two points on the part were manually inserted; this will translate any point on the part from the robot workspace to the scanner workspace that the scanner gathered while scanning. The program worked by inserting the location of the C-track in the robot workspace, which is the origin of the camera workspace along with points on the X axis of

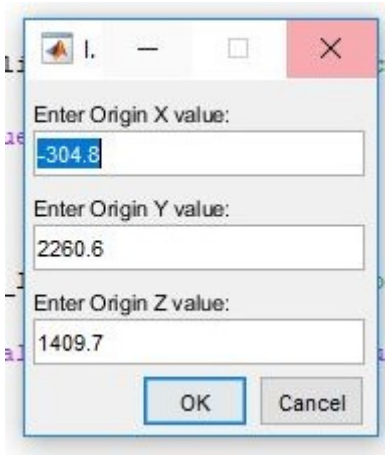

Figure 2.9: Matlab prompt to insert origin of the C-track

the C-track and points that lie on the XY plane of the C-track or on the XZ plane of the C-track. Points XY and XY along with the points on the X axis set up the orientation of the C-track and define the relation ship. The software that does this was made and can be seen in the Figure 2.9 below.

The results will give two mattresses, R and R_back; R is the relationship between a point in the global as seen from the local which means the location of the part being scanned with a known location in the robot workspace in the C-track workspace. To get this, the location of the point in the robot workspace is multiplied it by R in matrix 2.13. R_back is the Point in the local as seen from the global which means the point in the scanner workspace can be converted to the global workspace that is the robot workspace by multiplying it by R_back in matrix 2.14.

$$R = 10e+03 \times \begin{bmatrix} 0.0006 & -0.0008 & -0.0001 & 2.1252 \\ 0.0008 & 0.0006 & -0.0001 & -0.9384 \\ 0.0002 & 0.0000 & 0.0010 & -1.3391 \\ 0 & 0 & 0 & 0.0010 \end{bmatrix} \tag{2.13}$$

$$R\_back = 10e+03 \times \begin{bmatrix} 0.0006 & 0.0008 & 0.0002 & -0.3048 \\ -0.0008 & 0.0006 & 0.0000 & 2.2606 \\ -0.0001 & -0.0001 & 0.0010 & 1.4097 \\ 0 & 0 & 0 & 0.0010 \end{bmatrix} \tag{2.14}$$

2.8 Summary

This chapter showed the relationship between the locations of the reference frame of the C-track in relation to the robot workspace. The kinematic model that represents the relationship between the workspaces was derived along with the center of data points collected. Multiple experiments were done to locate and validate the location of the scanner in the C-track workspace, and it was determined that the location of the workspace of the C-track is the center of the two cameras of the C-track. These outcomes provide an opportunity to generate an optimum scan path planning technique capable of knowing the points to be collected beforehand. Knowing the positions of the robot arm, the 3D laser line scanner, and the C-track position while scanning along with the shape of the object being scanned can lead to creation of scan trajectories that take into consideration the dimension of the part being scanned. The limitation of the work is that the relationship between the location of the C-track and the location of the robot end effector is not always the same equation; it only depends on the current robot setup provided along with the current location of the C-track. Moving the C-track will not give the same results. By using the results, points collected from the scanner at this given position can be predicted. Future work will be generalizing the model and creating software that takes all the positions and orientations of the components in the work cell, such as the location of the C-track and orientation along with the location and orientation of the robot, to predict the location of given points on the C-track workspace.

CHAPTER 3: STUDYING THE EFFECT OF SCANNING SPEED AND RESOLUTION ON POINT CLOUD QUALITY

3.1 Abstract

3D scanning can be used for many applications in manufacturing and remanufacturing by offering a sustainable solution to end-of-use (EoU) core disposal and recovery. These manufacturing and remanufacturing activities require an accurate identification of the damage in order to generate recovery plans that suit the known damaged parts. Using 3D laser scanners as an inspection tool can facilitate this process by measuring the defect. In the preliminary study conducted, an error caused by different parameters was found in the point cloud gathered from the scanning process. Therefore, it was necessary to investigate the factors affecting the scanning accuracy and minimize the scanning errors in order to generate appropriate material deposition paths. Previous studies have identified several factors such as the view angle and standoff distance and investigated their effects on scanning quality. However, scanning speed and resolution are two additional factors affecting the accuracy of captured point cloud that have not been studied so far. Therefore, in this chapter, the effect of scanning speed and resolution is investigated in conjunction with the view angle and standoff distance on the scanning quality. An experiment was designed with four factors, three levels and three replications. Root Mean Square Error (RMSE) was used as the performance measure to analyze the difference between the laser-scanned 3D point cloud data and the model point cloud. Preliminary findings confirmed the results of the previous studies that changing the view angle and standoff distance affects the quality of the point cloud. Moreover, the findings showed that the scanning resolution is negatively associated with the scanning accuracy, meaning increasing the scanning resolution will decrease the scanning accuracy. In addition, the findings showed that the scanning speed has a negative relationship with the scanning accuracy.

3.2 Introduction

There are many types of technology for gathering dimensional information of a specific object. Two of the major technologies are touch probe and 3D scanning, each of which has its own advantages and disadvantages. The main advantages of using a 3D scanner over traditional Coordinate Measurement Machine (CMM) is that the CMM has a touch trigger probe that needs to make contact with the surface it is measuring and collect one coordinate point per touch, unlike the 3D scanner that has the ability to measure points without any contact with the object and capture a large number of points in a short period of time. In general, Coordinate Measure Machines (CMM) are used to extract data points, but they are relatively slow and have low resolution. On the other hand, non-contact methods using non-contact probes enhance accuracy by eliminating noise and giving the best possible fit according to the shape of the object [59]. CMM takes a long time for the touch trigger probe to capture the same number of data points that the 3D scanner collects since it captures one data point per touch. On the other hand, laser line scanners are less accurate than conventional touch-trigger probes such as CMMs. The accuracy of 3D scanners is strongly influenced by the characteristics of the object surface, shape, reflection, roughness, transparency and other properties. For example, it is difficult to scan and inspect shiny surfaces such as machine steel and aluminum using a 3D laser line scanner [4]. In addition, there are standardized procedures to evaluate the accuracy of touch-probe sensors by using a ball artifact. These procedures are not applicable for 3D scanning.Before developing an automated planning for laser inspections in industry, it is necessary to understand what causes outliers in scanning outputs. This can be achieved by experimentally testing the scanning parameters and analyzing their effects on scanning quality. Bevsic et al. [76] studied both measurement methods using the same evaluation procedure for the CMM on a sand blasted aluminum part that was designed to include complicated shapes and common parts such as planes and cylinders. They concluded that the same tools can't be used because the accuracy of the laser scanner is influenced by the characteristics, so further tests are needed

to take all of the influences into account, such as surface quality, surface orientation, and scan depth, which are not the case for CMMs. [76] [6]. The basic purpose of a 3D laser scanner is to gather data pertaining to the shape of an actual object so that it could build 3D models by propagating a laser beam on the surface of the target and then detect its shape through the reflections. There are several types of 3D laser scanners that can be used in various fields such as dentistry, mining, urban topography, reverse engineering, archaeology, etc. Time-of-flight 3D laser scanners, projected pattern 3D scanners, and modulated 3D light scanners are only a few examples of the different types of non-contact active 3D scanners [54]. There are many parameters that affect the output of 3D scanning, one of which is the influence of light that has been well studied and documented. Optimum results could be achieved when the colors have a strong red component, such as red, white and yellow, requiring a color setting at the light side while black and green surfaces give the poorest results [54]. In addition, gray surfaces do not have an impact on the results and thus, can be used in the scanning process [54]. Generally, white and matte surfaces tend to deliver more accurate point cloud data compared to black surfaces [18]. In addition to surface lighting and colors, surface glossiness is another factor that affects scanning quality [50]. The influence of light, color and brightness levels on the measurements can be reduced by doing a careful analysis of the reflected light time evolution which is imaged in the digitizing system's sensors [52]. Martinez et al. 2010 analyzed a touch-trigger probe system against a conventional Laser Tracking System (LTS) system and compared the results for reconstructed surfaces with different structured light intensity [1].

Scanning orientation is another factor that may affect the accuracy of any 3D laser scanner through influencing the incidence angle of the scanner, which is the angle between the normal vector of the surface and the laser beam itself [4, 50, 20]. The incidence angle is known to be closely linked to signal deterioration, where a larger angle would have a more stretched out footprint and the reflected signal is wider while having a low magnitude causing the sensor-to-surface relative position to be of great importance [50]. Due to the electro-

optical nature of the scanners and the principle of optical triangulation, the geometry and position inside the scanning window, which determines the incidence angle, tends to influence the measurement accuracy [4]. The main problem arises because of the falsely recorded outliers.These points are measured from different valid measurement points but usually do not really exist on the actual surface due to using different incidence angles. Outlier points particularly cause some difficulties in CAD/CAM applications [20]. The incidence angle also affects the reflectorless distance measurement of 3D laser scanners.

One of the more obvious factors that affect 3D Laser scanner measurements is the distance of the object from the sensor, which can have a significant influence on the quality of results. In very simplified terms, the shorter the distance of the object from the sensor, the higher the resolution and, thus, the lower the noise levels, and vice versa [6]. This can be explained by the Gaussian beam propagation, principle which dictates that the beam does not travel in a parallel manner but rather converges until a certain distance and then diverges. This divergence affects the quality of the results since the beams are not entirely reflected. This has been experimentally proven where a laser beam was directly aimed at a camera CCD sensor and its profile was measured at 20 mm increments from 40-200 mm. Since the sensor pixel size was known, it was easy to determine the varying width of the beam for confirming the Gaussian principle [53]. Too close or too far a distance can both be detrimental to the results since placing an object too far would put it out of the range of the laser but bringing it too close would open up the possibility of collisions between the points [46]. The relationship between the standoff distance/height and the accuracy of the scanning results can be determined by incrementally changing the distance between the object and the beam propagation point until an optimum working range can be found [18].

Any limitations related to the instruments and hardware can often lead to systematic errors in the propagation of the laser beam and the accumulation of the reflected light. The emission is affected by three factors: the beam divergence deviation, the beam deflection unit, and the axes error including three axes which are seldom aligned and stable. This is

usually dependent on the scanner resolution, which is related to the accuracy of the results [50].Resolution, in this context, refers to the capability of the scanner to detect minute features in the point cloud determined by the combination of two factors: the minimum angle increment between two continuous points and the laser spot's size [32]. Physical limitations of the scanner often cause noise in the gathered point cloud data, which could lead to deteriorated results such as holes in the artifacts scanned. In addition, herd to reach areas for the sensors are usually in grooves with low light, often which leads to low sampling density which can again cause the results to be inaccurate [5].

Most commercial scanners often face limitations in precise dimensional inspection of manufactured parts since there is at least one magnitude that is digitally less accurate compared to touch-trigger probes [4]. The surface material also affects the laser scanner measurements in a few cases such as reflective surface material in time-of-flight laser scanners. Moreover, roughness of the surface material creates variations in the final scan as it has been shown in many studies that the surface roughness of a flat surface correlates to a higher degree of laser beam scattering that leads to a higher noise level in the gathered point cloud [52]. Additionally, if the surface is shiny, e.g. aluminum or machined steel, then the accuracy will be severely affected since diffuse reflection is required to align the camera with the projected laser line, which is difficult for shiny surfaces [6].

There are several other material properties that affect the quality of scanning results through the reflectivity and roughness of the surface material [18]. Free-form surfaces, are common in many design and manufacturing fields such as marine propellers, is a good example. These surfaces contain a complicated sculpture that could potentially lead to a higher magnitude of errors if the measurements are not precise [13].

There are other factors that may potentially affect scanning quality. Scanning speed is one of the measurement parameters that needs to be fully explored before using 3D scanning technology for inspection purposes [13]. Furthermore, using scanners with higher resolution could potentially enhance the quality of gathered point cloud [53].

Although the scanning speed and resolution were mentioned in previous studies, the effect of changing these parameters on the scanning quality remains unknown. In this chapter, scanning speed and resolution are considered in conjunction with the previously studied parameters, i.e. standoff distance and view angle, to investigate their influence on scanning quality.

3.3 Methodology

In this work an experiment was designed with systematically varied scan parameters to study the effect of scanning speed and the resolution on the quality of the collected point cloud. This research examines the factors affecting scanning quality in order to obtain the least amount of noise in the scanning results and minimize the post processing efforts. Although the parameters of interest for this research are speed and resolution to test the methodology, an experiment was done involving parameters already discussed in the literature such as the standoff distance and view angle to make sure that the analysis of the results is correct. The findings confirmed the literature by using Root Mean Square (RMS) of the deviation.

Figure 3.1: The Test Setup with the 3D scanner mounted to the robot and the white board as the flat surface

The scanning errors are generated from the actual 3D scanner being used.There are

multiple factors that contribute to the scanning error. For example, in 3.2, the scanning error is noise in the surface, which does not represent the actual defect in the object. These errors are greater when the surface is not straight and the view angle of the scanner is not perpendicular to the scanner.

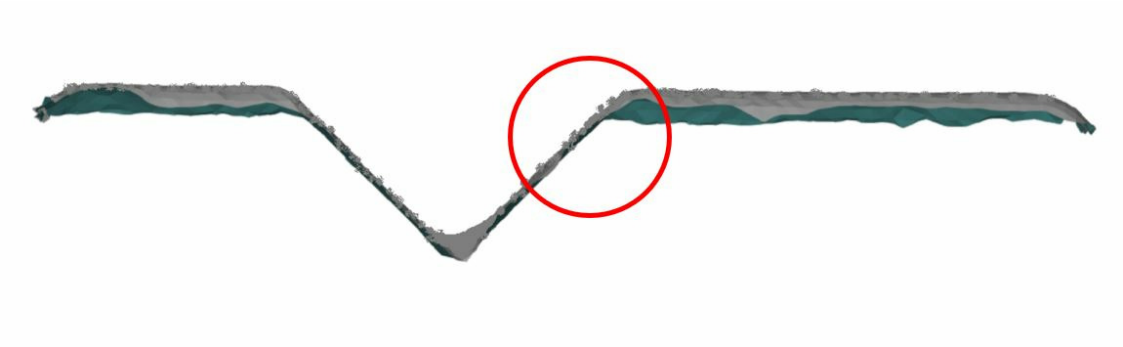

Figure 3.2: The shape of the scanned point cloud representing the defect.

There are n number of data points, and each data point is represented by a point in the x-axis, y-axis, and z-axis, which form d as shown in equation 3.1 below where d_n is an individual point on the surface of the scan. The scanning errors can be determined by a point-to-point objective quality metric which is based on comparing the scanned model with the CAD model and calculating the Root Mean Square Error (RMSE) of the variations [77]. For additive re-manufacturing, this would theoretically be the difference between the captured point cloud and the actual damage observed on a part. This functions by obtaining the value of the mean distance (root mean square error of distance), which is the change in the Z-axis between the scanned model and the CAD model. The ideal RMSE value is zero, meaning the lower the RMSE value, the closer the scan is to the CAD model.However, this is rare as the scanner collects noise because it is functioning due to many factors, some of which can be avoided while others can not. In Figure 3.2 the noise inside the circle does not come from the actual part, and in the part where the surface is smooth, the noise came from points in air and not on the actual surface made by the scanner while scanning.

$$E_{Scanning} = E_{RMS} = \sqrt{\frac{1}{n}(d_1^2 + d_2^2 + d_3^2 + ... + d_n^2)}. \tag{3.1}$$

$$where\ d_n = \Delta n_{scan} - \Delta n_{CAD} \tag{3.2}$$

3.4 Systematically Varied Scan Parameters Experiment

The objective of this task is to understand the impact of point cloud measurement parameters on scanning quality. Collecting a large point cloud data with systematically varied scan parameters is important for understanding the impact of those parameters. Automated point cloud measurement is critical to isolate all sources of variation caused by manual scanning. In this experiment the approach used was obtaining a sufficient database of physical measurements using the automated point cloud measurement test bed with varied scanning parameters by mounting the scanner to a robot to have a precise measurement that can be repeated and distinguished with different levels. In Figure 3.3 six tasks were accomplished in this experiment. First, a design for the test bed was made taking in consideration the limitation of the robot and the capability of the scanner used. Second, the experiment was designed and all the possible factors that are going to be studied along with the interaction of the other parameters were identified. Third, the levels were identified for each factor after knowing the limits of the view angles and the standoff distance then the scanner can function on. Fourth, the data was collected and the actual experiment was performed. Fifth, the right method was selected to compare the data. Sixth, the data gathered with the CAD model of the part being tested were compared. Following are the factors tested and the levels used in the experiment for the four parameters. The angle in which the scanner is in relation to the object being scanned is shown in Figure 3.4

The distance between the scanner and the object being scanned is shown in Table 3.4 and can be seen in Figure 3.4 as the offset Z. Scan line resolution of the experiment are shown in Table 3.5. The speed in which the joints of the robot are moving while preforming

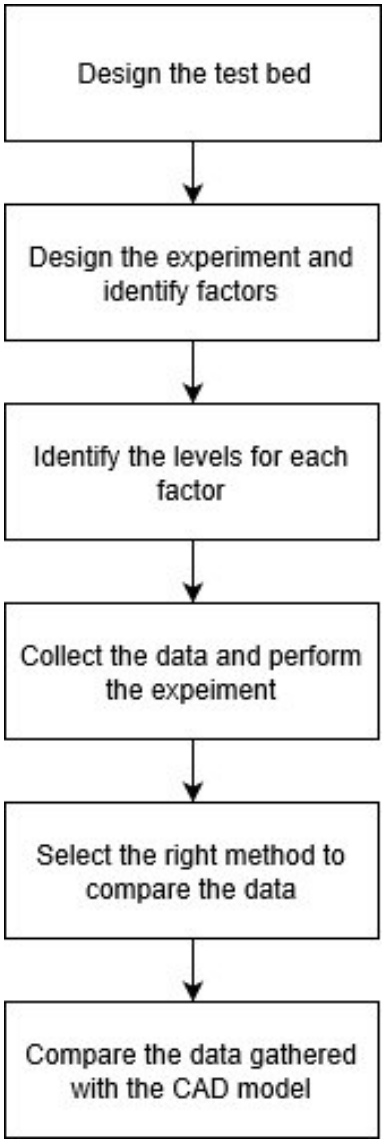

Figure 3.3: The steps taken to design and perform the experiment

Table 3.4: Standoff Distance Levels

Level	Value
1	11 Inch
2	8.8 Inch
3	6 Inch

the scanning process is defined as the scanning speed.The speed in relation to the robot maximum speed and how the robot is using it are shown in Table 3.6. Because the robot is

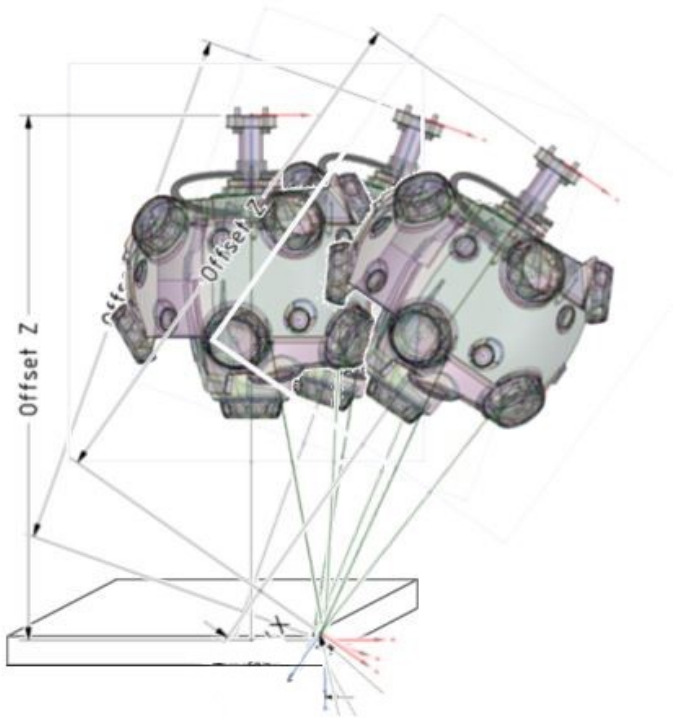

Figure 3.4: the scanner view angle in relationship to the part being scanned

for education purposes, the maximum speed limit is 1500mm/s at 50% which this means for the values in Table 3.6, the speeds of 5 to 25% are 150mm/s to 750 mm/s. After doing the previous experiment and getting the results, another experiment was designed using different levels and only the concerned parameters to validate the findings. In the new experiment levels were rearranged in ascending order and increments were even for both the speed and the resolution. The resolution levels for the new suggested values for validation are in Table 3.7

Therefore, the speed levels for the new suggested values for validation are in Table 3.8. These tables were selected based on observations from previous experiments and the limitation of the scanner. In this experiment the speed levels were higher than the first experiment as the change in the speeds was not noticeable because the values were set up next to each other and there was little change in each level. In this experiment the limits of the robot and scanner were identified to distinguish the effect of the change in the speed on

Table 3.5: Scanner resolution

Level	Value
1	1.0mm
2	0.8mm
3	0.2mm

Table 3.6: The Speed Levels

Level	Value
1	5%
2	15%
3	25%

the point cloud collected, and the maximum speed changed from 25% the maximum speed of the robot to 45% of the maximum speed to make the values spread across the spectrum of the range. These values translate to 150mm/s to 1350 mm/s.

3.5 Aim of the Experiment

To address this gap, this research seeks to answer the question of whether the quality of the point cloud is affected by changing the speed and resolution while scanning. In order to do this, these parameters need to be further studied to identify their effects on the scanning quality. This is important to give any future recommendations or to design a better scan trajectory, the effect of the parameters changes must be known to see if it is significant or not in order to design trajectories and select the appropriate parameters to perform a specific scanning task.

3.6 Approach

All the experiments were conducted with all the given levels and parameters, and the results were analyzed. It is better to over sample and work on a larger surface and keep the record to avoid redoing the experiment. Therefore, a trajectory was created to study multiple aspects in one run. The trajectory studied the repetition of the movement of the

Table 3.7: Scanner resolution

Level	Value
1	1.0 mm
2	0.6 mm
3	0.2 mm

Table 3.8: The Speed Levels

Level	Value
1	5%
2	25%
3	45%

robot over a specific section, which was the center of the flat surface. The data can be used when necessary to also test the effect of the direction of the movement from right to left or left to right along with the other parameters in each and every iteration as shown in Figure 3.6. The points selected on the white board are marked with a small marker and matched with the location of the trajectory, created in Figure 3.6 ,when the robot is moving.

A small section was cut from the collect point cloud and the analysis and results were based only on this section, as seen in Figure 3.7

3.7 Results

The gathered point cloud is shown the following three figures, which represent a scan of exactly the same shape using the same pattern, standoff distance, view angle, and resolution. The only difference is in the speed in which the scanner is moving with. As can be seen in Figure 3.8, there are many empty spots due to the speed in which the scanner is moving, and this is at level 1 in the experiment Figure 3.9 shows the point cloud when the speed is at level 2 in the experiment, Figure 3.10 shows the point cloud when the speed is at level 3.

The collected point clouds were segmented, and the area under study shown in Figure 3.7 was compared to the original CAD model. This area was selected because it has no scan

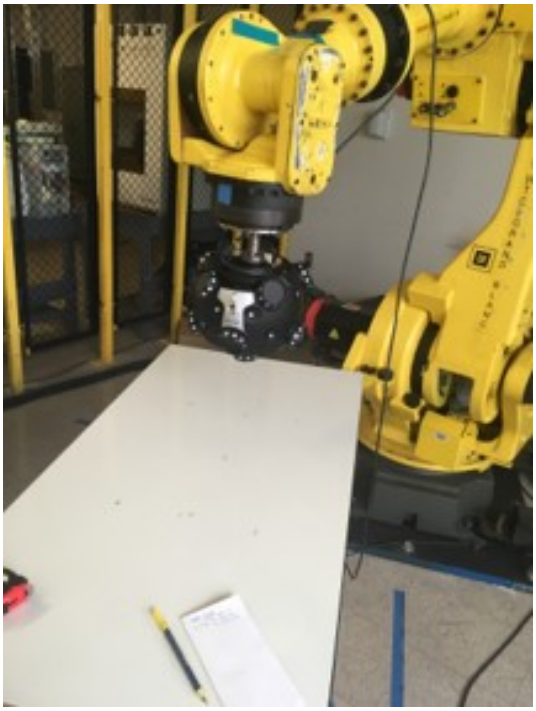

Figure 3.5: The scanner attached to the robot with the white board in place

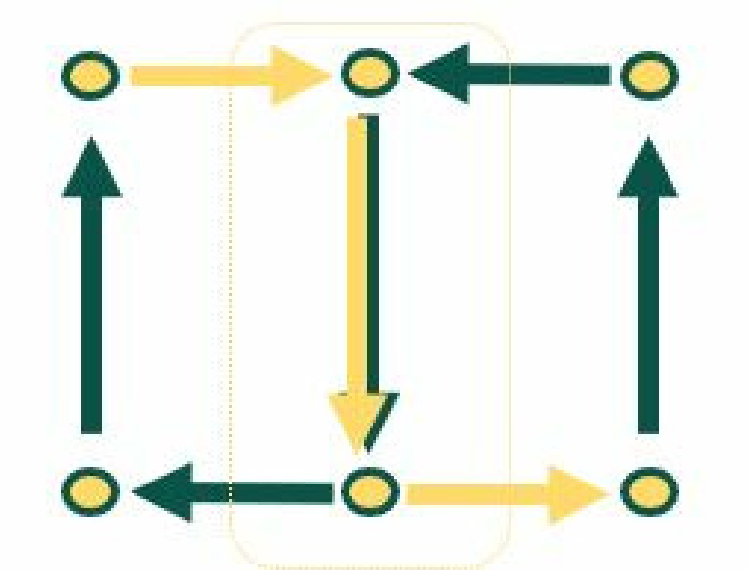

Figure 3.6: The scanner Path in the experiment

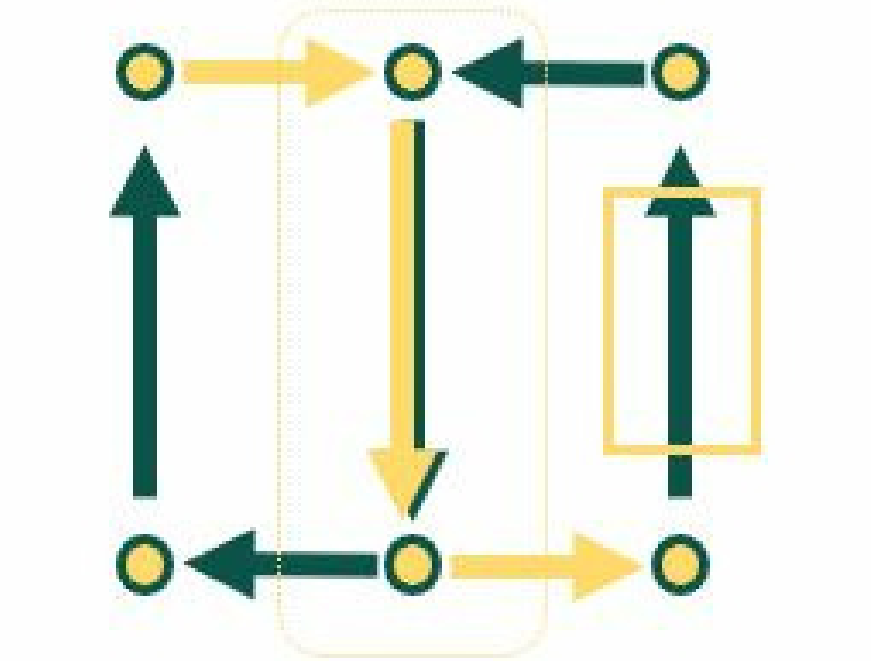

Figure 3.7: The area selected for the analysis

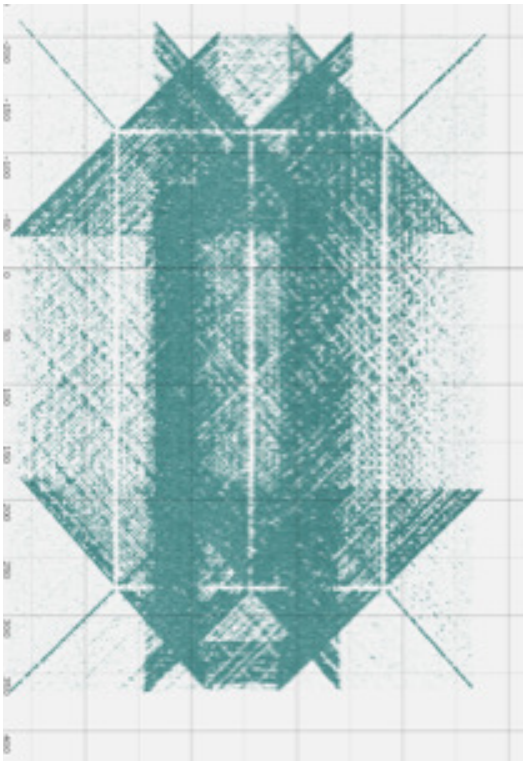

Figure 3.8: All parameters fixed except speed at highest setting at 25% equal to 750 mm/s.

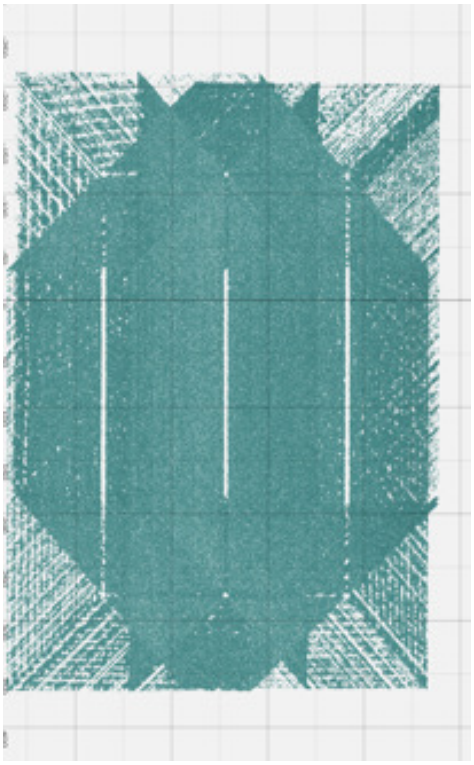

Figure 3.9: All parameters fixed except speed at medium setting at 15% equal to 450 mm/s.

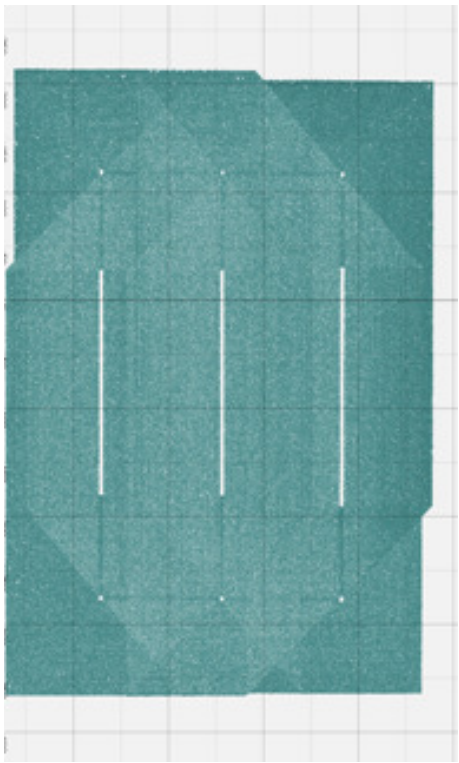

Figure 3.10: All parameters fixed except speed at lowest setting at 5% equal to 150 mm/s.

repetition, which is part of the scope of the study. Results were analyzed using analysis of variance (ANOVA) and also Pearson correlation. The results of the 81 experiments with all four factors with three levels shows that all four factors are significant as can be seen in Table 3.11. This confirms the literature regarding the standoff distance and the view angle. This also proves the validity of the algorithm and the tool used to analyze the point cloud.

Table 3.9: View Angle Levels

Level	Value
1	70°
2	80°
3	90°

As can be see in the table, the change is negative in the increment in the levels of the view angle and the stand off distance, because the levels are in descending order as can be seen in Table 3.9. For the view angle, the lowest level (1) has the highest deviation from normal in the angle and the highest level (3) has the lowest deviation from normal. Table 3.4 shows that the stand off distance of the lowest level (1) has the highest distance from the part and the highest level (3) has the lowest distance. This is unlike resolution and speed where it is arranged in ascending order as can be seen in Table 3.5 where the resolution lowest level (1) has the lowest resolution and the highest level (3) has the highest resolution. For speed as shown in Table 3.6, lowest level (1) has the lowest speed and the highest level (3) has the highest speed. The error is decreasing as we head toward the norm for the view angle and as we decrease the distance. and it is increasing as we increase the speed and the resolution as can be seen in Figure 3.11

Table 3.11: ANOVA table

Source	DF	SS	MS	F	P
View Angle	2	3.9476	1.9738	4.58	0.013
Standoff Distance	2	5.4058	2.7029	6.28	0.003
Resolution	2	37.4559	18.7279	43.48	0.000
Speed	2	7.3822	3.6911	8.57	0.000
Error	72	31.0107	0.4307		
Total	80	85.2022			

Table 3.12: ANOVA table

Table 3.10: Factors and levels

Factor	Type	Levels	Values
View angle	fixed	3	1, 2, 3
Standoff dist	fixed	3	1, 2, 3
Resolution	fixed	3	1, 2, 3
Speed	fixed	3	1, 2, 3

ANOVA: Response 1 versus View angle, Standoff distance, Speed, Resolution

Analysis of Variance for Response

As can be seen from Figure 3.13 after analyzing the data for validation, the error is increasing as we increase the speed and resolution. The same results were found for the initial experiment. However, the curve is not identical due to the different values that were selected for the validation experiment as can be seen in Table 3.5 for the resolution and Table 3.6 for the speed in comparison with Table 3.7 and Table 3.8, respectively.

It is increasing as we increase the speed and the resolution as can be seen in Figure 3.13

General Factorial Regression: Average error versus Resolution and Speed

Using Pearson correlation to validate the relationship of the change of the speed and resolution on the quality of the point cloud, a positive correlation were found as can be seen

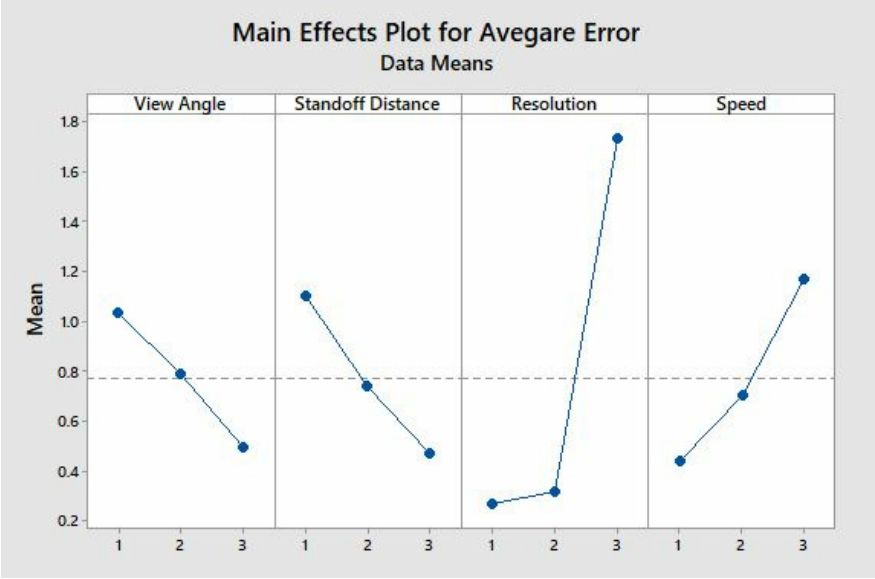

Figure 3.11: Plot of the standoff distance view angle speed and resolution

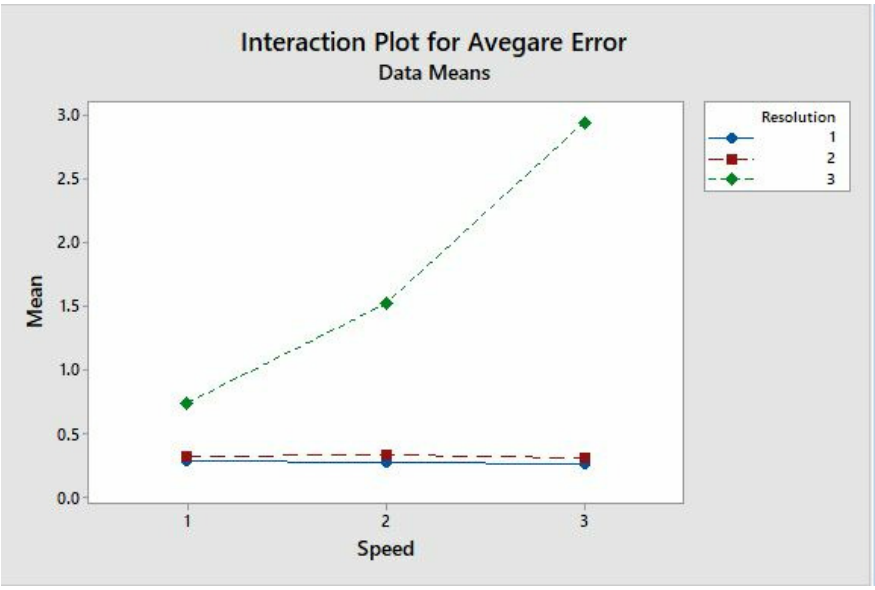

Figure 3.12: Interaction plot of the speed and resolution

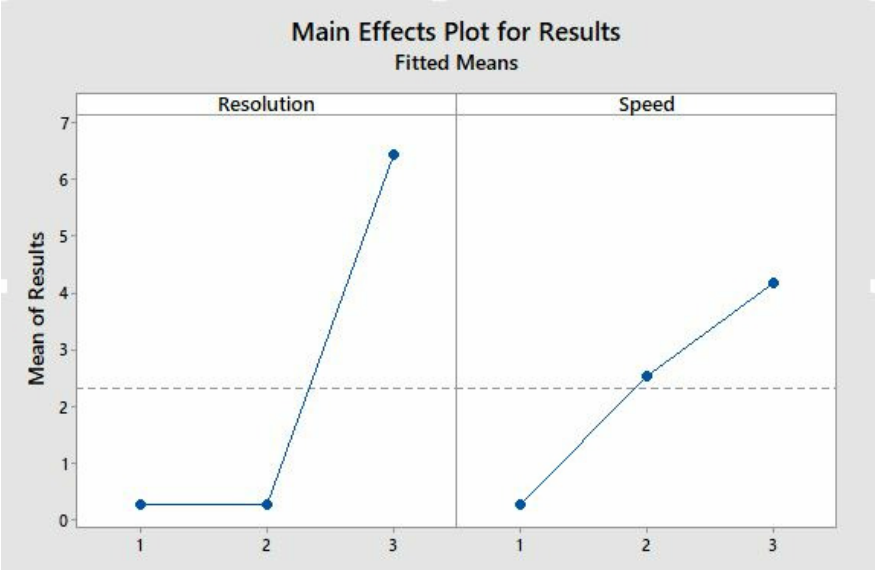

Figure 3.13: plot of the speed and resolution

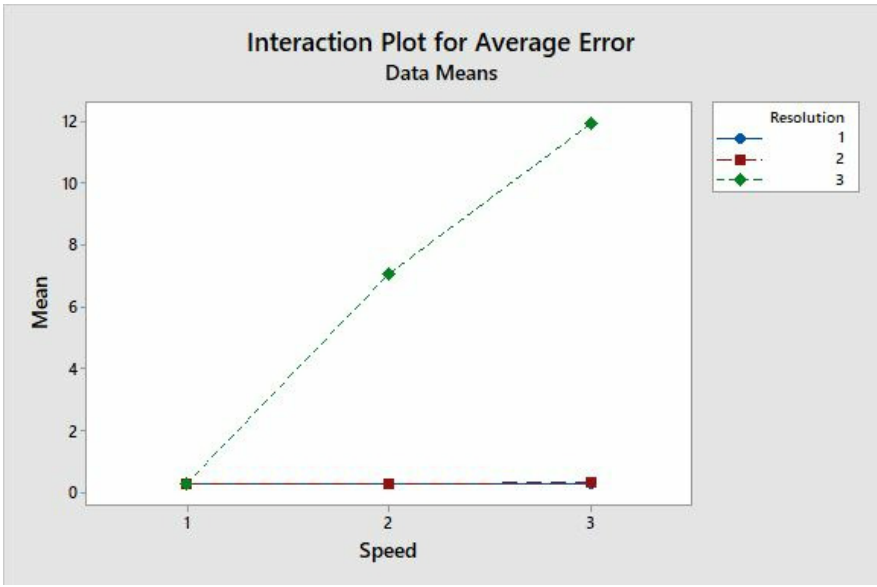

Figure 3.14: Interaction plot of the speed and resolution

Table 3.13: General Factorial Regression Factors and Levels

Factor	Levels	Values
Speed	3	1, 2, 3
Resolution	3	1, 2, 3

Table 3.14: Analysis of Variance Resolution and Speed

Source	DF	SS	MS	F	P
Model	8	432.373	54.047	162.28	0.000
Linear	4	295.701	73.925	221.96	0.000
Speed	2	69.068	34.534	103.69	0.000
Resolution	2	226.633	113.317	340.24	0.000
Interactions	4	136.672	34.168	102.59	0.000
Error	18	5.995	0.333		
Total	26	438.368			

in Table 3.15 and 3.16 this means that as the speed increase the is an increase in the noise or error in the point cloud. Table 3.15 shows the correlation for the experiment where I used all the four parameters, while Table 3.16 shows only for the validation experiment where I only studied the speed and the resolution.

Table 3.15: Pearson correlation results for the 81 experiments

Factor	correlation
Speed	0.2905554
Resolution	0.5834091

After validation see Table 3.16

Table 3.16: Pearson correlation results for the 27 experiments

Factor	correlation
Speed	0.3953238
Resolution	0.6239086

3.8 Limitations

In this experiment and analysis the movement direction was not part of the study, and the impact of repetition over the same area was not investigated. Each path was performed once over the same area. It was also assumed that there is no influence from the robot movement or vibration on noise created in point cloud as the robot is rigid and carries heavy items and our scanner is a very light scanner. Experiments were performed on a white matte surface and the results shown are only for this surface. The effect on different surfaces is not known but assumed to be the same. Finally the effect of ambient light was assumed to be irrelevant as the experiments were performed at the same time of day over several days.

3.9 Strategies for Improving the Point Cloud Quality

There are many strategies for improving the point cloud quality some of it related to the parameters while other are related to point Cloud Post Processing. Although post processing decrease the noise in the gathered point cloud, It can add up to the overall error in the point cloud if the wrong methods were used. Also, It is very important to select the right parameters and avoid collecting a large point cloud when the surface being inspected do not require a high resolution due to the surface simplicity. This leads to the importance of knowing the right parameters as it reduces the demand for processing power that consume time and resources. In the experiment with a simple flat surface it was evident that the increase in the resolution do not increase the quality of the gathered point cloud and in fact it adds to the error in the point cloud and thus selecting the right resolution level is important. With surfaces that has curvatures and arcs, it is important to increase the resolution of the scanner as it will capture the curvatures in a higher precision and will decrease the error in the point cloud. Smoothing and cleaning the point cloud can add to the overall error and will be shown in chapter 4 and this makes studying the parameters and increasing the accuracy of the scanner a very important task for the point cloud to be used for manufacturing and remanufacturing applications. Also, working in improving a good scanner point cloud is better than improving the point cloud that has a huge noise and this

leads to the importance of studying the parameters and the scanning procedures over the post processing of the point cloud.

3.10 Summary

As can be seen regarding the scanner used and the speeds that were selected, the change in the speeds was significant along with the change in the resolutions. Changing the resolution should result in a better results. However, that occurred to a certain extent, and then the effect become negative as the point cloud size got bigger and resulted in error as the point being sampled and calculated was higher. Therefore, further study is needed to make a final conclusion. The significant effect of the standoff distance and the view angle on the scanning quality was also confirmed in this experiment, and it supports the findings from the literature.

The future plan is to test the scanner using higher speeds and compare these results to generalize the findings. Then the scanning parameters need to be connected to the defect in the point cloud to monitor the quality of the manufactured parts. Therefore, machine learning most be used to predict the changes in the parameters on the point cloud. Knowing the effect of the parameters on the point cloud is important to compensate for it in the future steps in the re manufacturing digital thread an to reduce the effect of the parameters by having the right parameters for the scanner by setting up the optimal trajectory to preform the scanning task.

CHAPTER 4: ERROR PROPAGATION IN DIGITAL ADDITIVE REMANUFACTURING PROCESS PLANNING

4.1 Abstract

A point cloud is a digital representation of a part that consists of a set of data points in space. Typically point clouds are produced by 3D scanners that hover above a part and record a large number of points that represent the external surface of a part. Additive remanufacturing offers a sustainable solution to end-of-use (EoU) core disposal and recovery and requires quantification of part damage or wear that requires reprocessing. This chapter proposes an error propagation approach that models the interaction of each step of the additive remanufacturing process. This proposed model is formulated, and results of the error generated from the parameters of the scanner and point cloud smoothing are presented. Smoothing is an important step to reduce the noise generated from scanning, knowing that the right smoothing factor is important since over smoothing results in dimensional inaccuracies and errors, especially in cores with smaller degrees of damage. It is important to know the error generated from scanning and point cloud smoothing to compensate for the following steps and generate appropriate material deposition paths. Inaccuracies in 3D model renders can impact the remainder of the additive remanufacturing accuracy, especially because there are multiple steps in the process. Sources of error from smoothing, meshing, slicing, and material deposition are proposed in the error propagation model for additive remanufacturing. Results of efforts to quantify the scanning and smoothing steps within this model are presented.

4.2 Introduction

To be more sustainable and reduce material waste, Nasr et al. [78] suggested the use of remanufacturing as it plays a significant role in value recovery. Due to the flexibility of additive manufacturing processes, it offers a sustainable solution to end-of-use (EoU) core disposal and recovery [61, 62, 63, 64]. Despite the advantages and potential of addi-

tive manufacturing (AM), the accuracy of the geometry continues to be a limitation to its wider application [60]. While physical processes are important factors in the overall quality of manufacturing, failed builds were found that can be traced back to errors in the digital translations, with leads to the actual physical processes [60]. These errors are relevant to additive remanufacturing applications that aim to leverage additive processes for targeted material deposition and part reprocessing to original equipment manufacturer part specifications [79]. Thus far, error propagation in the digital thread of the additive remanufacturing processes has not been realized. Rickli et al. (2014) [9] describe a framework for an additive remanufacturing system that uses a 3D laser-line scanner to capture external defects. This framework is divided into three parts: condition assessment and digitization, material deposition, and re-processing and inspection. The steps that are taken in the condition assessment and digitization phase of this additive remanufacturing framework are scanning, smoothing, meshing and slicing, leading to tool path planning for material deposition (Figure 4.1). In this chapter, the focus is on the processes that affect the point cloud in order to use it in additive remanufacturing applications. Essentially, the defective part is received by a remanufacturing facility. The first step is to collect the 3D point cloud of the damaged part; there is some noise that the point cloud contains and this leads to the second step, smoothing the point cloud to reduce noise. In order to generate the tool path plan for additive remanufacturing, a meshed point cloud is needed to be used for slicing, Slicing is the plan for the material deposition in regard to the trajectory and the thickness of the layer in the additive manufacturing process and the actual material deposition. Smoothing reduces the noise in the point cloud and makes the neighboring points closer in features because it is based on the averaging of neighboring points. To generate the smoothed surface, points that are noise and not near the surface must be eliminated first; then a smoothing algorithm can be implemented. Smoothing is important to clean out errors that are not actually present in the object under the remanufacturing process, so this step is important as it influences subsequent meshing and slicing steps.

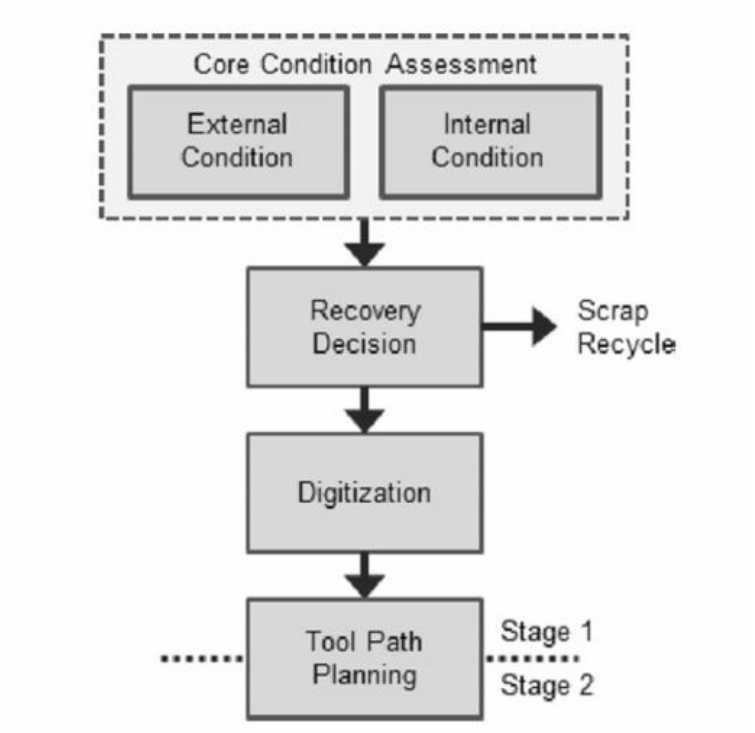

Figure 4.1: Flowchart of the main steps of EoL core condition assessment and digitization [9]

In this work experiments were conducted that demonstrate the error propagated in the remanufacturing digital thread. The focus of this chapter is on how the different steps in the remanufacturing process contribute to the overall error as each step adds up to the overall error. Specific contributions are: (1) The importance of the scanning factors in the remanufacturing digital thread and the overall error propagation in the process, and (2) The effect of the smoothing on error propagation and the effect it has in the remanufacturing process. The remainder of this chapter is organized as follows. Section 2 proposes error propagation models and outlines steps in the additive remanufacturing process. Section 4 present the results of the scanning and smoothing process within the context of additive remanufacturing, and section 5 presents the conclusions and future work.

4.3 Methodology

In this section, the proposed model for how the error is propagated in additive remanufacturing from the scanning to the material deposition is explained. Figure 4.4 lists

the digital additive remanufacturing factors that are considered in the proposed model in this chapter. Scanning is the first step, and it has the initial effect as it is the phase that is collecting the point cloud that is the base for subsequent steps that work on this collected point cloud. Smoothing work on the collected point cloud from the scanner removes outlier data points or brings it closer to the surface and reduces the error generated by the scanning phase. However, sometimes smoothing increases the error in the point cloud depending on if the outlier feature is present on the scanned object or it is just a noise in the scan. Meshing is transforming the point cloud by the creation of vertices, edges and faces which defines the shape of a polyhedral object to prepare the model for slicing. Depending on how dense is the point cloud this can adds up to the overall error as the dense point cloud represent the surface with more details and preserve the important features as shown in Figure 4.2 by [80]

Slicing uses the mesh generated from the smoothed point cloud to create a material deposition path plan for additive remanufacturing. Depending on the layer height the error can be added or decrease as using a higher layer height increase the error in the manufactured part as it is not confirming to the features in the object as shown in Figure 4.3 by [81]

. Material deposition is the final phase in which the plan that was generated from the part scan is executed.

There are errors generated in all the activities above, and the overall error equation 4.1 is listed below. It sums all the errors from additive remanufacturing steps, Figure 4.4. Here, error is defined as the difference between the scan, mesh, or slicing and the damage/defect geometry that is being remanufactured. The error generated from each of these steps is explained in detail in the following subsections. Since the objective of additive remanufacturing is to correct a damaged part, it is critical that the damage be captured and planned for accurately.

$$E_{Total} = E_{scanning} + E_{smoothing} + E_{meshing} + E_{slicing} + E_{printing} \tag{4.1}$$

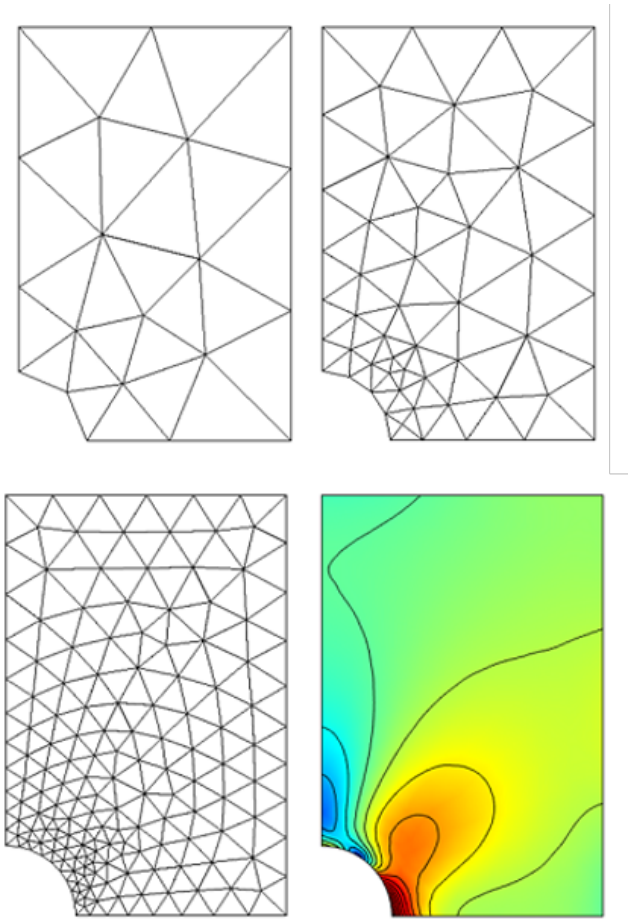

Figure 4.2: Effect of the density of the point cloud on preserving the features

4.3.1 Scanning Error

Scanning errors are generated from the actual 3D scanner being used. There are multiple factors that contribute to scanning error, in Figure 4.5 show that the scanning error is noise on the surface that does not represent an actual defect in the object. These errors are greater when the surface is not straight and the view angle of the scanner is not perpendicular to the scanner. Changes in scanner parameters affect the quality of the gathered point cloud. Thus, it is important to select the right parameters when scanning a part for remanufacturing to get a quality point cloud that is efficient for smoothing, meshing, and slicing steps..

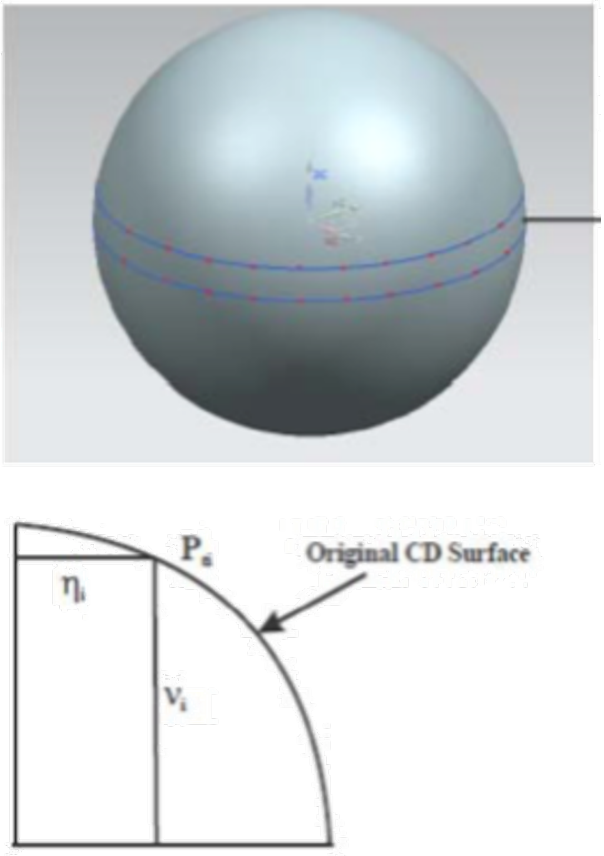

Figure 4.3: Effect of the slice height on the manufacturing error

Figure 4.5: The shape of the scanned point cloud representing the defect

The scanning errors can be captured by comparing the scanned model with the CAD model and calculating the Root Mean Square (RMS) of the variation in comparison to the CAD model, classified by Javaheri et al. [77] as point-to-point objective quality metrics. For

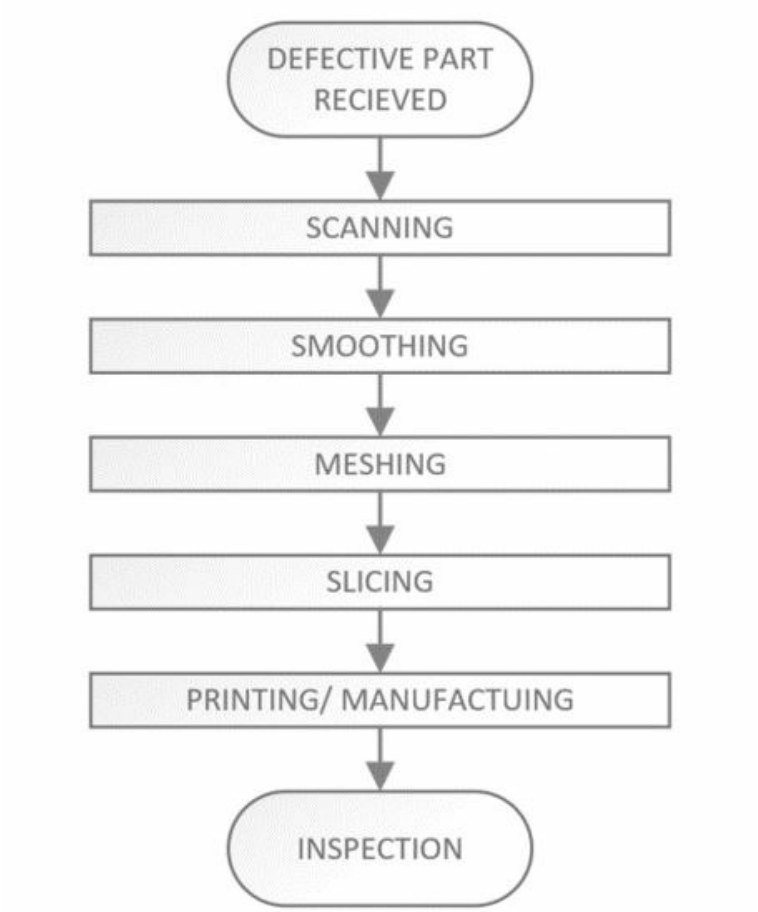

Figure 4.4: Point cloud capturing and processing steps in the remanufacturing.

additive remanufacturing, this would theoretically be the difference between the captured point cloud and the actual damage observed on a part. This functions by obtaining the value of the mean distance. d_RMS is equal to the root mean square of the distance, which is the change in the Z-axis between the scanned model and the CAD model. The lower the RMS value the closer the scan is to the CAD model, and the ideal is 0. There are n number of data points and each data point is represented by

$$E_{Scanning} = d_{RMS} = \sqrt{1/n(d_1^2 + d_2^2 + d_3^2 + \ + d_n^2)} \tag{4.2}$$

$$d_n = \Delta n_{Scan} - \Delta n_{CAD} \tag{4.3}$$

4.3.2 Smoothing Errors

Smoothing errors are generated from processing the point cloud after it was scanned. In Figure 4.6 below the smoothing reduces some of the noise data that are on the surface. However, although a smoothing algorithm cleans the point cloud, it can lead to errors in capturing the volume/surface. Therefore, some of the details necessary in the digital representation of the part might get compromised depending on the number of iterations and/or the smoothing factor.

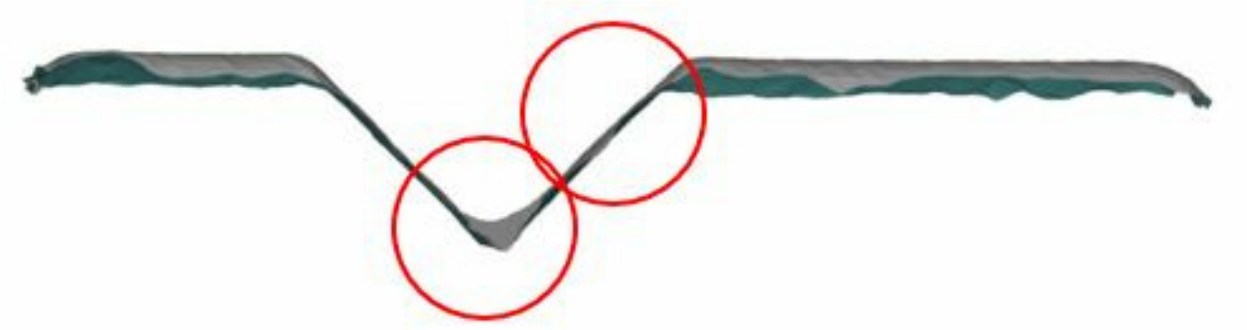

Figure 4.6: The shape of the scanned point cloud representing the defect after smoothing.

Numerous smoothing techniques exist that aim to reduce noise without affecting the accuracy of the scanned point cloud. For instance, Laplacian smoothing is a localized moving-point average smoothing function that takes the surrounding points and calculates

the average as it is moving from one location to another. This transforms the points in the point cloud to a new location based on the smoothing factor. The 'Smoothing Factor' essentially determines the influence of the nearest neighbors in point relocation. The higher the 'Smoothing Factor', the more influence the nearest neighbors have, thus leading to more smoothing. The comparison between the CAD and the scanned data is calculated by equation 4.4.

$$E_{Smoothing} = \sum_{i=1}^{k} min(P_s - P_{CAD})^2 \tag{4.4}$$

Where k is the number of adjacent vertices to node i, $\bar{x_j}$ is the position of the j^{th} adjacent vertex and $\bar{x_i}$ is the new position for node i. and $E_{Smoothing}$ is the error between the point cloud after smoothing and the CAD model were p_s is the point cloud scanned and p_{CAD} is the point cloud from the CAD model

4.3.3 Meshing Error

Meshing is the process of converting the scattered point cloud into triangles. Although this step may not essential in additive remanufacturing processes, it remains a part of digital processes due to practical reasons [60] as it offers a convenient interchange format to share the file without sharing the CAD file [82]. In Figure 4.7, meshing uses the point cloud to make a triangular mesh; therefore, when the number of the point cloud is low the curved surfaces may be sharper and more accurate as can be seen in the bottom of the groove compared to Figure 4.6.

The sources of the errors are dependent on the first two activities. In addition, the size and the density of the point cloud around the curved and detailed area affect the overall error. A larger point cloud will theoretically decrease the meshing error as it represents a higher details to the actual model as possible. Equations 4.4-4.7 are based on Sikder et al. [81] regarding slicing error, but they share similar concepts in calculating the error, When triangles are generated depending on a location of the triangle and the shape it takes, some

Figure 4.7: The shape of the scanned point cloud representing the defect after meshing the points.

features might be omitted or altered, for example, the circular shapes become more like n-gon (a polygon with n sides) shapes depending on the number of faces. The error is calculated by the difference between the faces and the CAD model. Meshing error where ef is the meshing error and $E_{Meshing}$ is the total surface error.

$$e_f = \sum_{i=1}^{\mu} min(\nu_i^2, \eta_i^2) \tag{4.5}$$

Surface error at i^{th} face

$$\varepsilon_i = \sum_{j=1}^{\lambda} e_p \tag{4.6}$$

Total surface face error

$$E_{Meshing} = \sum_{i=1}^{k} \varepsilon_i \tag{4.7}$$

Where ν_i, η_i is the vertical and Euclidian distance to the vertical and horizontal plane on the smoothed point cloud. By selecting the face of the represented shape closest to the mesh of the CAD model of the object, the calculated error is the distance between the CAD model and the triangulated mesh.

4.3.4 Slicing Error

In the slicing phase, the plan to create the material deposition or printing is done to correcting the defect. The areas that need to be filled are shown in Figure 4.8 below, which represent the point cloud of the defect aligned with the point cloud of the intact part.

Figure 4.8: The shape of the scanned point cloud of a defective part aligned with the scanned point cloud of an intact part.

The slicing error is generated when the defect geometry captured by the smoothed point cloud and mesh is converted into slices for material deposition. In Figure 4.9, the slicing plan shows that there are some small areas that are not covered due to the layer heights specified during slicing. These gaps can change depending on the slice height.

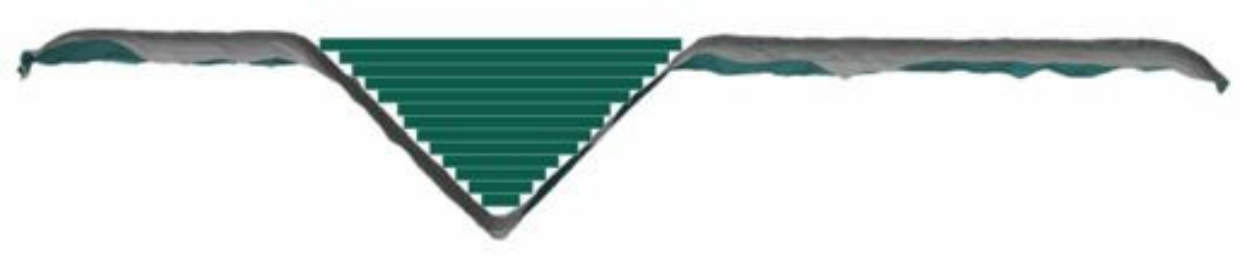

Figure 4.9: The slicing material deposition plan.

Sikder et al. [81] suggested an adaptive slicing algorithm to minimize the error based on the details needed at each layer. To minimize the surface error, they created an adaptive slicing algorithm that minimizes the slice thickness; then they calculated the error by using this technique. In Equation 4.8 the slicing error is calculated by the minimum distance between each slice and the surface in the created mesh. This covers the empty area that

is considered error an by selecting the closest point from the point cloud to the mesh. The calculated error is the distance between the triangle created in the meshing phase to the slices created in this phase, which is represented by the white area shown in Figure 4.9 above. Equation 4.9 is the total error in that slice. Equation 4.10 is the total slicing error.

$$e_p = \sum_{i=1}^{\mu} min(\nu_i^2, \eta_i^2) \tag{4.8}$$

Surface error at i^{th} face

$$\varepsilon_i = \sum_{j=1}^{\lambda} e_p \tag{4.9}$$

Total surface face error

$$E_{slicing} = \sum_{i=1}^{k} \varepsilon_i \tag{4.10}$$

Where ν_i, η_i is the vertical and Euclidian distance to the vertical and horizontal plane on the smoothed point cloud.

4.3.5 Printing Error

A printing error can be caused BY multiple factors in the printing process (the actual material deposition) or from previous steps to the actual material deposition mentioned (error 1-4) that might not completely cover the shape of the defect and thus generate a slicing plan that does not completely fill the defect space or overfills the defect space as shown in Figure 4.10.

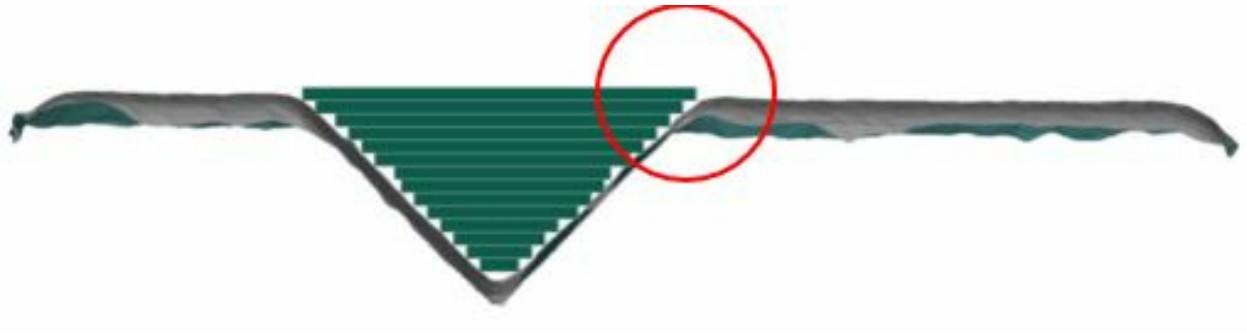

Figure 4.10: Printing and actual material deposition error.

Material deposition errors that may exist include a missing filament in the extruder, the inability to reach the specific location to add materials, and/or a smaller feature than the layer height of the material to be deposited. Brown and Pierson (2018) [60] suggested that errors are caused by three main sources: that include toolpath distortions, process capability errors, and process interaction errors. The errors in this phase are not known until the remanufactured part is inspected via destructive or non-destructive methods. Currently, this error is represented as Eprinting and is planned to be estimated through experiments in future research activities. The equations used for the scanning error can also be used to study error in this step. As noted in equation 4.1 the overall error in printing is an error propagated through the four previous steps, and it is shown into the inspection phase where the CAD model is compared with the gathered post production point cloud.

4.4 Experimental Design

Experiments were conducted based on scanning four models including three increasing degrees of defect, 2mm, 5mm and 8mm, and a blank model containing no defect. (The number corresponds to the depth of the defect). Each model was scanned three times at a resolution of 0.5mm. Consistency between scans of identical models was confirmed by using exactly the same path and attaching the scanner to a robotic arm

The selection of the resolution at 0.5 mm showed that it produces the least error based on the selected settings. And the speed, standoff distance, and view angle were ideal to ensure that the errors are at minimal levels. Figure 4.12 (below) shows the obtained

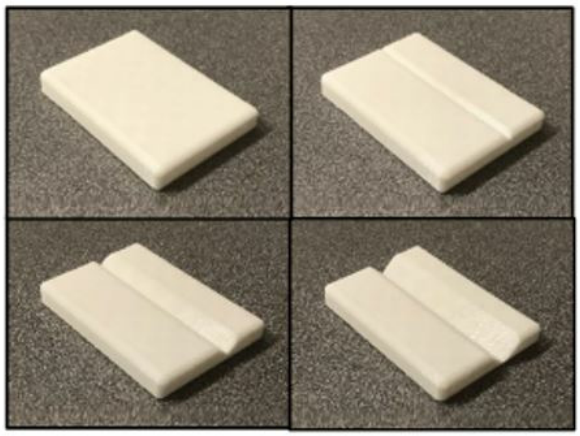

Figure 4.11: blank (top left), 2mm defect (top right), 5mm defect (bottom left), 8mm defect (bottom right).

Figure 4.12: 8mm defect model with noise after removing the surrounding area from the scanned data.

point-cloud of the 8mm defect model.

The model above was selected to compare the 8mm defect scan with the blank scan. Registration was needed to place the scan and the CAD model in the same coordinate system. The iterative close point algorithm (ICP) was used to roughly align the scans. Total errors are the summation of all the errors from all the processes. Scanning properties were set to ensure the best quality generated point cloud. A Metra-Scan 3D laser scanner was used to digitize parts. The scanner was bolted to the end-effector of a six-axis robot arm. The scan path was automated and chosen to fully cover the top surface of the part at a scan speed that ensured complete coverage. The scanner was prompted to begin scanning while the

part of interest was outside of the scanners capture frame as points in the initial scanning frame are often noisy or lost by the scanner. Lastly, to ensure that surrounding objects would not be included in the scan, the part of interest was raised up from the scanning table by a thin support that was undetectable by the laser-scanner as it moved on the scan path. In total, four models were scanned including three increasing degrees of defect, 2mm, 5mm and 8mm, and a blank model containing no defect. (The number corresponds to the depth of the defect). Each model was scanned 3 times at a resolution of 0.5mm. Consistency between scans of identical models was confirmed at a later point. Isolating the defect is key to evaluating the smoothing process via the 'Data Comparison' step. Without isolation, it is challenging to distinguish the effects of smoothing on the defect vs the effects on the entirety of the model. After the scan was performed, every point in the point cloud was represented and for each point the algorithm finds the nearest point to it in comparison to the blank that has no defect. Then the normal of each point was calculated, and from the normal the distance between the point was calculated. If the angle is less than the threshold, then the point chosen is inlier. Otherwise, if it exceeds the threshold, the point is outlier see Figure 4.13.

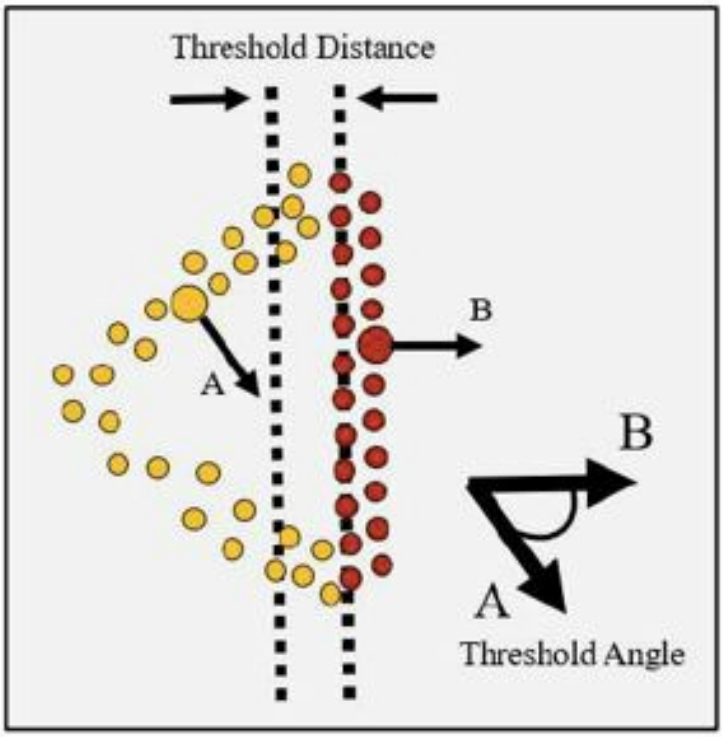

Figure 4.13: Threshold Distance and Threshold Angle Defect Detection Strategy.

The difficulty in defect detection is distinguishing defect points that are close to the blank surface. A distance comparison can only operate on a range outside of the resolution of the scanner, in this case 0.5 mm. This means that any points within 0.5mm of the actual surface are not captured. To compensate for these points, an angle comparison strategy was used that compares the vertex normal of each point in the defect point cloud to the corresponding point on the blank point cloud. The vertex normal was calculated in Matlab by fitting a plane to the nearest neighbors of the point of interest. The shape comparison algorithm by Avagyan et al. [83] was used by performing a detailed comparison of the shape of a model by geometrically adjusting its rotation and translated so they are in the same workspace with the scanned data using new viewpoint algorithms that they developed. The metric used involves measuring the height and width of the defect at each stage in the smoothing process. In this research, the "Number of Iterations" was kept constant at 20 iterations, and the "Smoothing Factor' varied from 0.1 to 1.6. Figure 4.14 depicts the

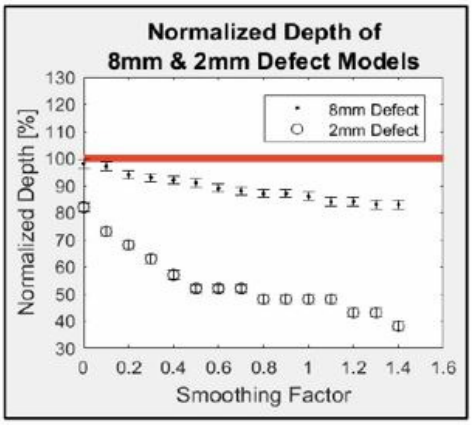

Figure 4.15: Normalized Depth of 8mm and 2mm Defect Models.

dimensions that were measured. The height is the depth of the defect and the width is the width of the defect. The green line is the actual collected scan data and the purple line is the CAD model.

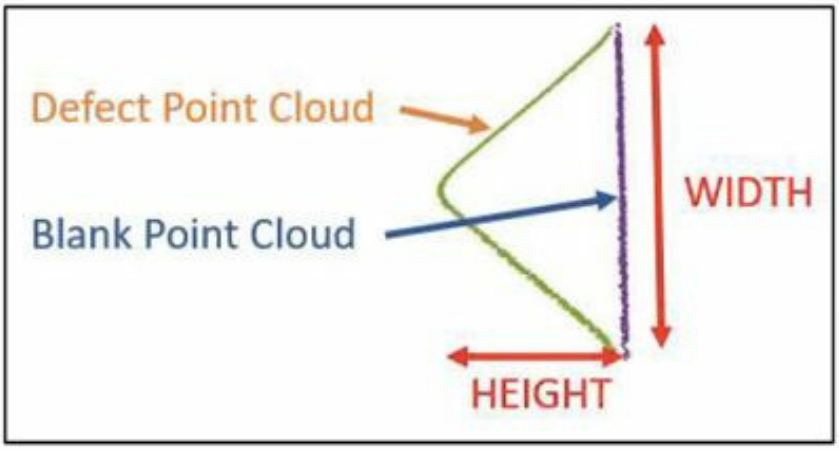

Figure 4.14: Height and width dimensions.

4.5 Results and Discussion

The major results are summarized in Figure 4.15 and Figure 4.16 (below). The graphs plot the normalized height and width on the y-axis and the smoothing factor on the x-axis. The normalization is the measured value divided by the expected value, thus the red horizontal line (at 100%) represents the true value of the defect, for reference.

Both Figure 4.15 and Figure 4.16 show the '2mm Defect' being more affected, relatively, by increasing smoothing in comparison to the '8mm Defect'. At a smoothing factor

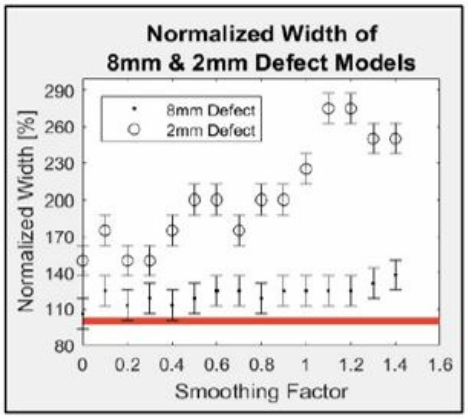

Figure 4.16: Normalized Width of 8mm and 2mm Defect Models.

of 1.0, the depth of the '2mm Defect' was 50% of its original value while the depth of the '8mm Defect' was 85% of its original value. Similarly, at a smoothing factor of 1.0, the width of the '2mm Defect' was 230% of its original value while the width of the '8mm Defect' was 130% of its original value. In absolute terms, at a smoothing factor of 1.0, the depth of both defects was smaller by about 1 millimeter, and the width was larger by about 2.5 millimeters. Error was more significant in measuring the width than the depth of the defect, as made obvious by the larger error bars in Figure 4.16. Due to the nature of the defect detection algorithm, points very close to the surface were not always recognized. This made it difficult to accurately define the width of the defect region. In Figure 4.17, this is illustrated by the widening of the contact point between point clouds, as the smoothing factor is increased. However, the depth measurements were unaffected by this, and any error in depth can be attributed to noise in the scan. Figure 4.17 (below) shows the evolution of the defect point cloud as smoothing is increased. Initially, increased smoothing rounds the left edge of the defect point cloud (orange) and flattens it near the face of the blank point cloud (blue). However, at a smoothing factor of 1.5 noise is generated within the defect point cloud, but at a smoothing factor of 1.6, the defect point cloud blows up.

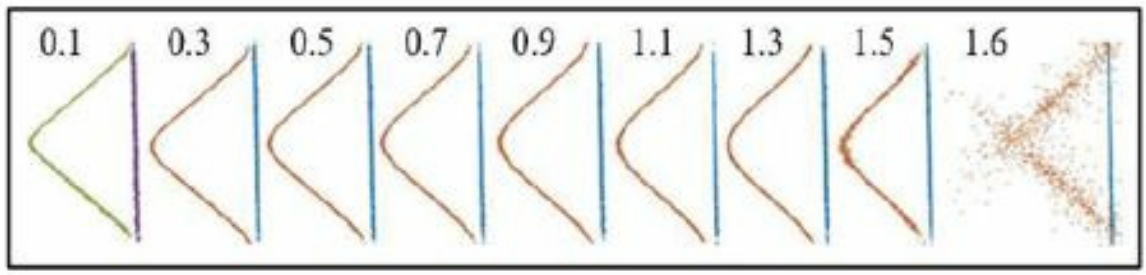

Figure 4.17: Point cloud evolution as smoothing factor varies from 0.1 to 1.6

In theory, over smoothing should continually flatten the defect point cloud; however, in the case of Laplacian smoothing, the point cloud starts expanding after a certain smoothing factor. Noise is generated as points try to move farther away from the actual surface, resulting in a much less accurate point cloud. This makes it important to carefully select the right smoothing factor. When taking the part with an 8mm defect and comparing the scanned data with the CAD model the RMS was 0.218 mm. After smoothing the part with an 8mm defect and comparing the scanned data with the CAD model the RMS was 0.20264; this is better than the prior smoothing that was 0.21851 mm. In this work error generated in the two studied phases were calculated. In the scanning phase, errors were generated due to two sources, systematic variation and random variation. The systematic errors are related to the factors that being used while executing the scanning process and are repeatable. The random errors are not related to factors being used dependent on where the part is located or the material of the part being scanned. In the second phase, smoothing, errors are generated due to the use of the wrong smoothing factors in the smoothing process; this increases the error in the scanned model and move or omit necessary feature in the scanned part. In the experiment, E-scanning and E-smoothing were calculated; the E-scanning was calculated to be +/- .218, and the E-smoothing was calculated to be +/- .20264. The total error for the first two phases is calculated in the following equation 4.11 the error is either negative or positive depending on the direction of the error. If the material deposition or the point cloud is getting less material to be deposited, then the error is negative. Otherwise, the error is

positive.

$$E_{total\ two\ phases} = \pm E_{Scanning} \pm E_{Smoothing} \tag{4.11}$$

The remaining phases of the digital additive remanufacturing steps are currently being studied. However, it is important to study all the phases and calculate the overall error and later introduce a way to compensate for the error in the following step. Errors are not necessarily positive enough where it need to be subtracted; sometimes the error is negative and can be compensated for in the next phase by adding more material or decreasing some material to get the intended outcome.

4.6 Summary

Remanufacturing consists of three sub-processes: condition assessment and digitization, material deposition, and reprocessing and inspection. This research aimed to improve the condition assessment and digitization phase by studying the effect that all the steps have on the point cloud quality used in the remanufacturing preprocessing. Scanning parameters influence the captured point cloud accuracy, and smoothing has an effect on correcting the point cloud to a certain extent. Inaccuracies in the digitization of end-of-life cores can result in incomplete material deposition and a failing additive remanufacturing procedure. The next step in this research is to quantify the error generated by meshing, slicing, and printing and how to compensate for it either positively or negatively in the prior or later activity. Outcomes from this work will aid researchers in creating point-cloud pre processing programs by knowing the effect of all the steps, integrating it in the planning phase of the remanufacturing activities, and designing a reconstruction plan for a defective part that is a crucial element in the additive remanufacturing framework.

CHAPTER 5: USING A PREDICTIVE MODEL TO OPTIMIZE THE PARAMETERS OF A CT SCANNER

5.1 Introduction

Although computed tomography (CT) scanning technologies have been well used to inspect a wide range of products, due to their inconstant material density and thickness, the CT scanner always requires an adjustment to the scanning parameters whenever a new object is loaded. This disadvantage makes the scanning process tedious and requires the involvement of a technician to execute the inspection task for the adjustments. Besides, the performance is not guaranteed every time. Thus, selecting the right scanning parameter is crucial to avoid wasting time as repeating the process can lead to a catastrophe in the manufacturing process if the decisions are not made about the production promptly and correctly. In order to improve the scanning parameter decision-making process, the Wenzel exaCT-S device was tested. Perception based on the that machine learning-based CT scanning parameter predictive method should be accessible in Wenzel's CT scanning software was tested. The users would be prompted to type in the density and thickness of the scanned item, and then the tool would use the inputs as the basis to simulate the scan setting and output a set of suggested parameter ranges that likely provide error-free scans. These predictive suggestions could reduce the time required to set scanning parameters (more valuable in future automated scanning procedures) and, if combined with continuous data collection in the future, predict wear or defection in a machine (i.e., scanning parameters that previously worked are no longer sufficient). 3D scanning technology has been developed for several years and classified by contact and non-contact types; the non-contact solution is further divided into active and passive forms. CT scanning belongs to active non-contact scanning technologies. Combining CT scanning with additive manufacturing is a popular research topic. Karme, A. et al. determined the possibilities and limitations of using CT-scanning as a quality control method in laser additive manufacturing (LAM) fabricated parts [84]. Du Plessis, A. et al. reviewed additive manufacturing (AM) applications, such as porosity and

defect analysis, volumetric density measurement, dimensional measurement, deformation, surface roughness or topography, multiscale CT and fast scanning, powder analysis, multi-materials, and also discussed the practicality and limitations of each [85]. Researchers mostly focus on product design measurement or defect analysis, but there have been few studies on how to improve the CT scanning setup, which is essential for the subsequent scanning process. Hothorn, T., and Lausen, B. derived a classifier with good performance on clinical image data to reduce glaucoma misclassification errors by comparing bagged classification trees (bagged-CTREE) to single classification trees and linear discriminate analysis (LDA) [86]. Considering that they introduced a knowledge-based decision support strategy to support routine clinical work, it is also helpful that a decision support model, such as a predictive method, can be applied to the scanning process.

This technology is related to the 3D scanning as they both has a scanner that can use different parameters to scan and gather the dimensional information. However, the CT-scanner can gather the internal structure as well. The methodology used was discussed in section 2 were a predictive model was made to optimize scanning setup parameters of a CT scanner with object density and thickness. In section 3, The results about the accuracy of the model were reveled and the results and discussions are and conclusion are in sections 4 and 5.

5.2 Methodology

Considering the property of a CT scanner, we designed 6 L shaped objects with different materials in this research. Their shapes are approximately the same for machining simplicity, and the material types are aluminum, clear plexiglass, brass, white nylon, black nylon, oak wood,as shown from left to right in Figure 5.1.

The density of the selected materials varied from 0.688 to 8.1397 mg/cm$\hat{3}$ by weighting them on a high-precision scale, shown below in Figure5.2. The exaCT-S scanning parameter setup process repeats for each sample material. After the scan parameter is set, the scan performance can be evaluated by observable blue, yellow, grey, black, and white areas on

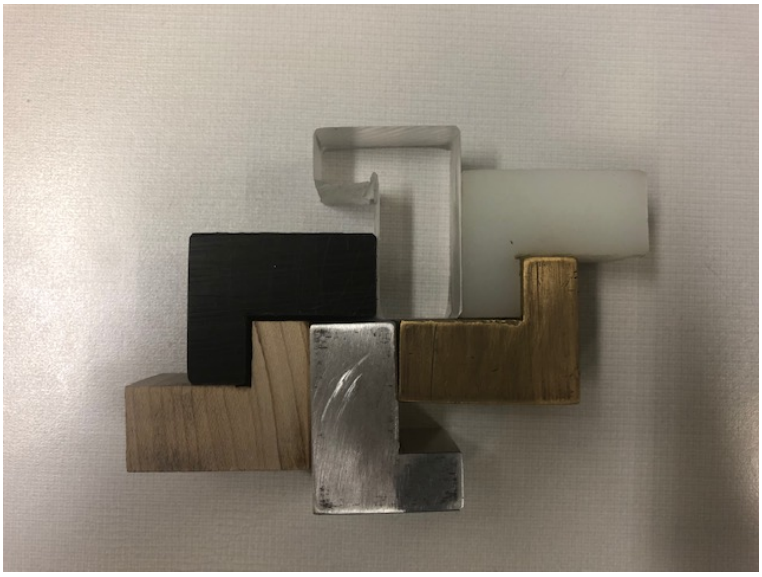

Figure 5.1: Six L shape objects for experiment and scanning

the user interface. The scan setting parameters with observations of no blue or yellow areas are classified error-free scan setting parameters.

Figure 5.2: Selected materials weight on a high precision scale to calculate density

Collected observations use five different filters, three voltage levels, three current levels, and three integration times in the experiment. In total, we collected 1620 observations (6 type materials * 5 filters * 3 voltages * 3 current * 3 integration times * 2 thicknesses), of which 70% were used to train a decision tree model (Figure 5.5) to predict and, 30% were used to test the model as shown in Figure 5.3 below.

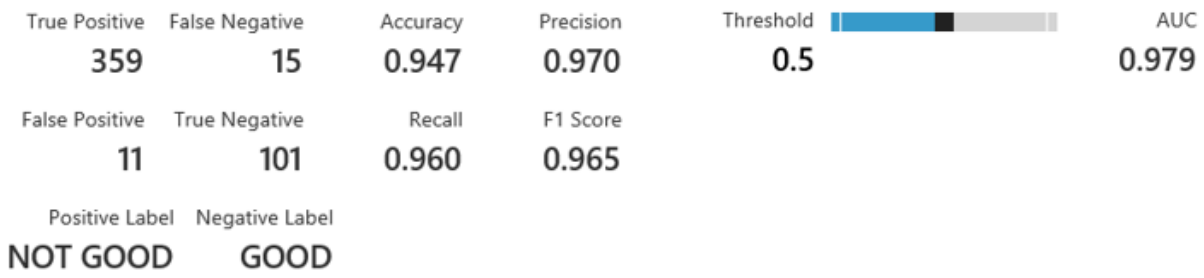

Figure 5.3: Confusion Matrix for good and bad prediction for the current gathered data with 70% model and 30% testing

There are four parameters that the technician changes each time a new part is loaded in the CT scanner. These input parameters are Filter Number, Voltage, Current, and Integration Time. The operator usually starts with the lowest filter and keeps adding the filter, the voltage, the current and finally the integration time until there are no blue or yellow spots in the software view. An experiment was designed to collect observations Various materials were tested with known densities and thicknesses. A large number of experiments were conducted, and all the observations were recorded. The observations were classified from good to not good based on the background color and the part color in the scanning software.A model designed to analyze the data to predict the good/bad outcomes can be found in Figure 5.4

A decision tree classifier created 100 decision trees based on the given data gathered in Table 5.17 these decision trees can be found in Figure 5.5.

Table 5.17: Decision Tree Classifier Parameters

Setting	**Value**
Number Of Leaves	20
Minimum Leaf Instances	10
Learning Rate	0.2
Number Of Trees	100
Allow Unknown Levels	True

Using machine learning, a boosted decision tree was created to predict the outcomes of the new given parameters based on the experimental observation. For each input parameter,

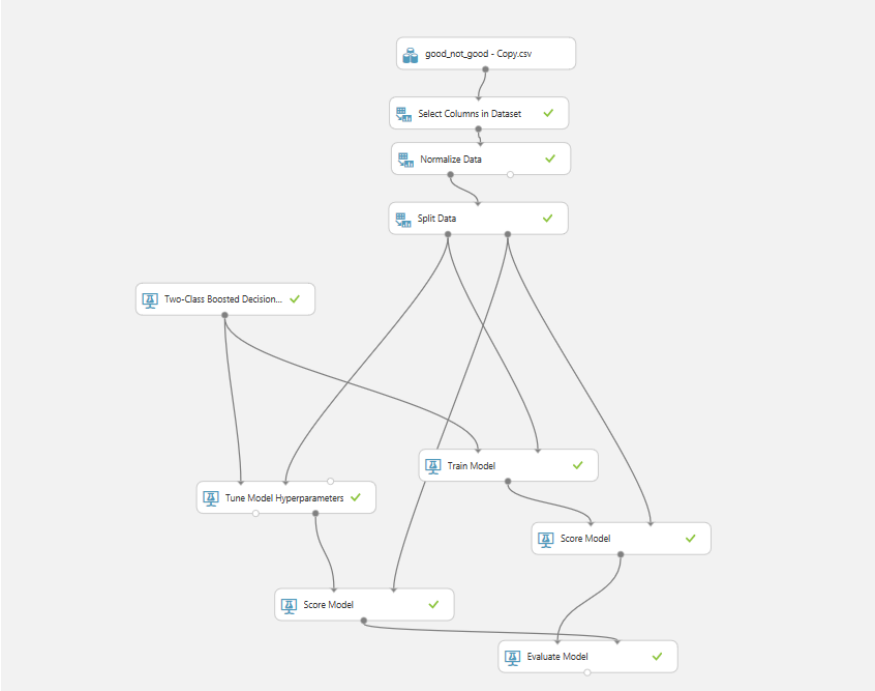

Figure 5.4: The model created to analyze the data predict the good/bad outcomes

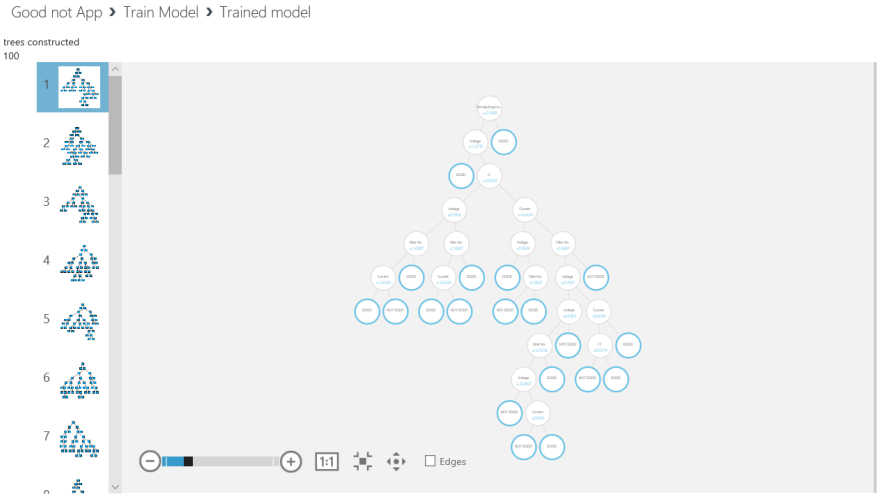

Figure 5.5: Decision tree example

Figure 5.6: Wenzel exaCT-S device at Wayne State University

such as the thickness and the material density, a suggested range of material parameters is predicted based on the historical data information.

5.3 Results

Through machine learning and classification algorithms, Wayne State University undertook a pilot study to learn and predict viable scanning parameters for the Wenzel exaCT-S device for a selection of material densities and thicknesses, as shown in Figure 5.6.

The material information is summarized below. Table 5.18.

Table 5.18: Material property information

Material	Up Thickness/mm	Bottom Thickness/mm	Volume/cm3	Weight/mg	Density (mg/cm3)
White Nylon	10.52	36.15	17.89644	16.9	0.944
Clear Plexiglass	11.13	37.95	18.86	22.43	1.19
Black Nylon	11.07	36.4	19.17	26.93	1.405
Brass	10.98	35.4	18.43	150.00	8.14
Oak Wood	11.1	36.01	17.86	12.29	0.688
Aluminum	11.15	36.32	18.54	52.03	2.81

The objective of this study was to demonstrate the ability to predict whether a scanning process on the exaCT-S would be successful given the filter number, voltage, current, integration time, material density, and material thickness. Results indicated that prediction model could be applied to guide the exaCT-S device's scan parameter selection process and reduce the time required to converge to feasible scanning parameters favorably. The results

(as can be seen from the confusion matrix) showed the ability to predict a scan with errors of 95% accuracy and 97% precision.

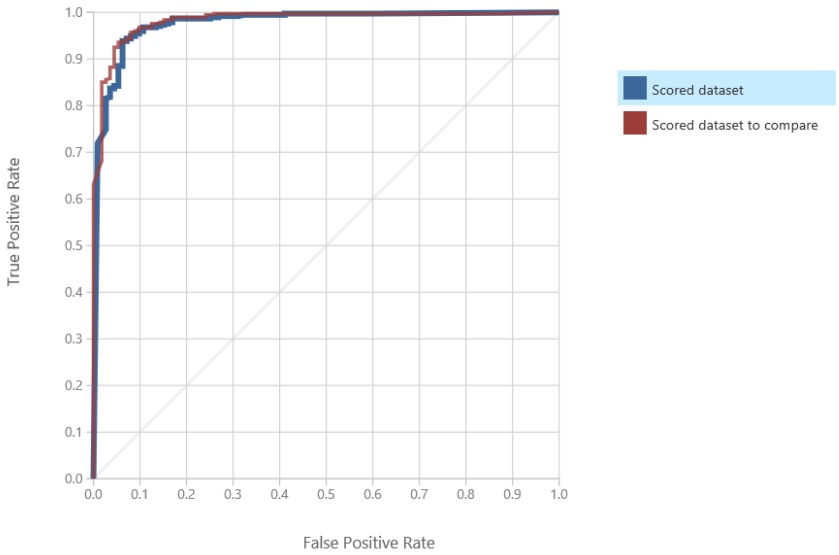

Figure 5.7: The accuracy of the model

These outcomes are promising and indicate that 1) the exaCT-S scan parameter selection process may be enhanced by integrating machine learning classification models that can suggest scan settings, and 2) more detailed studies are warranted to develop applicable ready scan parameter prediction models as can be seen in the graph in Figure 5.7 .

5.4 Discussion

The improvement we suggest to the existing software is that when the user first opens the software to scan, a pop-up window will appear called the assistive scanning tool. This tool suggests proper setting parameters for the intended scanning part according to density and thickness. This tool will have two empty boxes: 1) The first box will be for the material density and 2) the second box for the thickness of the longest edge or the spot that needs to be scanned. The pop-up windows or the application will be looking for approximate inputs in a database saved in the cloud that are shared among all the users of the scanner, match the model number, and suggest the four parameters. The user can click on and select the suggested parameters or modify it and execute the scan. The settings will be sent to the

cloud if changed and will be saved in the software. After the scan is complete, another pop-up window will appear and ask about rating the results of the performed scan. If the user chooses to accept, then the previously shared parameters will be reinforced as good scanning parameters; otherwise, it will be classified as bad scanning parameters. If a user keeps reporting bad scans results to a selected parameter that is reported by many users as good scanning parameters, then periodic maintenance is suggested to the CT scanner, and the user can will receive a phone call within a week from the company suggesting the service visit to replace the recommended part such as the reflector or do the recommended preventive maintenance. Investing in a prediction model to preset the optimal settings for the CT scanner can save the company money and reduce reliance on human capital to execute the task; it can also lead to less demand on buying other inspection devices as it reduces the bottleneck in the inspection stage. This model can be implemented and used for any CT scanner across multiple companies and organizations by having the data gathered or shared from similar CT scanners. This will provide a of understanding about the internal components of the CT scanner and its effect on the scanning quality. For the scanner used and the speeds that were selected, the change in the speeds was insignificant. Changing the resolution results in better quality scans to a certain extent, and after that, it has a negative effect. However, further study is needed to make a final conclusion The significant effect of the standoff distance and the view angle on the scanning quality were confirmed in this experiment, and it supports the findings of previous studies.

5.5 Summary

The preliminary results show that the prediction mode is accurate. Therefore, it is feasible to work on an optimization model to predict the right parameters. Currently I am working on several improvements and advancements to create an automated tool to predict the optimal parameters just by knowing the thickness and density of the part. The model has been created and many decision trees were generated to simulate different scenarios. This model needs to be inverted to give the parameters instead of taking the parameters and

knowing if the scan results are good or bad. I am also investigating ways to improve the scanning results by sharing the results across different platforms and connecting the gathered images of objects to the cloud. I will share it when ready in future publications.

CHAPTER 6: CONCLUSION

3D scanning parameters strongly affect the quality of the point cloud. Without knowing these effects and considering them in generating what is made might not be ideal and can miss-lead the inspection process as it will create a point cloud with many errors. In this dissertation, the focus was on studying the effect of the parameters on the point cloud that add up to the total error in the inspection and re manufacturing application. Although different parameters have been studied in the past and their effect was known, the effect of the speed and the scanner resolution had not investigated, get their effect is significant. For this work a robot was attached to the endeffector of a robot to make the experiment precise and reproducible and to eliminate the external factors and have specific levels for the parameters being tested. In chapter 2, we developed a link between the two work spaces, the scanner and the robot cell, as they are not integrated and the relationship between the two systems were not defined. A transformational relationship was found that can link the location of any point in the robot work space back to the scanner work space,which will help in knowing the points that will be collected and set the expectation of the scanner to the points that will be gathered. In chapter 3, we designed an experiment using the 3D scanner attached to the robot to investigate two additional parameters beyond than those studied in the literature. A literature review was done to identify the studied parameters, and the gap was identified. The two parameters that needed to be studied were the speed of the movement of the robot arm and the scanner resolution. These two parameters were studied along with two other known parameters in the literature. This was made to first validate the findings of the literature and make sure that the methodology used in the comparison was valid. The two parameters that were studied along with the speed and resolution are the standoff distance and the view angle of the scanner in relationship to the surface being scanned. The findings confirmed the literature and indicated that the changes in the speed and the scanner resolution are significant in the errors being generated to the point cloud that are not actually in the surface being scanned. In chapter 4, we proposed an error propagation

approach that models the interaction of each step of the additive remanufacturing process by incorporating all the processes that the point cloud undergo. Typically point clouds are collected in the first phases in the remanufacturing facility to identify the defects and generate the appropriate remanufacturing plan. There are errors that come with this point cloud due to the scanner parameters. These errors need to be added to the overall error of the point cloud that will be added to it in the remanufacturing data. This proposed model was formulated and results of the error generated from the parameters of the scanner and point cloud smoothing were presented. It is important to know the error generated from each step or process to be able to compensate for it in the following steps and generate appropriate material deposition paths. Sources of error from scanning, smoothing, meshing, slicing, and material deposition were proposed in the error propagation model for additive remanufacturing. In chapter 5, we tested parameter optimization on the scans with an experiment done on a CT scanner. We used machine learning to predict the ability to identify the outcomes of the scanner either good or a bad, by designing a machine learning algorithm and creating many classification trees. The results show the ability to use these techniques to predict the ability with high accuracy. The outcomes from this work will aid researchers in creating point-cloud preprocessing programs by knowing the effect of all the steps, integrating them in the planning phase of the remanufacturing activities, and designing a reconstruction plan for a defective part that is a crucial element in the additive remanufacturing framework.

APPENDIX

Journal Publications To Be Submitted

R1. M. Alkhateeb, M. Alzahrani, J. Rickli, "The influence of scanning speed and scanner resolution on the digital thread of the remanufacturing using additive manufacturing technologies,"

Conference Publications

C1. M. Mojahed, J. Rickli, N. Christoforou, "Error propagation in digital additive remanufacturing process planning," *ASME 2019 14th International Manufacturing Science and Engineering Conference MSEC 2019. American Society of Mechanical Engineers, 2019. (MSEC'19)*, Erie,PA USA, June 2019.

REFERENCES

[1] S. Martínez, E. Cuesta, J. Barreiro, and B. Álvarez, "Analysis of laser scanning and strategies for dimensional and geometrical control," *The International Journal of Advanced Manufacturing Technology*, vol. 46, no. 5-8, pp. 621–629, 2010.

[2] i3mainz, "terrestrial laserscanning : inschriften im bezugssystem des raumes (ibr)," http://www.spatialhumanities.de/en/ibr/technology/terrestrial-laserscanning.html, 06 2019.

[3] Y. Wang and H.-Y. Feng, "Outlier detection for scanned point clouds using majority voting," *Computer-Aided Design*, vol. 62, pp. 31–43, 2015.

[4] H.-Y. Feng, Y. Liu, and F. Xi, "Analysis of digitizing errors of a laser scanning system," *Precision Engineering*, vol. 25, no. 3, pp. 185–191, 2001.

[5] T. Weyrich, M. Pauly, R. Keiser, S. Heinzle, S. Scandella, and M. H. Gross, "Post-processing of scanned 3d surface data." *SPBG*, vol. 4, pp. 85–94, 2004.

[6] N. Van Gestel, S. Cuypers, P. Bleys, and J.-P. Kruth, "A performance evaluation test for laser line scanners on cmms," *Optics and lasers in engineering*, vol. 47, no. 3-4, pp. 336–342, 2009.

[7] D. Bračun, M. Jezeršek, and J. Diaci, "Triangulation model taking into account light sheet curvature," *Measurement Science and Technology*, vol. 17, no. 8, p. 2191, 2006.

[8] A. Djuric, "Reconfigurable kinematics, dynamics and control process for industrial robots." 2007.

[9] J. L. Rickli, A. K. Dasgupta, and G. P. Dinda, "A descriptive framework for additive remanufacturing systems," *International Journal of Rapid Manufacturing*, vol. 4, no. 2-4, pp. 199–218, 2014.

[10] K. H. Lee and H.-p. Park, "Automated inspection planning of free-form shape parts by laser scanning," *Robotics and Computer-Integrated Manufacturing*, vol. 16, no. 4, pp. 201–210, 2000.

[11] F. Xi and C. Shu, "Cad-based path planning for 3-d line laser scanning," *Computer-Aided Design*, vol. 31, no. 7, pp. 473–479, 1999.

[12] S. Son, H. Park, and K. H. Lee, "Automated laser scanning system for reverse engineering and inspection," *International Journal of Machine Tools and Manufacture*, vol. 42, no. 8, pp. 889–897, 2002.

[13] Y. Li and P. Gu, "Free-form surface inspection techniques state of the art review," *Computer-Aided Design*, vol. 36, no. 13, pp. 1395–1417, 2004.

[14] B. Morey, "Auto manufacturing focuses on vision," *Manufacturing Engineering*, vol. 149, no. 3, pp. 115–125, 2012.

[15] M. Rahayem, J. Kjellander, and S. Larsson, "Accuracy analysis of a 3d measurement system based on a laser profile scanner mounted on an industrial robot with a turntable," in *Emerging Technologies and Factory Automation, 2007. ETFA. IEEE Conference on.* IEEE, 2007, pp. 880–883.

[16] M. Callieri, A. Fasano, G. Impoco, P. Cignoni, R. Scopigno, G. Parrini, and G. Biagini, "Roboscan: an automatic system for accurate and unattended 3d scanning," in *3D Data Processing, Visualization and Transmission, 2004. 3DPVT 2004. Proceedings. 2nd International Symposium on.* IEEE, 2004, pp. 805–812.

[17] S. Larsson and J. Kjellander, "Motion control and data capturing for laser scanning with an industrial robot," *Robotics and Autonomous Systems*, vol. 54, no. 6, pp. 453–460, 2006.

[18] P. Manorathna, P. Ogun, S. Marimuthu, L. Justham, and M. Jackson, "Performance evaluation of a three dimensional laser scanner for industrial applications," in *Information and Automation for Sustainability (ICIAfS), 2014 7th International Conference on.* IEEE, 2014, pp. 1–6.

[19] S. Larsson and J. A. Kjellander, "Path planning for laser scanning with an industrial robot," *Robotics and autonomous systems*, vol. 56, no. 7, pp. 615–624, 2008.

[20] Y. Wang and H.-Y. Feng, "Effects of scanning orientation on outlier formation in 3d laser scanning of reflective surfaces," *Optics and Lasers in Engineering*, vol. 81, pp. 35–45, 2016.

[21] A. Yao, "Applications of 3d scanning and reverse engineering techniques for quality control of quick response products," *The international journal of advanced manufacturing technology*, vol. 26, no. 11-12, pp. 1284–1288, 2005.

[22] M. Korosec, J. Duhovnik, and N. Vukasinovic, "Identification and optimization of key process parameters in noncontact laser scanning for reverse engineering," *Computer-Aided Design*, vol. 42, no. 8, pp. 744–748, 2010.

[23] J. Chow, "Reproducing aircraft structural components using laser scanning," *The International Journal of Advanced Manufacturing Technology*, vol. 13, no. 10, pp. 723–728, 1997.

[24] R. G. Nedelcu and A. S. Persson, "Scanning accuracy and precision in 4 intraoral scanners: an in vitro comparison based on 3-dimensional analysis," *The Journal of prosthetic dentistry*, vol. 112, no. 6, pp. 1461–1471, 2014.

[25] M. Pieraccini, G. Guidi, and C. Atzeni, "3d digitizing of cultural heritage," *Journal of Cultural Heritage*, vol. 2, no. 1, pp. 63–70, 2001.

[26] S. Aung, R. Ngim, and S. Lee, "Evaluation of the laser scanner as a surface measuring tool and its accuracy compared with direct facial anthropometric measurements," *British journal of plastic surgery*, vol. 48, no. 8, pp. 551–558, 1995.

[27] W. Boehler and A. Marbs, "3d scanning instruments," *Proceedings of the CIPA WG*, vol. 6, pp. 9–18, 2002.

[28] G. Reinhart and W. Tekouo, "Automatic programming of robot-mounted 3d optical scanning devices to easily measure parts in high-variant assembly," *CIRP annals*, vol. 58, no. 1, pp. 25–28, 2009.

[29] H. ElMaraghy and X. Yang, "Computer-aided planning of laser scanning of complex geometries," *CIRP Annals-Manufacturing Technology*, vol. 52, no. 1, pp. 411–414, 2003.

[30] T. Hedberg, J. Lubell, L. Fischer, L. Maggiano, and A. B. Feeney, "Testing the digital thread in support of model-based manufacturing and inspection," *Journal of Computing and Information Science in Engineering*, vol. 16, no. 2, p. 021001, 2016.

[31] H. Zhao, J.-P. Kruth, N. Van Gestel, B. Boeckmans, and P. Bleys, "Automated dimensional inspection planning using the combination of laser scanner and tactile probe," *Measurement*, vol. 45, no. 5, pp. 1057–1066, 2012.

[32] W. Boehler, M. B. Vicent, and A. Marbs, "Investigating laser scanner accuracy," *The International Archives of Photogrammetry, Remote Sensing and Spatial Information Sciences*, vol. 34, no. Part 5, pp. 696–701, 2003.

[33] K. Deshmukh, J. L. Rickli, and A. Djuric, "Kinematic modeling of an automated laser line point cloud scanning system," *Procedia Manufacturing*, vol. 5, pp. 1075–1091, 2016.

[34] A. Contri, P. Bourdet, and C. Lartigue, "Quality of 3d digitised points obtained with non-contact optical sensors," *CIRP Annals-Manufacturing Technology*, vol. 51, no. 1, pp. 443–446, 2002.

[35] C. Lartigue, A. Contri, and P. Bourdet, "Digitised point quality in relation with point exploitation," *Measurement*, vol. 32, no. 3, pp. 193–203, 2002.

[36] F. Zhao, X. Xu, and S. Q. Xie, "Computer-aided inspection planningâĂŤthe state of the art," *Computers in industry*, vol. 60, no. 7, pp. 453–466, 2009.

[37] H. ElMaraghy, P. Gu, and J. Bollinger, "Expert system for inspection planning," *CIRP Annals-Manufacturing Technology*, vol. 36, no. 1, pp. 85–89, 1987.

[38] C.-H. Menq, H.-T. Yau, and G.-Y. Lai, "Automated precision measurement of surface profile in cad-directed inspection," *IEEE Transactions on Robotics and Automation*, vol. 8, no. 2, pp. 268–278, 1992.

[39] M. L. Kersten, S. Manegold *et al.*, "Cracking the database store," in *CIDR*, vol. 5, 2005, pp. 4–7.

[40] C. Gordon, F. Boukamp, D. Huber, E. Latimer, K. Park, and B. Akinci, "Combining reality capture technologies for construction defect detection: A case study," in *EIA9:*

E-Activities and Intelligent Support in Design and the Built Environment, 9th EuropIA International Conference, 2003, pp. 99–108.

[41] C. Boehnen and P. Flynn, "Accuracy of 3d scanning technologies in a face scanning scenario," in *3-D Digital Imaging and Modeling, 2005. 3DIM 2005. Fifth International Conference on.* IEEE, 2005, pp. 310–317.

[42] M. Sokovic, M. Cedilnik, and J. Kopac, "Use of 3d-scanning and reverse engineering by manufacturing of complex shapes," in *Proceedings of the 13th International Scientific Conference Achievements in Mechanical and Materials Engineering, AMME*, 2005, pp. 601–604.

[43] G. Dalton, "Reverse engineering using laser metrology," *Sensor review*, vol. 18, no. 2, pp. 92–96, 1998.

[44] J. Chow, T. Xu, S.-M. Lee, and K. Kengkool, "Development of an integrated laser-based reverse engineering and machining system," *The International Journal of Advanced Manufacturing Technology*, vol. 19, no. 3, pp. 186–191, 2002.

[45] Y. Reshetyuk, "Investigation of the influence of surface reflectance on the measurements with the terrestrial laser scanner leica hds 3000," *Zeitschrift für Geodasie, Geoinformation und Landmanagement*, vol. 131, no. 2, pp. 96–103, 2006.

[46] F. A. R. Martins, J. G. García-Bermejo, E. Z. Casanova, and J. R. P. González, "Automated 3d surface scanning based on cad model," *Mechatronics*, vol. 15, no. 7, pp. 837–857, 2005.

[47] X. Jin and X. Yang, "Off-line programming of a robot for laser re-manufacturing," *Tsinghua Science & Technology*, vol. 14, pp. 186–191, 2009.

[48] C. Shen and S. Zhu, "A robotic system for surface measurement via 3d laser scanner," *reconstruction*, vol. 1, p. 2, 2012.

[49] S. Yin, Y. Ren, Y. Guo, J. Zhu, S. Yang, and S. Ye, "Development and calibration of an integrated 3d scanning system for high-accuracy large-scale metrology," *Measurement*, vol. 54, pp. 65–76, 2014.

[50] S. Gerbino, D. M. Del Giudice, G. Staiano, A. Lanzotti, and M. Martorelli, "On the influence of scanning factors on the laser scanner-based 3d inspection process," *The International Journal of Advanced Manufacturing Technology*, vol. 84, no. 9-12, pp. 1787–1799, 2016.

[51] D. Blanco, P. Fernández, G. Valiño, J. Rico, and A. Rodríguez, "Influence of ambient light on the repeatability of laser triangulation digitized point clouds when scanning en aw 6082 flat faced features," in *AIP Conference Proceedings*, vol. 1181, no. 1. AIP, 2009, pp. 509–520.

[52] E. Cuesta, J. C. Rico, P. Fernández, D. Blanco, and G. Valiño, "Influence of roughness on surface scanning by means of a laser stripe system," *The International Journal of Advanced Manufacturing Technology*, vol. 43, no. 11-12, p. 1157, 2009.

[53] N. Vukašinović, D. Bračun, J. Možina, and J. Duhovnik, "The influence of incident angle, object colour and distance on cnc laser scanning," *The International Journal of Advanced Manufacturing Technology*, vol. 50, no. 1-4, pp. 265–274, 2010.

[54] N. Zaimovic-Uzunovic and S. Lemes, "Influences of surface parameters on laser 3d scanning," in *IMEKO Conference Proceedings: International Symposium on Measurement and Quality Control: Osaka, Japan*, 2010, pp. D024–026.

[55] S. Lemeš and N. Zaimović-Uzunović, "Study of ambient light influence on laser 3d scanning," in *Proceedings of the 7th International Conference on Industrial Tools and Material Processing Technologies*, 2009, pp. 327–330.

[56] S. Voisin, S. Foufou, F. Truchetet, D. L. Page, and M. A. Abidi, "Study of ambient light influence for three-dimensional scanners based on structured light," *Optical Engineering*, vol. 46, no. 3, p. 030502, 2007.

[57] T. Voegtle, I. Schwab, and T. Landes, "Influences of different materials on the measurements of a terrestrial laser scanner (tls)," in *Proc. of the XXI Congress, The International Society for Photogrammetry and Remote Sensing, ISPRS2008*, vol. 37, 2008, pp. 1061–1066.

[58] D. D. Lichti and B. Harvey, "The effects of reflecting surface material properties on time-of-flight laser scanner measurements," *tc*, vol. 2, p. 1, 2002.

[59] I. Popov, S. Onuh, and K. Dotchev, "Dimensional error analysis in point cloud-based inspection using a non-contact method for data acquisition," *Measurement Science and Technology*, vol. 21, no. 7, p. 075303, 2010.

[60] S. L. Brown and H. A. Pierson, "Digital design integrity for additive manufacturing: examining reliability issues in the digital preproduction process," *International Journal of Rapid Manufacturing*, vol. 7, no. 1, pp. 43–58, 2018.

[61] M. Hedges and N. Calder, "Near net shape rapid manufacture & repair by lens," in *Cost Effective Manufacture via Net-Shape Processing, Meeting Proceedings RTO-MP-AVT-139, Paper*, vol. 13, 2006.

[62] R. P. Mudge and N. R. Wald, "Laser engineered net shaping advances additive manufacturing and repair," *Welding Journal-New York-*, vol. 86, no. 1, p. 44, 2007.

[63] O. Yilmaz, N. Gindy, and J. Gao, "A repair and overhaul methodology for aeroengine components," *Robotics and Computer-Integrated Manufacturing*, vol. 26, no. 2, pp. 190–201, 2010.

[64] N. Gupta, C. Weber, and S. Newsome, "Additive manufacturing: Status and opportunities," *Science and Technology Policy Institute, Washington*, 2012.

[65] J. Wang, S. Prakash, Y. Joshi, and F. Liou, "Laser aided part repair-a review," in *Proceedings of the thirteenth annual solid freeform fabrication symposium, Austin, TX*. Citeseer, 2002.

[66] C. Chen, Y. Wang, H. Ou, Y. He, and X. Tang, "A review on remanufacture of dies and moulds," *Journal of Cleaner Production*, vol. 64, pp. 13–23, 2014.

[67] N. A. I. M. Rosli and A. Ramli, "Mapping bootstrap error for bilateral smoothing on point set," in *AIP Conference Proceedings*, vol. 1605, no. 1. AIP, 2014, pp. 149–154.

[68] Z. M. Bi and L. Wang, "Advances in 3d data acquisition and processing for industrial applications," *Robotics and Computer-Integrated Manufacturing*, vol. 26, no. 5, pp. 403–413, 2010.

[69] C. Piya, J. M. Wilson, S. Murugappan, Y. Shin, and K. Ramani, "Virtual repair: geometric reconstruction for remanufacturing gas turbine blades," in *ASME 2011 International Design Engineering Technical Conferences and Computers and Information in Engineering Conference*. American Society of Mechanical Engineers, 2011, pp. 895–904.

[70] L. A. Freitag, "On combining laplacian and optimization-based mesh smoothing techniques," *ASME applied mechanics division-publications-amd*, vol. 220, pp. 37–44, 1997.

[71] M. Pauly, N. J. Mitra, and L. J. Guibas, "Uncertainty and variability in point cloud surface data." *SPBG*, vol. 4, pp. 77–84, 2004.

[72] R. Lindenbergh, N. Pfeifer, and T. Rabbani, "Accuracy analysis of the leica hds3000 and feasibility of tunnel deformation monitoring," in *Proceedings of the ISPRS Workshop, Laser scanning*, vol. 36, 2005, p. 3.

[73] S. M. Odeyinka and A. M. Djuric, "Fanuc family inverse kinematics modeling, validation and visualization," SAE Technical Paper, Tech. Rep., 2016.

[74] P. Arachchige, M. Abderrahmane, and A. M. Djuric, "Modeling and validation of rapid prototyping related available workspace," *SAE International Journal of Materials and Manufacturing*, vol. 7, no. 2, pp. 291–299, 2014.

[75] M. Abderrahmane, A. M. Djuric, W. Chen, and C. Yeh, "Study and validation of singularities for a fanuc lr mate 200ic robot," in *IEEE International Conference on Electro/Information Technology*. IEEE, 2014, pp. 432–437.

[76] I. Bešić, N. Van Gestel, J.-P. Kruth, P. Bleys, and J. Hodolič, "Accuracy improvement of laser line scanning for feature measurements on cmm," *Optics and Lasers in Engineering*, vol. 49, no. 11, pp. 1274–1280, 2011.

[77] A. Javaheri, C. Brites, F. Pereira, and J. Ascenso, "Subjective and objective quality evaluation of 3d point cloud denoising algorithms," in *Multimedia & Expo Workshops (ICMEW), 2017 IEEE International Conference on*. IEEE, 2017, pp. 1–6.

[78] N. Nasr and M. Thurston, "Remanufacturing: A key enabler to sustainable product systems," *Rochester Institute of Technology*, pp. 15–18, 2006.

[79] S. Ford and M. Despeisse, "Additive manufacturing and sustainability: an exploratory study of the advantages and challenges," *Journal of Cleaner Production*, vol. 137, pp. 1573–1587, 2016.

[80] W. Frei, "Meshing considerations for linear static problems," *URL: https://www. comsol. com/blogs/meshing-considerations-linear-staticproblems*, 2013.

[81] S. Sikder, A. Barari, and H. Kishawy, "Effect of adaptive slicing on surface integrity in additive manufacturing," in *ASME 2014 International Design Engineering Technical Conferences and Computers and Information in Engineering Conference*. American Society of Mechanical Engineers, 2014, pp. V01AT02A052–V01AT02A052.

[82] I. Gibson, D. W. Rosen, and B. Stucker, "Design for additive manufacturing," in *Additive Manufacturing Technologies*. Springer, 2010, pp. 299–332.

[83] V. Avagyan, A. Zakarian, and P. Mohanty, "Scanned three-dimensional model matching and comparison algorithms for manufacturing applications," *Journal of Manufacturing Science and Engineering*, vol. 129, no. 1, pp. 190–201, 2007.

[84] A. Karme, A. Kallonen, V.-P. Matilainen, H. Piili, and A. Salminen, "Possibilities of ct scanning as analysis method in laser additive manufacturing," *Physics Procedia*, vol. 78, pp. 347–356, 2015.

[85] A. Du Plessis, I. Yadroitsev, I. Yadroitsava, and S. G. Le Roux, "X-ray microcomputed tomography in additive manufacturing: a review of the current technology and applications," *3D Printing and Additive Manufacturing*, vol. 5, no. 3, pp. 227–247, 2018.

[86] T. Hothorn and B. Lausen, "Bagging tree classifiers for laser scanning images: a data- and simulation-based strategy," *Artificial intelligence in medicine*, vol. 27, no. 1, pp. 65–79, 2003.

ABSTRACT

3D SCANNING AND THE IMPACT OF THE DIGITAL THREAD ON MANUFACTURING AND RE-MANUFACTURING APPLICATIONS

by

MOJAHED MOHAMMAD F. ALKHATEEB

August 2019

Advisor: Dr. Jeremy L. Rickli

Major: Industrial Engineering

Degree: Doctor of Philosophy

3D laser line scanners are becoming a powerful technology for capturing point cloud datasets and collecting dimensional information for many objects. However, the use of point cloud is limited due to many factors. These include the lack of on deep understanding of the effect of point cloud parameters on scan quality. This knowledge is critical to gaining an understanding of the measurement in point cloud. Currently, there are no adequate measurement procedures for 3D scanners. There is a need for standardized measurement procedures to evaluate 3D scanner accuracy due to uncertainties in 3D scanning, such as surface quality, surface orientation and scan depth [6]. The lack of standardized procedures does not allow the technology to be fully automated and used in manufacturing facilities that would allow 100% in-line inspection. In this dissertation I worked on accomplishing four tasks that will achieve the objective of having a standardized measurement procedure that is critical to develop an automated laser scanning system to avoid variations and have consistent data capable of identifying defects. The four tasks are: (1) linking the robot workspace with the scanner workspace; (2) studying the effect of the scanning speed and the resolution on point cloud quality by conducting an experiment with systematically varied scan parameters on scan quality. The parameters that were tested are the effect of view angle, standoff distance, speed, and resolution. Knowing the effect of these parameters is important in order to generate the scan path that provides the best coverage and quality of points collected; (3) studying the overall error of that is associated with the transformation

of the point cloud in a remanufacturing facility using additive manufacturing. There is also a need to know the impact of all the scanning parameters especially the speed and the resolution; (4) modeling a machine learning tool to optimize the parameters of different scanning techniques after collecting the scanning results to select the optimal ones that provide the best scan quality. With the success of this work, the advancement and practice of automated quality monitoring in manufacturing will increase.

AUTOBIOGRAPHICAL STATEMENT

Mojahed Mohammad F. Alkhateeb is currently a doctoral candidate in the department of industrial and systems engineering at Wayne State University. He received a M.Sc. degree in industrial and systems engineering from the University of Michigan - Dearborn, MI USA in 2013. Prior to that he received a B.Sc. degree in industrial engineering from King Abdulaziz University - Jeddah, Saudi Arabia in 2009. His primary research interests include testing the effect of different scanning parameters on the quality of the scanning outcome. His research has been published in MSEC. He has participated in many conferences in WSU and other organizations including ISERC, and ASME where his paper was accepted and recommended for journal publication. He also received an NSF travel award to attend the conference. Mojahed will start as an assistant professor in the department of industrial engineering at King Abdulaziz University - Rabigh, Saudi Arabia in Fall 2019.